

5.13 Paleointensities

L. Tauxe, University of California San Diego, La Jolla, CA, USA

T. Yamazaki, Geological Survey of Japan, Tsukuba, Ibaraki, Japan

© 2007 Elsevier Ltd. All rights reserved.

5.13.1	Introduction	2
5.13.2	Introduction to the Theory of Paleointensity	2
5.13.3	Paleointensity with Thermal Remanence	3
5.13.3.1	Linearity Assumption	5
5.13.3.2	Alteration during Heating	6
5.13.3.2.1	KTT family of experiments	7
5.13.3.2.2	Shaw family of experiments	10
5.13.3.3	Methods that Minimize Alteration	12
5.13.3.3.1	Reduced number of heating steps	12
5.13.3.3.2	Use of controlled atmospheres to reduce alteration	14
5.13.3.3.3	Measurement at elevated temperature	14
5.13.3.3.4	Use of microwaves for thermal excitation	14
5.13.3.3.5	Using materials resistant to alteration	15
5.13.3.4	Use of IRM Normalization	15
5.13.4	Paleointensity with Depositional Remanences	16
5.13.4.1	Physical Alignment of Magnetic Moments in Viscous Fluids	16
5.13.4.1.1	Nonflocculating environments	18
5.13.4.1.2	Flocculating environments	19
5.13.4.2	PostDepositional Processes	21
5.13.4.3	Note on Aeolian Deposits	22
5.13.4.4	Normalization	22
5.13.5	Remagnetization	23
5.13.5.1	Magnetic Viscosity	23
5.13.5.2	Chemical Alteration	24
5.13.6	Evaluating Paleointensity Data	24
5.13.6.1	Thermally blocked remanences	24
5.13.6.2	Depositional Remanences	24
5.13.7	Current State of the Paleointensity Data	24
5.13.7.1	Paleomagnetic Databases	24
5.13.7.2	Conversion to Virtual Dipole Moment	29
5.13.7.2.1	Absolute paleointensity data	29
5.13.7.2.2	Relative paleointensity data	30
5.13.8	Discussion	31
5.13.8.1	Selection Criteria from the PINT06 Database	31
5.13.8.2	What is the Average Strength of the Geomagnetic Field?	33
5.13.8.3	Are There Any Trends?	34
5.13.8.3.1	Intensity versus polarity interval length	34
5.13.8.3.2	Source of scatter in the CNS	35
5.13.8.3.3	The oldest paleointensity records	35
5.13.8.3.4	The paleointensity 'saw-tooth'	35
5.13.8.4	High-Resolution Temporal Correlation	39
5.13.8.4.1	Sediments	39

2 Paleointensities

5.13.8.4.2	Ridge crest processes	40
5.13.8.5	Atmospheric Interaction	40
5.13.8.6	Frequency of Intensity Fluctuations and the Climatic Connection	44
5.13.9	Conclusions	46
References		47

s0005 5.13.1 Introduction

p0005 The geomagnetic field acts both as an umbrella, shielding us from cosmic radiation and as a window, offering one of the few glimpses of the inner workings of the Earth. Ancient records of the geomagnetic field can inform us about geodynamics of the early Earth and changes in boundary conditions through time. Thanks to its essentially dipolar nature, the geomagnetic field has acted as a guide, pointing to the axis of rotation thereby providing latitudinal information for both explorers and geologists. A complete understanding of the geomagnetic field requires not only a description of the direction of field lines over the surface of the Earth, but information about its strength as well. While directional information is relatively straightforward to obtain, intensity variations are much more difficult and are the subject of this chapter.

p0010 In his treatise *De Magnete*, published in 1600, William Gilbert described variations in field strength with latitude based on the sluggishness or rapidity with which a compass settled on the magnetic direction. Magnetic intensity was first measured quantitatively in the late 1700s by French scientist Robert de Paul, although all records were lost in a shipwreck. Systematic measurement of the geomagnetic field intensity began in 1830 (see, e.g., Stern^{b1000} (2003) for a review). Despite studies of the geomagnetic field that included some mention of its strength, stretching back to at least the time of Gilbert, basic questions such as what is the average field strength and whether there are any predictable trends remain subject to debate. To study field intensity in the past requires us to use ‘accidental’ records; we rely on geological or archeological materials which can reveal much about the behavior of the Earth’s magnetic field in ancient times.

p0015 There have been several fine reviews of the field of paleointensity recently (see, e.g., Valet^{b1265}, 2003) and the subject is developing very rapidly. Paleointensity data derived from archeological materials will be considered elsewhere (see 00094). This chapter reviews the theoretical basis for paleointensity

experiments in igneous and sedimentary environments especially with regard to experimental design. We then turn to new and updated existing databases. Finally, we highlight current topics of interest.

5.13.2 Introduction to the Theory of Paleointensity

s0010

In principle, it is possible to determine the intensity of ancient magnetic fields because the primary mechanisms by which rocks become magnetized (e.g., thermal, chemical, and detrital remanent magnetizations or TRM, CRM, and DRM, respectively) can be approximately linearly related to the ambient field for low fields such as the Earth’s. Thus we have by assumption

$$M_{\text{NRM}} \simeq \alpha_{\text{anc}} H_{\text{anc}}$$

and

$$M_{\text{lab}} \simeq \alpha_{\text{lab}} H_{\text{lab}} \quad [1]$$

where α_{lab} and α_{anc} are dimensionless constants of proportionality; M_{NRM} and M_{lab} are natural and laboratory remanent magnetizations, respectively; and H_{anc} and H_{lab} are the magnitudes of the ancient and laboratory fields, respectively. If α_{lab} and α_{anc} are the same, we can divide the two equations and rearrange terms to get

$$H_{\text{anc}} = \frac{M_{\text{NRM}}}{M_{\text{lab}}} H_{\text{lab}}$$

In other words, if the laboratory remanence has the same proportionality constant with respect to the applied field as the ancient one, the remanences are linearly related to the applied field, and the natural remanence (NRM) is composed solely of a single component, all one needs to do to get the ancient field is measure M_{NRM} , give the specimen a laboratory proxy remanence M_{lab} and multiply the ratio by H_{lab} .

In practice, paleointensity is not so simple. The remanence acquired in the laboratory may not have the same proportionality constant as the original

remance (e.g., the specimen has altered its capacity to acquire remance or was acquired by a mechanism not reproduced in the laboratory). The assumption of linearity between the remance and the applied field may not hold true. Or, the natural remance may have multiple components acquired at different times with different constants of proportionality.

p0030 In Sections 5.13.3 and 5.13.4 we will discuss the assumptions behind paleointensity estimates and outline various approaches for getting paleointensity data. We will start by considering thermal remanences and then address depositional ones. (To our knowledge, no one has deliberately attempted paleointensity using other remance types such as chemical or viscous remanences.) In Section 5.13.5 we will briefly consider ways in which these remanences can be compromised by remagnetization processes. Section 5.13.6 considers how paleointensity data can be evaluated as to their reliability, and Section 5.13.7 reviews the published data and database initiatives. We concentrate here on data prior to the Holocene as the Holocene is discussed in 00000. Finally, Section 5.13.8 highlights some of the major issues posed by the paleointensity data.

AU2

5.13.3 Paleointensity with Thermal Remanence

s0015

It appears that ^{b0300}Folgheraiter (1899) was the first to ^{p0035}propose that normalized thermal remanences of pottery be used to study the ancient magnetic field, although ^{b0350}Königsberger and/or Thellier are most often given credit. ^{b0355}Königsberger (1936) described an experimental protocol for ^{b0360}estimating the ratio of natural remance to a laboratory-acquired TRM (**Figure 1(a)**) and assembled data from igneous and metamorphic rocks that spanned from the Pre-Cambrian to the recent (**Figure 1(b)**). He noted that with few exceptions, the ratio $M_{\text{NRM}}/M_{\text{lab}}$ decreased with increasing age, and discussed various possible explanations for the trend, including changing geomagnetic field strength and shaking by earthquakes. His preferred reason for the trend in normalized remance, however, was that magnetized bodies lose their magnetism over time, a phenomenon we now recognize as magnetic viscosity. In fact ^{b0550}Königsberger (1938a, 1938b) believed that the trend in normalized remance could be used to ^{b0555}date rocks. It was ^{b0560}Thellier (1938) who argued

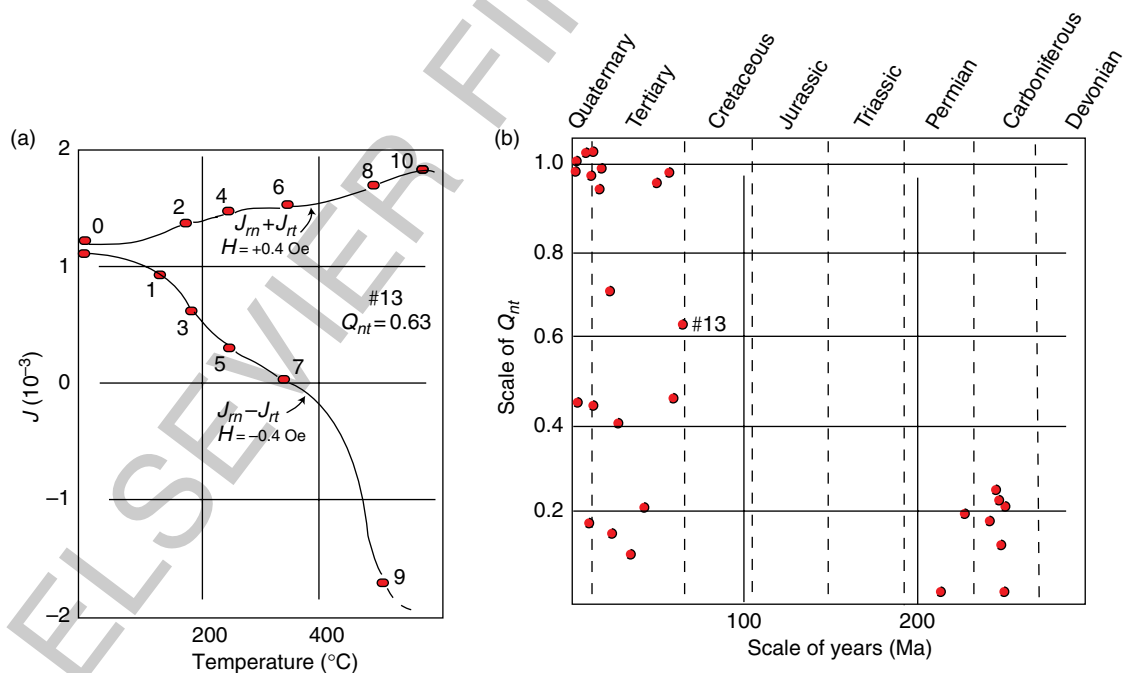


Figure 1 (a) Example of thermal normalization experiment of Königsberger (1938). A specimen is heated to given temperature and cooled in a field of + 0.4 Oe (40 μT) (e.g., step labeled # 1). Then the specimen is heated to same temperature and cooled in field of -0.4 Oe (e.g., step # 2). The two curves can be decomposed to give M_{NRM} and M_{lab} , the ratio of which was termed Q_{nt} by Königsberger. (b) Q_{nt} data for a number of specimens compiled by Königsberger (1938b). The specimen from (a) is labelled # 13. These data were interpreted by Königsberger to reflect the decay of magnetic remanence with time.

AU3,4 f0005

4 Paleointensities

strongly for the use of the thermal remanences of archeological artifacts normalized by laboratory TRMs for studying the past magnetic fields.

p0040 Königsberger's approach was largely empirical; he knew that TRMs were proportional to the magnetic fields in which they were cooled and that remanences tended to decay over time, and he was well aware of the relationship between coercivity and thermal blocking. Nonetheless, he had very few tools at his disposal to discriminate among the myriad possible explanations for his observed trend that the NRM/TRM ratio appeared to decay with increasing age; for example, he did not call on apparent polar wander to explain deviant directions, relying instead on the idea that parts of lava flows tend to cool below their Curie temperatures before they stop moving.

p0045 The theoretical basis for how ancient magnetic fields might be preserved was clarified with the Nobel Prize-winning work of Néel (1949, 1955). Modern theory of TRM is discussed in detail in 00093 (see also h1157 Tauxe (2005) and a recent review by Valet, 2003) but we review only the essential ideas here.

p0050 Briefly, a magnetized rod in the absence of a magnetic field will tend to be magnetized in one of several (often two) 'easy' directions. In order to overcome the intervening energy barrier and get from one easy direction to another, a magnetic particle must have energy sufficient to leap through some intervening 'hard' direction. According to the Boltzmann distribution law, the probability of a given particle having an energy ϵ is proportional to $e^{-\epsilon/kT}$ where k is Boltzmann's constant and T is the temperature in kelvin (yielding thermal energy for the product kT). Therefore, it may be that at a certain time, the magnetic moment may have enough thermal energy to flip the sense of magnetization from one easy axis to another.

p0055 If we had a collection of magnetized particles with some initial statistical alignment of moments giving a net remanence M_0 , the random flipping of magnetic moments from one easy axis to another over time will eventually lead to the case where there is no preferred direction and the net remanence will have decayed to zero. The rate of approach to magnetic equilibrium is determined by the 'relaxation time' which describes the frequency of moments flipping from one easy axis to another.

p0060 Relaxation time according to Néel theory is given by

$$\tau = \frac{1}{C} \exp \frac{[\text{anisotropy energy}]}{[\text{thermal energy}]} = \frac{1}{C} \exp \frac{[Kv]}{[kT]} \quad [2]$$

where C is a frequency factor with a value of something like 10^{10} s^{-1} , v is volume, and K is an 'anisotropy constant'. Equation [2] is sometimes called the 'Néel equation'.

The energy barrier for magnetic particles to flip through a 'hard direction' into the direction of the applied field H (the anisotropy energy) requires less energy than to flip the other way, so relaxation time must be a function of the applied field. The more general equation for relaxation time is given by

$$\tau = \frac{1}{C} \exp \frac{[Kv]}{[kT]} \left[1 - \frac{H}{H_c} \right]^2 \quad [3]$$

where H and H_c are the applied field and the field required to overcome the anisotropy energy and change the moment of the particle (known as the 'coercivity').

From eqn [2] we know that τ is a strong function of temperature. As described by Néel (1955), there is a very sharply defined range of temperatures over which τ increases from geologically short to geologically long timescales (see Dunlop and Özdemir (1997) and Tauxe (2005) for more details). Taking reasonable values for magnetite, the most common magnetic mineral, we can calculate the variation of relaxation time as a function of temperature for a cubic grain of width = 25 nm as shown in **Figure 2**. At room temperature, such a particle has a relaxation time longer than the age of the Earth, while at a few hundred degrees centigrade, the grain has a relaxation time that allows the magnetization to flip frequently between easy axes and can maintain an

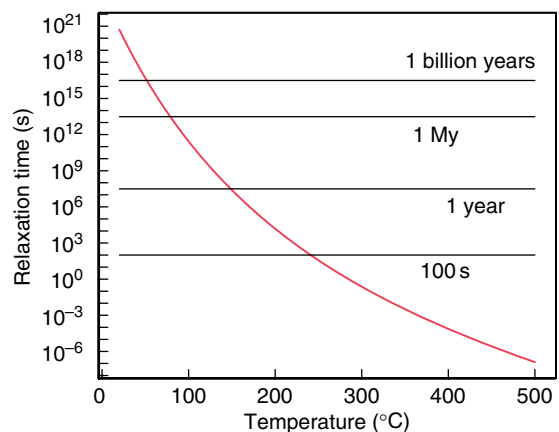


Figure 2 Variation of relaxation time versus temperature for a 25-nm-width cube of magnetite. From Tauxe L (2005) *Lectures in Paleomagnetism*, earthref.org/Magic/Books/Tauxe/2005, San Diego.

f0010

equilibrium with the external field. Such populations will have a slight statistical preference for the direction of the applied field because of the small difference in relaxation time between directions closer to the applied field direction from eqn [3].

The temperature at which T is equal to about 10^2 - 10^3 s is defined as the 'blocking temperature', T_b . At or above the blocking temperature, but below the Curie temperature (the temperature at which all spontaneous magnetization is lost), a population of these grains is in equilibrium with the applied field and are called 'superparamagnetic.' Further cooling increases the relaxation time such that the magnetization is effectively blocked and the rock acquires a thermal remanence.

Consider a lava flow which has just been extruded (see **Figure 3**). First, the molten lava solidifies into rock. While the rock is above the Curie temperature, there is no remanent magnetization; thermal energy dominates the system. As the rock cools through the Curie temperature of its magnetic phase(s), exchange energy (the energy that encourages electronic spins to align with each other) becomes more important and the rock acquires a magnetization. The magnetization, however, is free to track the prevailing magnetic field because anisotropy energy is still less important than the energy encouraging alignment with the magnetic field (the magnetostatic energy). At this high temperature, the magnetic moments in the lava flow are superparamagnetic and tend to flop from one easy direction to another, with a slight statistical bias toward the direction with the minimum angle to the applied field (**Figure 3(c)**). The equilibrium magnetization of superparamagnetic grains is only slightly aligned, and the degree of alignment is a quasi-linear function of the applied

field for low fields like the Earth's. The magnetization approaches saturation at higher fields, depending on the details of the controls on anisotropy energy like shape, size, mineralogy, etc.

5.13.3.1 Linearity Assumption

s

From theory we expect thermal remanences of small p single-domain particles to be approximately linearly related to the applied field for low fields like the Earth's. However, as particle size increases, TRMs can become quite nonlinear even at relatively low fields (see **Figure 4**). Predicted TRM curves with respect to the applied field for randomly oriented populations of single-domain particles ranging in size from 20 to 100nm widths are plotted in **Figure 4(a)**. We calculated these curves assuming quasi-equidimensional grains (1.5:1) and highly elongate grains (10:1). For the elongate grains, the TRM is predicted to be distinctly nonlinear even for the 80 nm particles. (The approximate range of the present Earth's field is shown as the shaded box.) Particles of magnetite larger than about 90 nm will have more complicated remanent states (flower, vortex, multidomain) and will not necessarily follow the predicted curves which are based on single-domain theory.

We note in passing that Kletetschka *et al.* (2006) p have postulated that multidomain particles have TRMs that are highly nonlinear at fields below some threshold value with linear behavior at higher field values. This behavior was observed using a Schonstedt oven, which has very poor field control and we were unable to reproduce the observations in the SIO laboratory which has excellent field control; linear behavior was observed in fields as low as 10 nT (Yongjae Yu, personal communication, 2006).

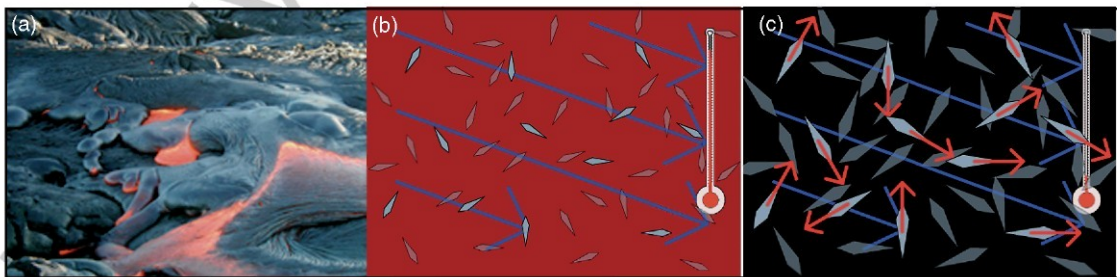


Figure 3 (a) Picture of lava flow. courtesy of Daniel Staudigel. (b) While the lava is still well above the Curie temperature, crystals start to form, but are nonmagnetic. (c) Below the Curie temperature but above the blocking temperature, certain minerals become magnetic, but their moments continually flip among the easy axes with a statistical preference for the applied magnetic field. As the lava cools down, the moments become fixed, preserving a thermal remanence. (a) Courtesy of Daniel Standigel. (b) and (c) Modified from animation of Genevieve Tauxe available at http://magician.ucsd.edu/Lab_tour/movs/TRM.mov. Figure from Tauxe L (2005) *Lectures in Paleomagnetism*, earthref.org/Magic/Books/Tauxe/2005, San Diego.

6 Paleointensities

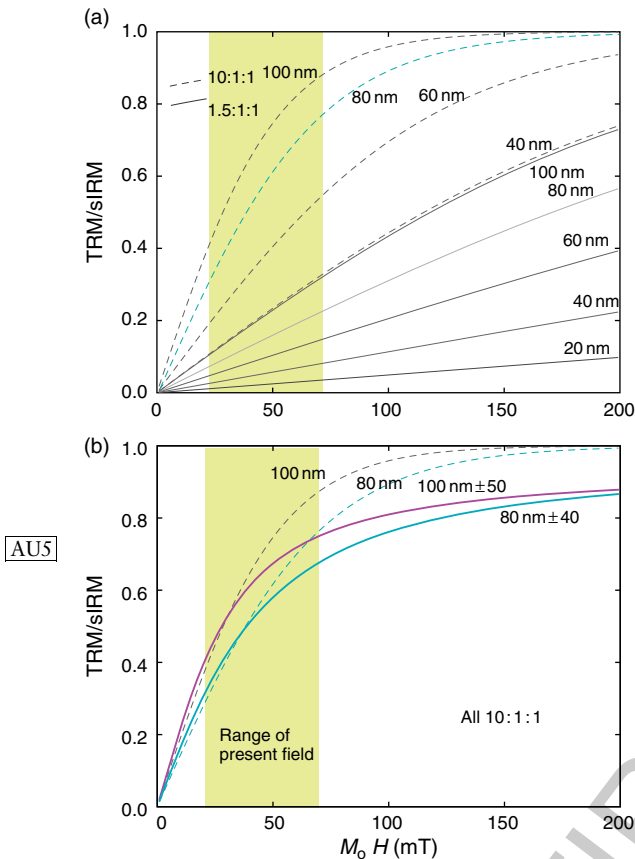


Figure 4 Predicted TRM expressed as a fraction of saturation for various particle sizes and distributions of magnetite. Note the nick point for which the linearity assumption fails is a strong function of particle size, but linearity holds true for equant particles in fields less than a $100 \mu\text{T}$. Strongly elongate particles will behave in a more nonlinear fashion.

Figure 4(b) shows the effect of having a distribution of grain sizes. We calculated curves for populations with normally distributed particle widths (all with 10:1 elongation) with mean widths of 80 and 100 nm, respectively. The effect of the distribution of particle sizes is to depress the TRM below that for a uniform distribution because smaller particles have much lower TRMs at a given field strength that the effect is asymmetric (the difference between 80 and 100 nm width at say $100 \mu\text{T}$ is much less than the difference between 60 and 80 nm at the same field). (Note also, grains smaller than about 20 nm are superparamagnetic at room temperature and do not contribute to the TRM at all, so distributions that include small particles will have suppressed TRMs relative to their theoretical saturation remanences.)

Dunlop and Argyle (1997) discovered strongly nonlinear TRM acquisition behavior in synthetic specimens with mean grain sizes in the single-domain grain range. Although their lab fields were mostly much higher than those of the Earth's field (up to 9 mT !), the results should give practitioners of paleointensity pause. Moreover, Selkin *et al.* (2007) have found nonlinear TRM behavior in natural specimens with single-domain behavior and the nonlinearity is distinct in fields as low as $50 \mu\text{T}$.

The modeling exercises shown in **Figure 4** and the experimental results of Dunlop and Argyle (1997) and Selkin *et al.* (2007) suggest that it would be a wise practice to incorporate a test of TRM linearity into paleointensity experiments as a matter of routine. If the relationship between TRM and applied field is known empirically, then biased results can be corrected to the true ancient intensity.

5.13.3.2 Alteration during Heating

The second assumption for absolute paleointensity determinations is that the laboratory and ancient proportionality constants are the same (i.e., $\alpha_{\text{lab}} = \alpha_{\text{anc}}$ in eqn [1]). Simply measuring the NRM and giving the specimen a total TRM does nothing to test this assumption. For example, alteration of the specimen during heating could change the capacity to acquire thermal remanence and give erroneous results with no way of assessing their validity.

There are several ways of checking the ability of the specimen to acquire thermal remanence in paleointensity experiments. The most commonly used are experiments that employ stepwise replacement of the natural remanence with a laboratory thermal remanence (Königsberg/Thellier-Thellier or KTT family of experiments) and those that compare anhysteretic remanence before and after heating ('Shaw' family of experiments). Other approaches attempt to prevent the alteration from occurring, for example, by heating in controlled atmospheres or vacuum, or by using microwaves to heat just the magnetic phases, leaving the rest of the specimen cool. Another approach is to find materials that are particularly resistant to alteration (e.g., submarine basaltic glass or single plagioclase crystals). Finally, some methods attempt to normalize the remanence with IRM and avoid heating altogether. We will briefly describe each of these in turn, beginning with KTT family of experiments.

s0030 5.13.3.2.1 KTT family of experiments

p0120 Detection of changes in the proportionality constant caused by alteration of the magnetic phases in the rock during heating has been a goal in paleointensity experiments since the earliest days. As we have already seen (Figure 1(a)), Königsberger (1936, 1938a, 1938b) heated up specimens in stages, progressively replacing the natural remanence with partial thermal remanences (pTRMs), an experiment that was elaborated on by Thellier (1938) and Thellier and Thellier (1959). The so-called ‘KTT’ approach is particularly powerful when lower-temperature steps are repeated, to verify directly that the ability to acquire a thermal remanence has not changed.

p0125 The stepwise approach relies on the assumption that pTRMs acquired by cooling between any two temperature steps (e.g., 500°C and 400°C in Figure 5) are independent of those acquired between any other two temperature steps. This assumption is called the ‘Law of independence’ of pTRMs. The approach also assumes that the total TRM is the sum of all the independent pTRMs (see Figure 5), an assumption called the ‘Law of additivity.’

p0130 There are several possible ways to progressively replace the NRM with a pTRM in the laboratory. In the original KTT method (see, e.g., Figure 1(a)), the specimen is heated to some temperature (T_1) and

cooled in the laboratory field B_{lab} . After measurement the combined remanence (what is left of the natural remanence plus the new laboratory pTRM) is

$$M_1 = M_{\text{NRM}} + M_{\text{pTRM}}$$

Then the specimen is heated a second time and cooled upside down (in field $-B_{\text{lab}}$). The second remanence is therefore

$$M_2 = M_{\text{NRM}} - M_{\text{pTRM}}$$

Simple vector subtraction allows the determination of the NRM remaining at each temperature step and the pTRM gained (see Figure 6(a)). These are nowadays plotted against each other in what is usually called an ‘Arai plot’ (Nagata *et al.*, 1963) as in Figure 6(b). The KTT method implicitly assumes that a magnetization acquired by cooling from a given temperature is entirely replaced by reheating to the same temperature (i.e., $T_b = T_{\text{ub}}$), an assumption known as the ‘Law of reciprocity.’

As magnetic shielding improved, more sophisticated approaches were developed. In the most popular paleointensity technique (usually attributed to Coe, 1967), we substitute cooling in zero field for the first heating step. This allows the direct measurement of the NRM remaining at each step. The two equations now are

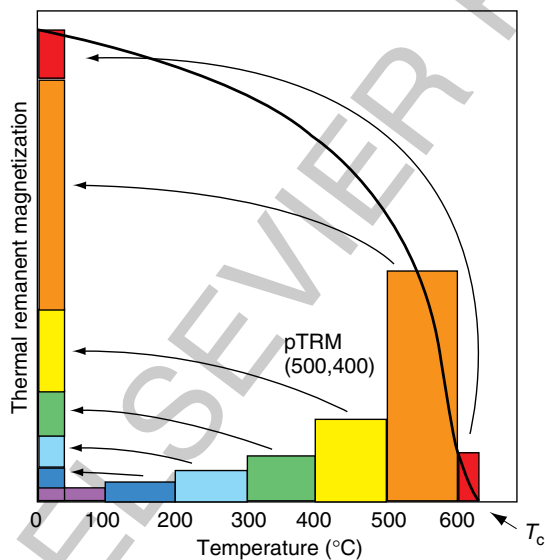
$$M_1 = M_{\text{NRM}}$$

and

$$M_2 = M_{\text{NRM}} + M_{\text{pTRM}}$$

The laboratory M_{pTRM} in this ‘zero-field/in-field’ (or ZI) method is calculated by vector subtraction. Alternatively, the first heating and cooling can be done in the laboratory field and the second in zero field (Aitken *et al.*, 1998; see also Valet *et al.*, 1998), here called the ‘in-field/zero-field’ or (IZ) method.

In all three of these protocols, lower temperature in field cooling steps can be repeated to determine whether the remanence-carrying capacity of the specimen has changed. These steps are called ‘pTRM checks.’ Differences between the first and second M_{pTRM} s at a given temperature indicate a change in capacity for acquiring thermal remanences and are grounds for suspicion or rejection of the data after the onset of such a change. Some have proposed that paleointensity data can be ‘fixed’ even if the pTRM checks show significant alteration (e.g., Valet *et al.*, 1996 and McClelland and Briden, 1996). The argument is that if pTRM checks can be brought back into accordance with the original pTRM



f0025 **Figure 5** Laws of independence and additivity. Partial thermal remanences (pTRMs) acquired by cooling between two temperature steps are independent from one another and sum together to form the total TRM. Figure redrawn from McElhinny MW (1973) Paleomagnetism and Plate Tectonics.

8 Paleointensities

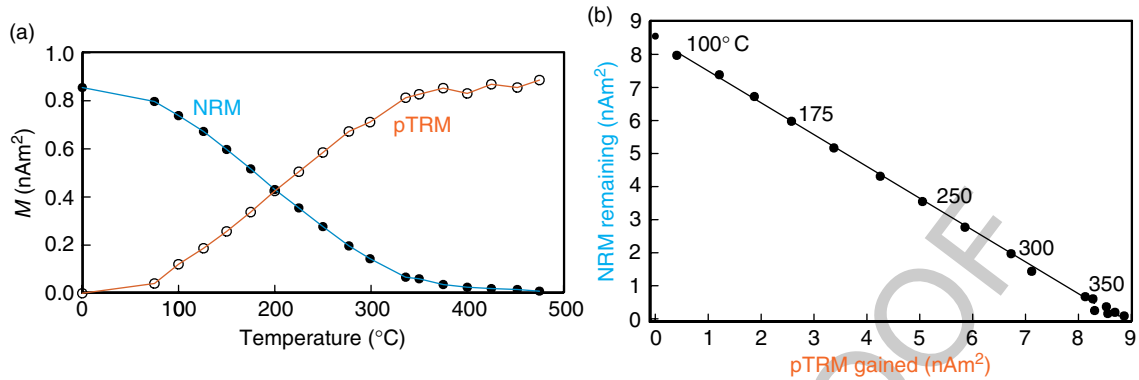


Figure 6 Illustration of the KTT method for determining absolute paleointensity. (a) Thermal demagnetization of NRM shown as filled circles and the laboratory-acquired pTRM shown as open symbols. (b) Plot of NRM component remaining versus pTRM acquired for each temperature step. Figure from Tauxe L (2005) *Lectures in Paleomagnetism*, earthref.org/Magic/Books/Tauxe/2005, San Diego.

measurements using a correction factor, then if that same correction factor is applied to all subsequent pTRM measurements, the effect of the alteration has been accounted for and the data can be considered ‘reliable.’ We consider this correction to carry some risk and ‘corrected’ data should be clearly marked as such.

Despite its huge popularity and widespread use, the approach of progressively replacing the natural remanence with a thermal remanence has several drawbacks. Alteration of the ability to acquire a pTRM is not the only cause for failure of the assumption of equality of α_{lab} and α_{anc} . Both experiment (Bol’shakov and Shcherbakova, 1979; Shcherbakova *et al.*, 2000) and theory (e.g., Dunlop and Xu (1994) and Xu and Dunlop (1994) suggest that the essential assumption of equivalence of blocking and unblocking temperatures may break down for larger particles.

Micromagnetic modeling of hysteresis behavior can shed some light on what might be going on. In simulated hysteresis experiments, particles can be subjected to a large DC applied magnetic field, sufficient to completely saturate them. As the field is lowered, certain particles form vortex structures at some applied field strength (see Figure 7). These vortex structures are destroyed again as the field is ramped back up to saturation. However, the field at which the vortex is destroyed is higher than the field at which it formed. This is the phenomenon responsible for ‘transient hysteresis’ (see Fabian, 2003; Yu and Tauxe, 2004).

One can imagine that something similar to transient hysteresis could occur if we cooled a particle from its Curie temperature, and then heated it back

up again. Just below the Curie temperature, the particle would be in a saturated state (because the magnetization is quite low and the vortex structure is just an attempt by the particle to reduce its external field). As the specimen cools down, the magnetization grows. At some temperature a vortex structure may form. As the specimen is heated back up again, the vortex may well remain stable to higher temperatures than its formation temperature by analogy to the behavior in the simulated hysteresis experiment.

If the particle is large enough to have domain walls in its remanent state, then the scenario is somewhat different and not easily tractable by theory (see 00093). At just below its Curie temperature the particle is at saturation. As the particle cools, domain walls will begin to form at some temperature. The remanent state will have some net remanence, proportional to the applied field for moderate field strengths. As the temperature ramps up again, the walls ‘walk around’ within the particle seeking to minimize the magnetostatic energy and are not destroyed until temperatures very near the Curie temperature.

The fact that blocking and unblocking of remanence occur at different temperatures in some particles means that a pTRM blocked at a given temperature will remain stable to higher temperatures; the unblocking temperature is not equal to the blocking temperature. This means that $\alpha_{\text{lab}} \neq \alpha_{\text{anc}}$ and the key assumptions of the KTT-type methods are not met. The Arai plots may be curved (see Dunlop and Özdemir (1997) for a

AU6

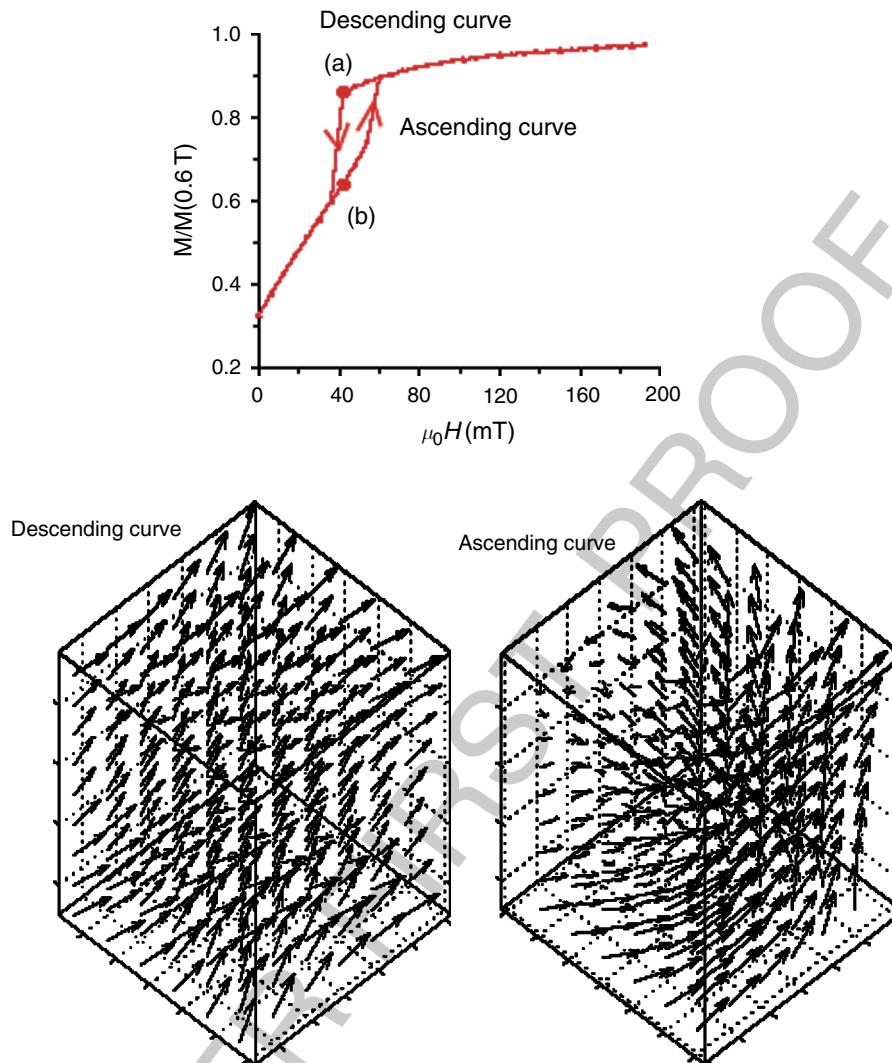


Figure 7 Example of irreversible behavior when particle is brought from a saturated state at high field to zero fields and back up again. A vortex structure forms on the descending curve in the simulated hysteresis loop at the sharp drop in magnetization at about $40 \mu\text{T}$ (labeled 'a'). A snapshot of the micromagnetic state is shown to the lower left. This feature intensifies as the field drops to zero, resulting in a loss of magnetization. When the field ramps back up again, the vortex remains stable well past its formation field (labeled 'b'). A snapshot of the micromagnetic state on the ascending curve is shown in the lower right. The vortex is not destroyed until a higher field, when the loop is closed. Figure modified from Yu and Tauxe L (2004) On the use of magnetic transient hysteresis in paleomagnetism for granulometry. *Geochemistry, Geophysics, Geosystems* 6: Q01H14 (doi: 10.1029/2004GC000839).

more complete discussion) and if any portion of the NRM/TRM data are used instead of the entire temperature spectrum, the result could be biased. For example, the lower-temperature portion might be selected on the grounds that the higher-temperature portion is affected by alteration, or the higher-temperature portion might be selected on the grounds that the lower-temperature portion is affected by viscous remanence. Both of these interpretations would be wrong.

In order to detect inequality of blocking and unblocking and the presence of unremoved portions of the pTRM known as 'high-temperature pTRM tails,' several embellishments to the KTT-type experiment have been proposed and more are on the way. In one modification, a second zero-field step is inserted after the in-field step in the ZI method. This so-called 'pTRM-tail check' (e.g., Riisager and Riisager, 2001) assesses whether the pTRM gained in the laboratory at a given

temperature is completely removed by reheating to the same temperature. If not, the specimen is said to have a ‘pTRM tail,’ a consequence of an inequality of the unblocking temperature T_{ub} and the original blocking temperature T_b in violation of the law of reciprocity and grounds for rejection. A second modification is to alternate between the IZ and ZI procedures (the so-called ‘IZZI’ method first conceived with Agnès Genevey and described by Yu *et al.*, 2004.) The IZZI method is also extremely sensitive to the presence of pTRM tails and may obviate the need for the pTRM-tail check step. An example of a complete IZZI experiment is shown in **Figure 8**.

p0175 There are several other violations of the fundamental assumptions that require additional tests and/or corrections in the paleointensity experiment besides alteration or failure of the law of reciprocity. For example, if the specimen is anisotropic with respect to the acquisition of thermal remanence, the anisotropy tensor must be determined and the intensity corrected (e.g., Fox and Aitken, 1980). The detection and correction for anisotropy can be very important in certain paleomagnetic (and archeomagnetic) materials. The correction involves determining the TRM (or the ARM proxy) anisotropy tensor and matrix multiplication to recover the original

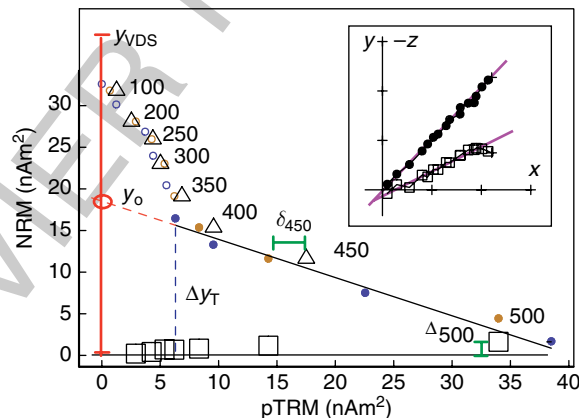
magnetic vector (see Selkin *et al.*, 2000, for a more complete discussion). Moreover, because the approach to equilibrium is a function of time, slower cooling results in a larger TRM, hence differences in cooling rate between the original remanence acquisition and that acquired in the laboratory will lead to erroneous results (e.g., Halgedahl *et al.*, 1980). Compensating for differences in cooling rate is relatively straightforward if the original cooling rate is known and the specimens behave according to single-domain theory. Alternatively, one could take an empirical approach in which the rock is allowed to acquire a pTRM under varying cooling rates (e.g., Genevey and Gallet, 2003), an approach useful for cooling rates of up to a day or two.

5.13.3.2 Shaw family of experiments

s0035

The previous section was devoted to experiments in which detection of nonideal behavior is done by repeating various temperature steps. In this section we will consider an alternative approach, long in use in paleointensity studies, which employs the laboratory proxy anhysteretic remanence (ARM). The so-called ‘Shaw method’ (e.g., Shaw, 1974) is based on ideas first explored by van Zijl *et al.* (1962a, 1962b). In its simplest form, we measure the NRM, then

p0180



f0040 **Figure 8** Data from an IZZI experiment. Circles are the pTRM gained at a particular temperature step versus the NRM remaining. Solid symbols are those included in the slope calculation. Blue (darker) symbols are the in-field–zerofield steps (IZ) and the brown (lighter) symbols are the zerofield–in-field steps (ZI). The triangles are the pTRM checks and the squares are the pTRM tail checks. The difference between the first pTRM check and the original measurement is δ_i as shown by the horizontal bar labeled δ_{450} . The difference between the first NRM measurement and the repeated one (the pTRM tail check) is shown by the vertical bar labeled Δ_{500} . The vector difference sum (VDS) is the sum of all the NRM components (tall vertical bar labeled VDS). The NRM fraction is shown by the vertical dashed bar. The insets are the vector components (x , y , z) of the zero-field steps. The solid symbols are (x , y) pairs and the open symbols are (x , z) pairs. The specimen was unoriented with respect to geographic coordinates. The laboratory field was applied along the z -axis in the in-field steps. Redrawn from Tauxe L and Staudigel H (2004) Strength of the geomagnetic field in the Cretaceous Normal Superchron: New data from submarine basaltic glass of the Troodos Ophiolite. *Geochemistry, Geophysics, Geosystems* 5(2): Q02H06 (doi:10.1029/2003GC000635).

progressively demagnetize the NRM with alternating fields (AF) to establish the coercivity spectrum of the specimen prior to heating. The specimen is then given an anhysteretic remanence (M_{ARM_1}) by subjecting the specimen to progressively higher peak AF which decay in the presence of a small bias field. The use of ARM has been justified because it is in many ways analogous to the original TRM (*see* 00093). M_{ARM_1} is then progressively demagnetized to establish the original relationship between the coercivity spectrum of the M_{NRM} (presumed to be a thermal remanence) and ARM prior to any laboratory heating.

p0185 As with the KTT-type methods, M_{NRM} is normalized by a laboratory thermal remanence. But in the case of the Shaw-type methods, the specimen is given a total TRM, (M_{TRM_1}) which is AF demagnetized as well. Finally, the specimen is given a second ARM (M_{ARM_2}) and demagnetized for the last time.

p0190 The general experiment is shown in **Figures 9(a)** and **9(b)**. If the first and second ARMs do not have the same coercivity spectrum as in **Figure 9(b)**, the coercivity of the specimen has changed and the NRM/TRM ratio is suspect.

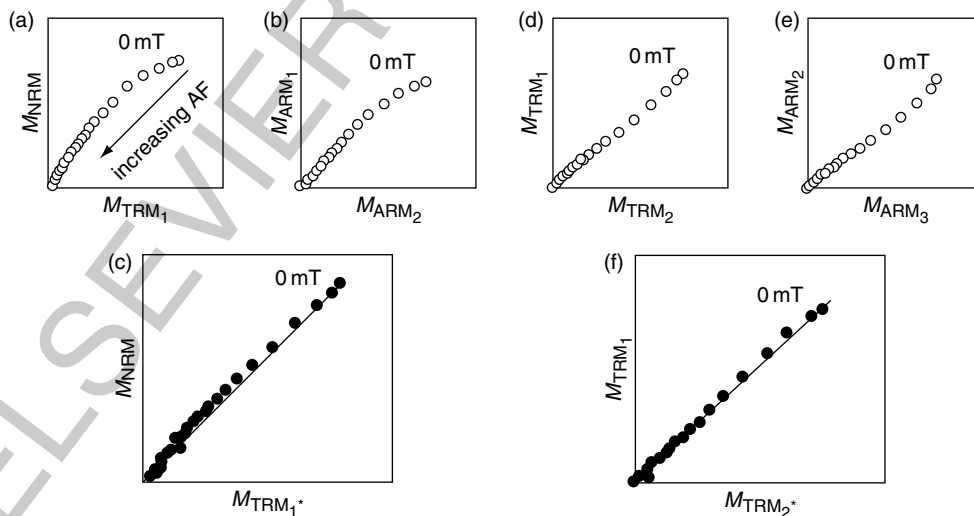
p0195 Rolph and Shaw (1985) suggested that the ratio M_{ARM_1}/M_{ARM_2} at each demagnetizing step be used to 'correct' for the alteration bias of M_{TRM_1} by

$$M_{TRM_1}^* = M_{TRM_1} \frac{M_{ARM_1}}{M_{ARM_2}}$$

So doing can, in some cases, restore linearity between NRM and TRM as shown in **Figure 9(c)**.

^{b1273} Valet and Herrero-Bervera (2000) argued that p0200 only data requiring no correction and utilizing the entire coercivity spectrum should be used. They further pointed out that many specimens are required to lend credibility to a paleointensity experiment. As the former requirement generally leaves very few specimens, Valet and Herrero-Bervera reasoned that a quicker experimental procedure would ultimately result in more acceptable data, hence a better overall outcome, even if the results from many experiments are discarded. To speed up the measurement process, they employed a truncated Shaw method in which no ARMs are imparted, but both the NRM and the laboratory TRM are completely demagnetized using AF. Linearity of the two when plotted as in **Figure 9(a)** is taken as the sole criterion for acceptance.

^{b1260} Tsunakawa and Shaw (1994) suggested that a ten- p0205 dency for chemical alteration could also be detected if the specimen is heated to above the Curie temperature twice, each followed by AF demagnetization (see **Figures 9(d)–9(f)**). During the second heating step, the specimen is left at high temperature for a longer period of time than the first heating step to encourage alteration to continue so that it may be detected by the method. If the slope $M_{TRM_1}/M_{TRM_2}^*$



f0045 **Figure 9** Shaw family of methods (see text). (a) Plot of pairs of NRM and the first TRM for each AF demagnetization step. (b) Plot of pairs of the first ARM and the second ARM for each AF demagnetization step. (c) Plot of pairs of NRM and TRM adjusted by the ratio of ARM_1/ARM_2 for that AF step from (b) (TRM_1^*). (d) Same as (a) but for the first and second TRMs. (e) Same as (a) but for the second and third ARMs. ^{b1595} (f) Same as (c) but for first and second TRM where TRM_2^* is adjusted using ARM_2/ARM_3 ratio from (e). Figure redrawn from Yamamoto *et al.* (2003).

differs by more than the experimental error, the experimental results are rejected.

p0210 The issue of contamination of the remanence by multidomain particles has also been considered in the Shaw-type methods. It has long been known (Ozima *et al.*, 1964) that specimens can lose much of their remanence by cooling to temperatures below about -160°C and warming in zero field. This behavior is generally attributed to magnetocrystalline-dominated remanences cycling through the so-called ‘Verwey transition’ at which the axis of magnetocrystalline anisotropy changes, erasing the magnetic memory of these particles (see, e.g., Dunlop and Özdemir, 1997). This behavior is frequently assumed to occur most readily in multidomain particles, hence their contribution could be minimized if specimens are pretreated to low temperatures (low-temperature demagnetization, or LTD) prior to measurement. Yamamoto *et al.* (2003) and Yamamoto and Tsunakawa (2005) argued that one of the major causes of failure in paleointensity experiments is the effect of multidomain particles, which violate the essential assumption that the original blocking temperature is the same as the laboratory unblocking temperature. They therefore treat specimens to LTD prior to AF demagnetization of each remanence. This ‘LTD–DHT’ method gave improved results for the otherwise disappointingly difficult Hawaiian 1960 lava flow (see, e.g., Tanaka and Kono (1991), Valet and Herrero-Bervera (2000), and Valet (2003)).

p0215 The LTD–DHT experiment assumes that mainly the multidomain particles are affected by the LTD step. However, Carter-Stiglitz *et al.* (2002, 2003) found that single-domain magnetites can and do lose substantial remanence by LTD as well. This behavior means that LTD treatment may demagnetize part of the desired as well as the undesired NRM. It is possible that the SD remanence removed by LTD may be the low-coercivity contribution and unimportant to the paleointensity.

p0220 One other note of caution for all paleointensity experiments using specimens with multidomain grains was raised by Dunlop and Argyle (1997). They showed experimentally that the acquisition of TRM in grains with domain walls was very non-linear, even in low fields like the Earth’s, a problem that no one has addressed yet for multidomain specimens.

p0225 The primary reasons stated for using the Shaw method are that (1) it is faster and (2) alteration is minimized, as the specimen is only heated once

(albeit to a high temperature). The first rationale is no longer persuasive because modern thermal ovens have high capacities and the KTT method is certainly not slower than the Shaw method on a per specimen basis. This is particularly true for the LTD–DHT Shaw method as this experiment takes approximately 8 h to complete per specimen. The second rationale may have some validity. The key features of any good experiment are the built-in tests of the important assumptions.

5.13.3.3 Methods that Minimize Alteration s0040

Several alternative approaches have been proposed which instead of detecting nonideal behavior, such as alteration, attempt to minimize it. These methods include reducing the number of heating steps required (as in the Shaw methods), heating specimens in controlled atmospheres, reducing the time at temperature by, for example, measuring the specimens at elevated temperature, and using microwaves to excite spin moments as opposed to direct thermal heating. Finally, there has been some effort put into finding materials that resist alteration during the heating experiments.

5.13.3.3.1 Reduced number of heating steps s0045

Kono and Ueno (1977) describe in detail a single heating per temperature step method suggested by Kono (1974) whereby the specimen is heated in a laboratory field applied perpendicular to the NRM. M_{pTRM} is gotten by vector subtraction. Reducing the number of heatings can reduce the alteration to some extent. However, this method has only rarely been applied because it can only be used for strictly univectorial NRMs (an assumption that is difficult to test with the data generated by this method) and requires rather delicate positioning of specimens in the furnace or fancy coil systems that generally have a limited region of uniform field, reducing the number of specimens that can be analyzed in a single batch. While pTRM checks are possible with this method, they necessitate additional heating steps and are not generally performed.

A second strategy for reducing the number of heating steps was proposed by Hoffman *et al.* (1989), and modified by Hoffman and Biggin (2005; see also Dekkers and Böhnell, 2006). In the Hoffman–Biggin version, at least five specimens from a given cooling unit are sliced into four specimens each, one of which is dedicated to rock-magnetic analysis. The

remaining specimens (at least 15) are heated a total of five times giving remanence measurements $\mathbf{M}_1 - \mathbf{M}_5$. (Please note that bold face parameters are vectors, while normal text variables are scalars, in this case the magnitudes.) In the first three heating steps, the specimens are treated to increasingly high temperatures (T_0 , T_1 , and T_2) and cooled in zero field. The first heating step ostensibly removes any secondary overprint (e.g., a viscous remanent magnetization (VRM)) and M_1 serves as the baseline for normalizing all subsequent steps so that data from different specimens can be combined. After the three zero-field heating steps, the specimens are heated again to T_2 and cooled with the laboratory field switched on between T_2 and T_0 after which it is switched off. This treatment step gives the pTRM acquired between T_2 and T_0 by vector subtraction of $\mathbf{M}_4 - \mathbf{M}_3$. The fifth heating step is to T_1 followed by a zero-field cooling. This final step serves both to supply the pTRM acquired between T_2 and T_1 by vector subtraction of $\mathbf{M}_4 - \mathbf{M}_5$ and a kind of ‘pseudo pTRM check’ step as explained later.

p0245 In interpreting results, there are two data points from each specimen with estimates for NRM remaining versus pTRM gained, denoted T_1 and T_2 . The NRM remaining part of T_1 and T_2 are ratios M_2/M_1 and M_3/M_1 , respectively. The pTRMs gained at T_1 and T_2 are $|\mathbf{M}_5 - \mathbf{M}_4|/M_1$ and $|\mathbf{M}_4 - \mathbf{M}_3|/M_1$. Because all remanences are normalized by the NRM remaining after zero-field cooling from T_0 (M_1) measured for each specimen, we can combine data from the different specimens together on a single Arai-like plot (see **Figure 10**).

p0250 ^{b0425}Hoffman and Biggin (2005) have several criteria that help screen out ‘unreliable’ data. First, they require that the directions of the zero-field steps trend to the origin on an orthogonal plot and have low scatter. This helps eliminate data for which the characteristic remanence has not been isolated (although three zero-field steps is not generally considered sufficient for this purpose). Second, they require the y -intercept to be between 0.97 and 1.03 and that the correlation coefficient must be ≥ 0.97 . If the T_1 data are displaced from the line connecting the T_2 point and a y -intercept of 1.0, then the specimen may have altered during laboratory heating (e.g., open symbols in **Figure 10**) and can be rejected.

p0255 Noting that the results of the multispecimen procedure when applied to the 1971 Hawaiian flow (shown in **Figure 10**) were significantly different than the known field ($37 \mu\text{T}$), ^{b0425}Hoffman and Biggin (2005) suggested that the data, which are heavily

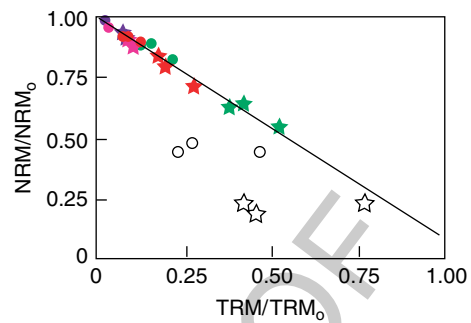


Figure 10 Illustration of multispecimen approach for specimens from the 1971 Hawaiian lava flow. Different colors represent data from different specimens. Different symbols are different heating steps. Open symbols are from specimen that failed initial selection criteria. Best-fit line represents a slope that predicts a ‘paleo’ field of $33 \mu\text{T}$, whereas the actual field was $37 \mu\text{T}$. Redrawn from Hoffman KA and Biggin AJ (2005) A rapid multi-sample approach to the determination of absolute paleointensity. *Journal of Geophysical Research* 110: B12108 (doi:10.1029/2005JB003646).

f0050

influenced by data from a single, low blocking temperature specimen (green symbols in **Figure 10**), could be reweighted to remove the bias. Furthermore, they proposed averaging all the data by accepted specimen, and including the y -intercept in the calculation. These modifications yielded a concordant result with the known field within error. Finally, they redefined many of the parameters typically used in paleointensity experiments (see Section 5.13.6) for use with the multispecimen method.

The primary advantage of the multispecimen ^{b0425} approach put forward by Hoffman and Biggin (2005) is the speed with which measurements can be made, allowing many more specimens to be analyzed. While the method may be fast, it loses multiple pTRM checks and any ability to assess the equivalence of blocking and unblocking. Moreover, the method strongly emphasizes the lower-blocking-temperature portion of the blocking temperature spectrum (especially in the moment-corrected version). This means that the remanence is contaminated by viscous or multidomain remanences leading to a concave downward curve in the Arai plot, the multispecimen result will overestimate the true value of the paleointensity. Finally, it is experimentally very difficult to turn the laboratory field off precisely when the ‘specimen’s’ internal temperature is T_0 because only the oven temperature is known and the specimen temperature lags behind that of the oven by variable and unknown amounts, depending

p0260

on the exact disposition of the specimens in the oven. This bias will lead to scatter and contribute to a systematic bias (the field will always be turned off at too high a temperature, thereby underestimating the pTRM gained).

p0265 On the positive side, the presentation of all specimen data on a single Arai diagram (also proposed by Chauvin *et al.*, 2005) is an interesting modification of the traditional Arai diagram. Plotting all the KTT data from specimens from a given cooling unit on a single Arai diagram allows instant assessment of the reproducibility of data and of course can be done with traditional experimental results.

p0270 Dekkers and Böhlen (2006) argue that their multi-specimen procedure, which employs a single heating/cooling step with the laboratory field oriented parallel to the NRM, can be used on specimens of any domain state. The fundamental assumption of this method is the assumed linearity of pTRM with applied field which the authors claim is independent of domain state. As already discussed, this may not be true, particularly for multidomain grains, which may explain the high degree of scatter in their experimental results.

s0050 **5.13.3.3.2 Use of controlled atmospheres to reduce alteration**

p0275 Alteration during heating is caused by oxidation (or reduction) of the magnetic minerals in the specimen. There have been several strategies to reduce this effect with varying degrees of success. Thellier (1938) tried using vacuum and nitrogen atmospheres. Taylor (1979) developed a technique for paleointensity determination that encapsulated specimens in silica glass. By placing an oxygen 'getter' such as titanium in the evacuated glass tube along with the specimen, he suggested that oxygen fugacity could be maintained and alteration would be reduced. This technique was tested by Sugiura *et al.* (1979) who claimed some improvement in experimental results on lunar glass specimens. More recently, Valet *et al.* (1998) performed paleointensity experiments by heating in argon atmospheres and cooling in nitrogen atmospheres. They reported a significant improvement in their argon results over those performed in air. The difficulty of heating and cooling in vacuum and controlled atmospheres are (1) difficulty in achieving a uniform and reproducible temperature in the oven and (2) unintended oxidation or reduction reactions. It appears that reduction in alteration can be achieved using these techniques, although the

overwhelming majority of paleointensity experiments are done in air.

5.13.3.3.3 Measurement at elevated temperature

s0055

Boyd (1986) suggested that measurements could be made more rapidly if they were measured at elevated temperatures instead of cooling back to room temperature for measurement. The idea was that alteration could be detected immediately and the experiment aborted, before wasting time finishing the entire measurement sequence. This idea was recently warmed up by Le Goff and Gallet (2004) who developed a vibrating sample magnetometer equipped with magnetic field coils which allow the specimen to be measured at temperature and in controlled fields, greatly speeding up the measurement process and, one hopes, reducing the effects of cooling rate and specimen alteration. Preliminary data are promising.

5.13.3.3.4 Use of microwaves for thermal excitation

s0060

Until now we have not concerned ourselves with HOW the magnetic moment of a particular grain flips its moment. Earlier, we mentioned 'thermal energy' and left it at that. But how does thermal energy do the trick?

An external magnetic field generates a torque on the electronic spins, and in isolation, a magnetic moment will respond to the torque in a manner similar in some respects to the way a spinning top responds to gravity: the magnetic moment will precess about the applied field direction, spiraling in and come to a rest parallel to it. Because of the strong exchange or superexchange coupling in magnetic phases, spins tend to be aligned parallel (or antiparallel) to one another and the spiraling is done in a coordinated fashion, with neighboring spins as parallel as possible to one another. This phenomenon is known as a 'spin wave.'

Raising the temperature of a body transmits energy (via 'phonons') to the electronic spins, increasing the amplitude of the spin waves. This magnetic energy is quantized in 'magnons.' In the traditional KTT experiment, the entire specimen is heated and the spin waves are excited to the point that some may flip their moments as described in Section 5.13.3.

As in most kitchens, there are two ways of heating things up: the conventional oven and the microwave oven. In the microwave oven, molecules with certain

vibrational frequencies (e.g., water) are excited by microwaves. These heat up, passing their heat on to the rest of the pizza (or whatever). If the right microwave frequency is chosen, ferromagnetic particles can also be excited directly, inviting the possibility of heating only the magnetic phases, leaving the matrix alone (e.g., Walton *et al.*, 1993). The rationale for developing this method is to reduce the degree of alteration experienced by the specimen because the matrix often remains relatively cool, while the ferromagnetic particles themselves get hot. (The magnons get converted to phonons, thereby transferring the heat from the magnetic particle to the matrix encouraging alteration, but there may be ways of reducing this tendency (see Walton 2004).)

p0305 The same issues of nonlinearity, alteration, reciprocity, anisotropy, and cooling rate differences, etc. arise in the microwave approach as in the thermal approach. Ideally, the same experimental protocol could be carried out with microwave ovens as with thermal ovens. In practice, however, it has proved quite difficult to repeat the same internal temperature, making double (or even quadruple) heatings problematic although progress toward this end may have been made recently (e.g., Böhnell *et al.*, 2003.) It is likely that the issues of reciprocity of blocking and unblocking in the original (thermally blocked) and the laboratory (microwave unblocked) and differences in the rate of blocking and unblocking will remain a problem for some time as they have for thermally blocked remanences. It is also worth echoing the concerns raised by Valet (2003) and LeGoff and Gallet (2004) that the theoretical equivalence between thermal unblocking and microwave unblocking has not yet been explained. In fact, Walton (2005) pointed out that resonance within the magnetic particles is wavelength dependent. This raises the possibility that unblocking may occur in an entirely different manner in microwave processes than in thermal ones (by chords instead of scales to use a musical metaphor) leading to serious questions about the applicability of the method for recovery of paleointensity estimates. Nonetheless, if alteration can be prevented by this method, and the theoretical underpinnings can be worked out, it is worth pursuing.

s0065 5.13.3.3.5 Using materials resistant to alteration

p0310 Another very important approach to the paleointensity problem has been to find and exploit materials that are themselves resistant to alteration. There are

an increasing variety of promising materials, ranging from quenched materials, to single crystals extracted from otherwise alteration-prone rocks, to very slowly cooled plutonic rocks (e.g., layered intrusions). Quenched materials include volcanic glasses (e.g., Pick and Tauxe, 1993), metallurgical slag (e.g., Ben Yosef *et al.*, 2005), and welded tuffs (unpublished results). Single crystals of plagioclase extracted from lava flows (see review by Tarduno *et al.*, 2006) can yield excellent results while the lava flows themselves may be prone to alteration or other nonideal behavior. Parts of layered intrusions (e.g., Selkin *et al.*, 2000b) can also perform extremely well during the paleointensity experiment.

While some articles have called the reliability of submarine basaltic glass results into question (e.g., Heller *et al.*, 2002), Tauxe and Staudigel (2004) and Bowles *et al.* (2005) addressed these concerns in great detail and the reader is referred to those papers and the references therein for a thorough treatment of the subject. In any case, results from alteration-resistant materials are quite promising and more results will be available in the near future.

5.13.3.4 Use of IRM Normalization

Sometimes it is difficult or impossible to heat specimens because they will alter in the atmosphere of the lab, or the material is too precious to be subjected to heating experiments (e.g., lunar samples and some archeological artifacts). Looking again at Figure 4 suggests an alternative for order of magnitude estimates for paleointensity without heating at all. TRM normalized by a saturation remanence (IRM) is quasi-linearly related to the applied field up to some value depending on mineralogy and grain-size population.

Cisowski and Fuller (1986; see also, e.g., Kletetschka *et al.*, 2004) advocated the use of IRM normalization of the NRM of lunar samples to estimate paleointensity. They argued that, especially when both remanences were partially demagnetized using alternating field demagnetization, the NRM:IRM ratio gave order-of-magnitude constraints on absolute paleointensity and reasonable relative paleointensity estimates. Their argument is based on monomineralic suites of rocks with uniform grain size. They further argue optimistically that multidomain contributions can be eliminated by the AF demagnetization.

As can be seen by examining Figure 4, at best only order-of-magnitude estimates for absolute

paleointensity are possible. The monomineralic and uniform grain size constraints make even this unlikely. Finally, the behavior of multidomain TRMs and IRMs is not similar under AF demagnetization, the former being much more stable than the latter. Nonetheless, if magnetic uniformity can be established, it may in fact be useful for establishing relative paleointensity estimates as is done routinely in sedimentary paleointensity studies (see Section 5.13.6). The caveats concerning single-component remanences are still valid and perhaps complete AF demagnetization of the NRM would be better than a single ‘blanket’ demagnetization step. Moreover, we should bear in mind that for larger particles, TRM can be strongly nonlinear with applied field at even relatively low fields (30 μT) according to the experimental results of Dunlop and Argyle (1997; see also figure 1(a) of Kletetschka *et al.* 2006). The problem with the IRM normalization approach is that domain state, linearity of TRM, and nature of the NRM cannot be assessed. The results are therefore difficult to interpret in terms of ancient fields.

s0075 5.13.4 Paleointensity with Depositional Remanences

p0335 Sediments become magnetized in quite a different manner than igneous bodies. Detrital grains are already magnetized, unlike igneous rocks which crystallize above their Curie temperatures. Magnetic particles that can rotate freely will turn into the direction of the applied field which can result in a DRM. Sediments are also subject to post-depositional modification through the action of organisms, compaction, diagenesis, and the acquisition of VRM all of which will affect the magnetization and our ability to tease out the geomagnetic signal. In the following, we will consider the syn-depositional processes of physical alignment of magnetic particles in viscous fluids (giving rise to the primary DRM), then touch on the post-depositional processes important to paleointensity in sedimentary systems.

s0080 5.13.4.1 Physical Alignment of Magnetic Moments in Viscous Fluids

p0340 The theoretical and experimental foundation for using DRM for paleointensities is far less complete than for TRM. Tauxe (1993) reviewed the literature available through 1992 thoroughly and the reader is referred to that paper for background (see also Valet,

2003). In the last decade there have been important contributions to both theory and experiment and we will outline our current understanding here.

Placing a magnetic moment \mathbf{m} in an applied field \mathbf{B} results in a torque Γ on the particle $\Gamma = \mathbf{m} \times \mathbf{B}$. The magnitude of the torque is given by $\Gamma = mB \sin \theta$, where θ is the angle between the moment and the magnetic field vector. This torque is what causes compasses to align themselves with the magnetic field. The torque is opposed by the viscous drag and inertia and the equation of motion governing the approach to alignment is

$$I \frac{d^2\theta}{dt^2} = -\lambda \frac{d\theta}{dt} - mB \sin \theta \quad [4]$$

where λ is the viscosity coefficient opposing the motion of the particle through the fluid and I is the moment of inertia. Nagata (1961) solved this equation by neglecting the inertial term (which is orders of magnitude less important than the other terms) as

$$\tan \frac{\theta}{2} = \tan \frac{\theta_0}{2} e^{(-mBt/\lambda)} \quad [5]$$

where θ_0 is the initial angle between \mathbf{m} and \mathbf{B} . He further showed that by setting $\lambda = 8\pi r^3 \eta$ where r is the particle radius and η to the viscosity of water ($\sim 10^{-3} \text{ kg m}^{-1} \text{ s}^{-1}$), the time constant γ of eqn [5] over which an initial θ_0 is reduced to $1/e$ of its value is

$$\gamma = \frac{\lambda}{mB} = \frac{6\eta}{MB} \quad [6]$$

where M is the volume-normalized magnetization.

Now we must choose values η , M , and B . As noted by many authors since Nagata himself (see recent discussion by Tauxe *et al.*, 2006), plugging in reasonable values for η , M , and B and assuming isolated magnetic particles, the time constant is extremely short (microseconds). The simple theory of unconstrained rotation of magnetic particles in water, therefore, predicts that sediments with isolated magnetic particles should have magnetic moments that are fully aligned and insensitive to changes in magnetic field strength. Yet even from the earliest days of laboratory redeposition experiments (e.g., Johnson *et al.*, 1948; see Figure 11(a)) we have known that depositional remanence (DRM) can have a strong field dependence and that DRMs are generally far less than saturation magnetizations ($\sim 0.1\%$). Much of the research on DRM has focussed on explaining the strong field dependence observed for laboratory redepositional DRM.

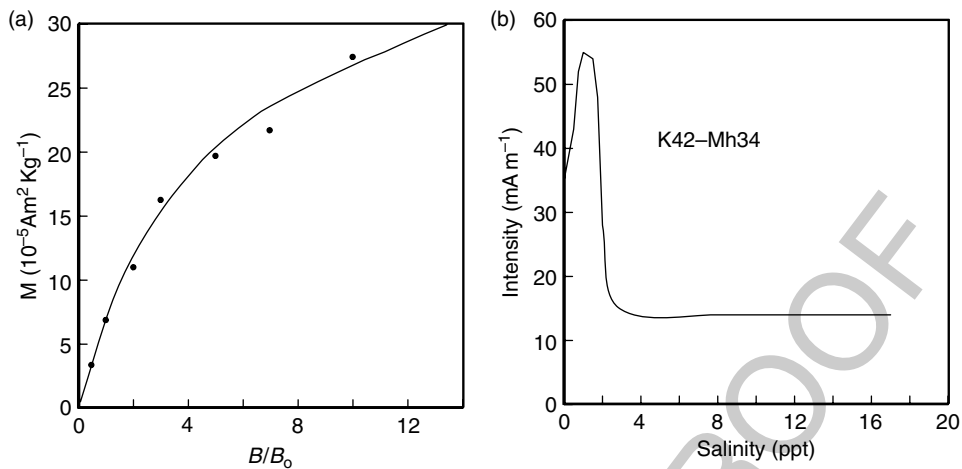


Figure 11 (a) Depositional remanence versus applied field for redeposited glacial varves. B_0 was the field in the lab. Data from Johnson *et al.* (1948). (b) Relationship of DRM intensity and salinity for synthetic sediment composed of a mixture of kaolinite and maghemite. Data of Van Vreumingen, 1993b. Figure from Tauxe L (2005) *Lectures in Paleomagnetism*, earthref.org/Magic/Books/Tauxe/2005, San Diego.

The observation that DRM is usually orders of magnitude less than saturation and that it appears to be sensitive to changing geomagnetic field strengths implies that the time constant of alignment is much longer than predicted by eqn [6]. To increase γ , one can either increase viscosity or decrease magnetization.

One can increase γ by using the viscosity in the sediment column (e.g., Denham and Chave, 1982) instead of the water column. However, something must act to first disrupt the alignment of particles prior to burial, so calling on changes in viscosity is at best an incomplete explanation.

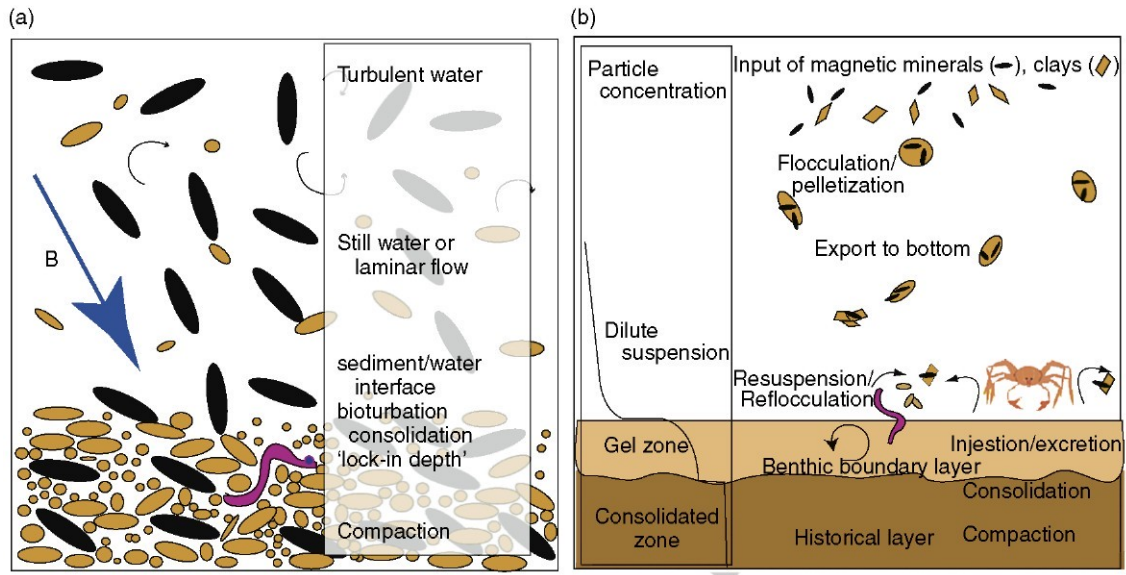
There are several ways of increasing γ by reducing the value of M hence inhibiting the alignment in the first place. For example, one could use values for M much lower than the saturation magnetizations of common magnetic minerals (e.g., Collinson, 1965; Stacey, 1972). However, even using the magnetization of hematite, which is two orders of magnitude lower than magnetite, results in a time constant of alignment that is still less than a second.

There are two mechanisms by which the time constant of alignment can be reduced which account for experimental results of laboratory redeposition experiments: Brownian motion and flocculation. Collinson (1965) called on Brownian motion to disrupt the magnetic moments by analogy to paramagnetic gases. Reasonable parameter assumptions suggest that particles smaller than about 100 nm will be affected by Brownian motion suggesting a possible role in DRM

of isolated magnetite grains free to rotate in water. Furthermore, Yoshida and Katsura (1985) presented experiments on the magnetization of suspensions in response to applied fields that were entirely consistent with a Brownian motion model. Flocculation was fingered by Shcherbakov and Shcherbakova (1983) (see also Katari and Bloxham, 2001) who noted that in saline environments, sedimentary particles tend to flocculate and that isolated magnetic particles would be highly unlikely. When magnetic moments are attached to nonmagnetic 'fluff' it is the net magnetization of the floc that must be used in eqn [6], that is, much smaller than the magnetization of the magnetic mineral alone.

The role of water chemistry (e.g., pH and salinity) has been investigated by several authors since the early 1990s (Lu *et al.*, 1990; van Vreumingen, 1993a, 1993b; Katari and Tauxe, 2000; and Tauxe *et al.*, 2006). In Figure 11(b) we replot data from one of the van Vreumingen experiments. The data were obtained by depositing a synthetic mixture of kaolinite, illite, and maghemite under various conditions of salinity. There is an intriguing increase in intensity with small amounts of NaCl followed by a dramatic decrease in intensity which stabilizes for salinities greater than about 4 ppt.

Both the increase and the decrease can be explained in terms of Brownian motion and flocculation, which is encouraged by increasing salinity. The initial increase in intensity with small amounts of NaCl could be the result of the maghemite particles



f0060 **Figure 12** (a) Schematic drawing of traditional view of the journey of magnetic particles from the water column to burial in a nonflocculating (freshwater) environment. Magnetic particles are black. Redrawn from Tauxe, 1993. (b) View of depositional remanence in a flocculating (marine) environment. Redrawn from Tauxe *et al.* (2006).
 AUZ

adhering to the clay particles, increasing viscous drag, hence reducing the effect of Brownian motion. The subsequent decrease in intensity with higher salinities could be caused by building composite flocs with decreased net moments, hence lowering the time constant of alignment. The decrease in net moment with increasing flocculation was also supported by the redeposition experiments of Lu *et al.* (1990), Katari and Tauxe (2000), and Tauxe *et al.* (2006).

There are therefore two completely different systems when discussing DRM: ones in which magnetic particles remain isolated (e.g. freshwater lakes; see **Figure 12 (a)**) and ones in which flocculation plays a role (e.g., marine environments; see **Figure 12(b)**). For the case of magnetite in freshwater, Brownian motion may well be the dominant control on DRM efficiency. In saline waters, the most important control on DRM is the size of the flocs in which the magnetic particles are embedded. In the following we briefly explore these two very different environments.

s0085 5.13.4.1.1 Nonflocculating environments

p0390 In freshwater we expect to have isolated magnetic particles whose magnetic moments would presumably be a saturation remanence. The overwhelming majority of laboratory redeposition experiments have been done in deionized water (e.g., Kent, 1973; Lovlie, 1974), hence are in the nonflocculating

regime. However, only a few studies have attempted to model DRM using a quantitative theory based on Brownian motion (e.g., Collinson, 1965; King and Rees, 1966; Stacey, 1972; Yoshida and Katsura, 1985). Here we outline the theory to investigate the behavior of DRM that would be expected from a Brownian motion mechanism (henceforth a Brownian remanent magnetization or BRM).

To estimate the size of particles effected by p0395 Brownian motion, Collinson used the equation

$$\frac{1}{2} mB\phi^2 = \frac{1}{2} kT \quad [7]$$

where $\langle f \rangle$ is the Brownian deflection about the applied field direction (in radians), k is Boltzmann's constant ($1.38 \times 10^{-23} \text{ J K}^{-1}$), and T is the temperature in kelvin. The effect of viscous drag on particles may also be important when the magnetic moments of the particles are low (see Coffey *et al.* (1996) for a complete derivation), for which we have

$$\frac{\phi^2}{\delta} = \frac{kT}{4\pi\eta r^3}$$

where δ is the time span of observation (say, 1 s). According to this relationship, weakly magnetized particles smaller than about a micron will be strongly effected by Brownian motion. Particles that have a substantial magnetic moment, however, will be partially stabilized (according to eqn [7]) and might remain unaffected by Brownian motion to smaller

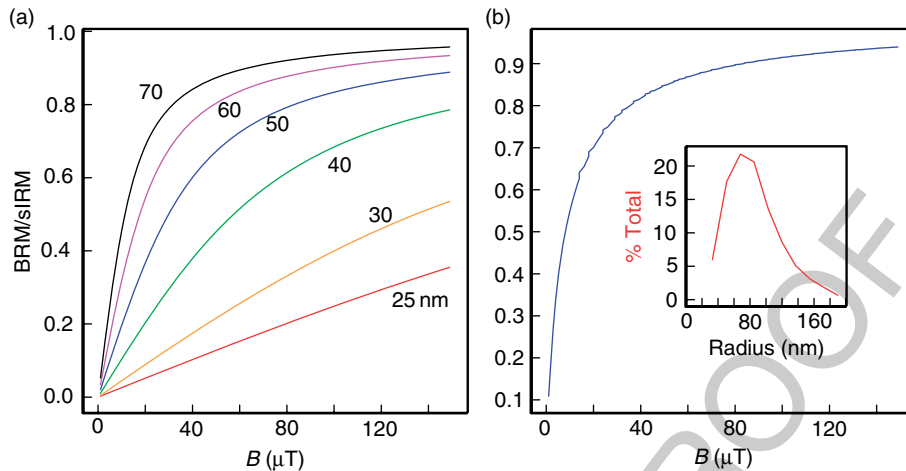


Figure 13 (a) Numerical simulations of Brownian remanent magnetization (BRM) for various sizes of magnetite. (b) BRM simulated for distribution of particle sizes of magnetite shown in inset.

particle sizes (e.g., $0.1 \mu\text{m}$). In the case of isolated particles of magnetite, therefore, we should use eqn [7] and BRM should follow the Langevin equation for paramagnetic gases, that is,

$$\frac{\text{BRM}}{\text{sIRM}} = \coth\left(\frac{mB}{kT}\right) - \frac{kT}{mB} \quad [8]$$

To get an idea of how BRMs would behave, we first find m from $M(r)$ (here we use the results from micromagnetic modeling of Tauxe *et al.* (2002)). Then, we evaluate eqn [8] as a function of B for a given particle size (see **Figure 13(a)**). We can also assume any distribution of particle sizes (e.g., that shown as the inset to **Figure 13(b)**), and predict BRM/sIRM for the distribution (blue line in **Figure 13(b)**). It is interesting to note that BRMs are almost never linear with the applied field unless the particle sizes are very small.

BRMs would be fixed when the particles are no longer free to move. The fixing of this magnetization presumably occurs during consolidation, at a depth (known as the lock-in depth) where the porosity of the sediment reduces to the point that the particles are pinned (see **Figure 12(a)**). Below that, the magnetization may be further affected by compaction (e.g., Deamer and Kodama, 1990) and diagenesis (e.g., Roberts, 1995).

s0090 5.13.4.1.2 Flocculating environments

p0405 DRM in flocculating environments (saline waters) has been studied in the laboratory by Lu *et al.* (1990), van Vreumingen (1993a, 1993b), Katari and Tauxe (2000), and Tauxe *et al.* (2006), and

theoretically by Shcherbakov and Shcherbakova (1983), Katari and Bloxham (2001), and Tauxe *et al.* (2006). We summarize the current state of the theory in the following.

Katari and Bloxham (2001) rearranged eqn [5] by replacing time with settling distance l , a parameter that is more easily measurable in the laboratory using the empirical relationship of settling velocity to radius of Gibbs (1985). They got

$$\tan \frac{\theta}{2} = \tan \frac{\theta_0}{2} \exp(-mBl/8.8\pi\eta r^{3.78}) \quad [9]$$

As in Nagata (1961), a magnetic moment \mathbf{m} making an initial angle θ_0 with the applied field \mathbf{B} will begin to turn toward the direction of the magnetic field. After time t (or equivalently, settling distance, l), the moment will make an angle θ with the field. Tauxe *et al.* (2006) showed that the new coordinates of \mathbf{m} (x', y', z') are related to the initial values (x_0, y_0, z_0) by

$$x' = \cos \theta \cdot y' = \sqrt{\frac{1 - x_0^2}{1 + z_0^2/y_0^2}} \quad \text{and} \quad z' = y' \frac{z_0}{y_0} \quad [10]$$

From the preceding, we can make a simple numerical model to predict the DRM for an initially randomly oriented assemblage of magnetic moments, after settling through l . For an initial set of simulations, Tauxe *et al.* (2006) followed Katari and Bloxham, using the viscosity of water, m of 5 fAm^2 (where femto (f) = 10^{-15}), and a settling length l of 0.2 m . **Figures 14(a)** and **14(b)**, show the predicted DRM curves as a function of magnetic field and radius. We see that particles, in general, are either nearly aligned with the magnetic field, or nearly random with only a

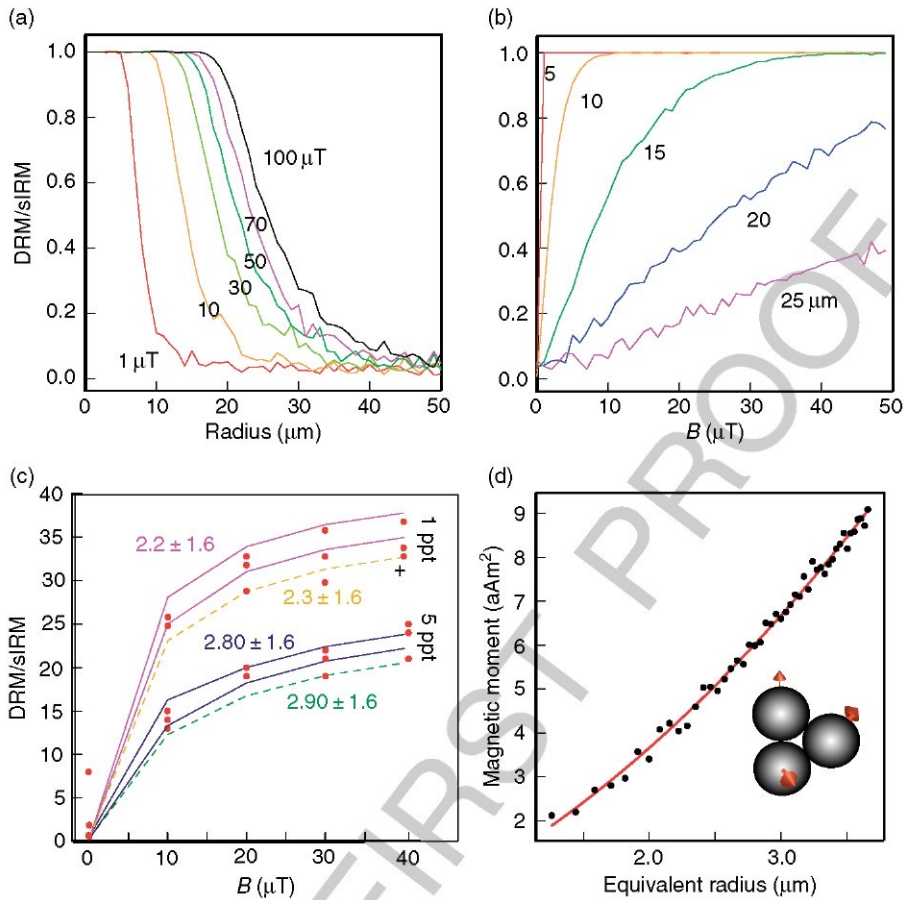


Figure 14 (a) Results of numerical experiments of the flocculation model using the parameters: $\lambda = 0.2$ m and the viscosity of water. M/M_0 is the DRM expressed as a fraction of saturation, holding m constant and varying B . For a given field strength, particles are either at saturation or randomly oriented, except for within a very narrow size range. (b) Same as (a) but plotted versus applied field (B) in a flocculating environment. The assumed mean and standard deviations of truncated log-normal distributions for floc radii are shown in the legends and are indicated using the different line styles in the figure. (c) Results of settling experiments as a function of field (B) in a flocculating environment. The assumed mean and standard deviations of truncated log-normal distributions for floc radii are shown in the legends and are indicated using the different line styles in the figure. (d) m versus equivalent radius for composite flocs as in inset. Line given by polynomial fit $m = ar^2 + br + c$, where $a = 3.61 \times 10^{-7}$, $b = 1.2 \times 10^{-12}$, $c = -2.1 \times 10^{-19}$ is based on a fundamental floc of 1 mm with a measured saturation remanence. Figures redrawn from Tauxe et al., 2006.

narrow band of radii in between the two states for a given value of B . Increasing B increases the size for which particles can rotate into the field, giving rise to the dependence of DRM intensity on applied field strength. Taking a given particle size and predicting DRM as a function of the applied field (Figure 14(b)) predicts the opposite behavior for DRM than the Brownian motion theory (Figure 13) in that the larger the floc size, the weaker the DRM and also the more linear with respect to the applied field. The theories of Brownian motion, which predicts low DRM efficiency for the smallest particles increasing to near saturation values for particles around 0.1 mm and composite flocs theory, which predicts decreased DRM efficiency for larger floc sizes can therefore

explain the experimental data of van Vreumingen 1993 shown in Figure 11 (b).

The flocculation model of DRM makes specific predictions which can in principle be tested if the model parameters can be estimated or controlled. Tauxe et al. (2006) tested the theory by dispersing natural sediments in settling tubes to which varying amounts of NaCl had been introduced. Prior to dispersal, each specimen of mud was given a saturation IRM. They measured DRM as a function of floc size (increasing salinity enhanced floc size) and the applied field (see Figure 14(c)). In general their results suggest the following: (1) The higher the NaCl concentration, the lower the net moment (confirming previously published efforts); (2) the higher

the salinity, the faster the particles settled (a well-known phenomenon in coastal environments, see, e.g., Winterwerp and van Kesteren, 2004); (3) the higher the applied field, the higher the DRM, although a saturation DRM appears to be nearly achieved in the 1 ppt NaCl set of tubes by 30 μ T (Figures 14(c) and 4) the relationship of DRM to B was far from linear with applied field in all cases. Moreover, in the Katari and Bloxham (2001) model of DRM, a single magnetic particle is assumed to be embedded in each floc; hence the magnetization of the flocs is independent of floc size. In this view, the saturation DRM (sDRM) should equal the sum of all the individual flocs, that is, sIRM in the case of these experiments. sDRM was well below sIRM in all experiments (see, e.g., Figure 14(c)) and no Katari–Bloxham-type model can account for the results.

p0420 ^{b0475} Tauxe *et al.* (2006) modified the simple theory of Katari and Bloxham (2001) by incorporating the understanding of flocculation from the extensive literature on the subject. In nature, flocs are formed by coalescing of ‘fundamental flocs’ into composite flocs. Each fundamental floc would have tiny magnetic particles adhering to them and would have the sIRM imparted prior to settling. As the composite flocs grow by chance encounters with other flocs, the net moment of the composite floc will be the vector sum of the moments of the fundamental flocs (see, e.g., inset to Figure 14(d)). They modeled the magnetization of flocs as a function of floc radius (assuming a quasi-spherical shape) through Monte Carlo simulation, an example of which is shown in Figure 14(d). By choosing reasonable log-normal distributions of flocs for settling tube, their model predicts the curves shown in Figure 14(c), in excellent agreement with the redeposition data.

s0095 5.13.4.2 PostDepositional Processes

p0425 It appears that by combining the effects of Brownian motion for nonflocculating environments and a composite floc model for flocculating environments we are on the verge of a quantitative physical theory that can account for the acquisition of depositional remanence near the sediment/water interface. At some point after deposition, this DRM will be fixed because no further physical rotation of the magnetic particles in response to the geomagnetic field is possible. The depth at which moments are pinned is called the lock-in depth. If lock-in depth is selective and some magnetic particles would be fixed while others remain free, there will be some depth (time)

interval over which remanence is fixed, resulting in some temporal smoothing of the geomagnetic signal. Physical rotation of particles in response to compaction can also change the magnetic remanence. Other processes not involving postdepositional physical rotation of magnetic particles, including ‘viscous’ (in the sense of magnetic viscosity) remagnetization and diagenetic alteration resulting in a chemical remanence, may also modify the DRM. All of these processes influence the intensity of remanence and hamper our efforts to decipher the original geomagnetic signal. We will briefly discuss the effects specific to sediments in the following; chemical alteration and viscous remagnetization effect of both TRMs and DRMs will be addressed in Section 5.13.5.

The ‘standard model’ of depositional remanence p0430 (DRM) acquisition was articulated, for example, by Verosub (1977) and Tauxe (1993). In this view, detrital remanence is acquired by locking in different grains over a range of depths. This phased lock-in leads to both significant smoothing and to an offset between the sediment/water interface and the fixing of the DRM. Many practitioners of paleomagnetism still adhere to this concept of DRM which stems from the early laboratory redeposition experiments which were carried out under nonflocculating conditions (see Section 5.13.4.1). Several studies on natural marine sediments (e.g., deMenocal *et al.*, 1990; Lund and Keigwin, 1994; and Kent and Schneider, 1995; see also Channell *et al.*, 2004) are frequently cited which suggest a high degree of mobility of magnetic particles after deposition resulting in sedimentary smoothing and delayed remanence acquisition.

The work of deMenocal *et al.* (1990) called for a p0435 deep lock-in depth of up to \sim 16 cm for marine sediments based on a compilation of deep sea sediment records with oxygen isotopes and the Matuyama–Brunhes boundary (MBB). However, Tauxe *et al.* (1996) updated the compilation with twice the number of records and, using the same logic, concluded that, on average, the magnetization is recorded within the top few centimeters.

Several papers have revived the deep lock-in p0440 debate (e.g., Bleil and von Dobeneck, 1999; and Channell *et al.*, 2004). The former used a complicated lock-in model to explain results not observed anywhere else (substantial reversely magnetized intervals in apparently Late Brunhes Age equatorial sediments). The latter noted that in North Atlantic drift deposits, the mid-point of the MBB is ‘younger’ isotopically than records with lower sedimentation rates, implying a deep lock-in. However, drift

deposits by nature collect sediments from a large catchment area. A particular bit of plankton from the surface waters of the North Atlantic will be transported along the bottom for some time before it finds a permanent home in the drift. The age offset between the isotopic (acquired at the surface) and magnetic ages (acquired at the final point of deposition) obviates the need for a deep lock-in depth.

p0445 The most-quoted examples of significant smoothing in natural sediments are those of Lund and Keigwin (1994) and Kent and Schneider (1995). On close examination, the evidence is weak. Lund and Keigwin (1994) postulated that the PSV record of Bermuda Rise, western North Atlantic Ocean was systematically subdued with respect to the PSV recorded in Lake St. Croix stemming from the observed difference in sediment accumulation rate, the Lake St. Croix record having been deposited at a rate several times that of the Bermuda Rise record. They suggested that smoothing the Lake St. Croix data with a 10 or 20 cm moving average window reproduced the Bermuda Rise data with high-frequency features smoothed out, and the amplitude of variation significantly reduced. However, they ignored the age constraints present in the original St. Croix record. Tauxe *et al.* (2006) showed that a substantially better fit of the Bermuda data could be achieved when the available age constraints are used and no smoothing was required by the data.

p0450 The study of Kent and Schneider (1995) showed three records of relative paleointensity across the MBB and interpreted these in terms of sedimentary smoothing. These records came from low and moderate sediment accumulation rates. Hartl and Tauxe (1996) augmented the database of peri-MBB relative paleointensity records using an additional ten records obtained from a wide range of sediment accumulation rates and showed that the single low-sedimentation-rate core of Kent and Schneider (V16–58) most probably had a poorly constrained timescale. Once again, little, if any, smoothing of sedimentary paleointensity records is required.

p0455 As sediments lose water and consolidate, compaction can have a strong effect on DRM intensity (e.g., Anson and Kodama, 1987). Consolidation is a continuous process starting from the sediment–water interface when sedimentary particles first gel (see, e.g., **Figure 12(b)**) and continuing until the sediment is completely compacted, perhaps as deep as hundreds of meters. The effect on magnetic remanence

depends on volume loss during compaction which depends largely on clay content, so clay-rich sediments will have the largest effect.

5.13.4.3 Note on Aeolian Deposits

s0100

The theoretical and experimental foundations of relative paleointensity studies have all been done on water-borne sedimentary deposits. Nonetheless it is clear that aeolian sediments, in particular, loess, can retain a natural remanence that appears to record the direction of the geomagnetic field (e.g., Heller and Liu, 1982). Details of how the geomagnetic field is impressed on loess deposits are not well known, but mechanisms must include viscous remanence, pedogenic modification (chemical remanence), and perhaps also a remanence acquired at deposition (see e.g., Spassov *et al.*, 2003 for discussion). What controls the intensity of remanence acquired during deposition of wind-blown dust is unknown, yet there have been several attempts to use the normalized remanence in loess as a proxy for geomagnetic intensity variations (e.g., Zhu *et al.*, 1994; Pan *et al.*, 2001; and Liu *et al.*, 2005). These studies rely heavily on the theoretical and experimental work developed for water-lain sediments (see also Spassov *et al.*, 2003); theoretical and experimental efforts must be carried out for the mechanism involved in remanence acquisition in loess.

AU9

5.13.4.4 Normalization

s0105

Until now we have considered only how magnetic moments behave when placed in a magnetic field and are allowed to rotate freely. Paleointensity studies in sediments make the *a priori* assumption that DRM is quasi-linear with the applied field (although as we have seen in the section on DRM theory that is only true under certain circumstances). However, we have not yet considered the effect of changing the magnetic content of the sediment which of course will have a profound effect on the intensity of the remanence. Such changes must be compensated for through some sort of normalization process (see e.g., Kent, 1982). Methods of normalization were reviewed thoroughly by King *et al.* (1983) and Tauxe (1993) but there have been a few contributions to the subject published since. Here we briefly summarize the most commonly used methods of normalization.

Most studies use some easily measured bulk magnetic parameter such as saturation remanence (Johnson *et al.*, 1948), magnetic susceptibility (χ , Harrison, 1966) or anhysteretic remanence

p0470

(^{b0460}Johnson *et al.*, 1975) which will compensate for changes in concentration of the magnetic minerals in a relatively crude way. ^{b0655}Levi and Banerjee (1976) proposed a more sophisticated approach in which the natural remanence was partially demagnetized as was the anhysteretic remanent normalizer to ensure that the same coercivity fraction was used to normalize the remanence as was carrying the natural remanence. Following up on this line of reasoning, ^{b1300}Tauxe *et al.* (1995) suggested that the natural remanence be normalized by anhysteretic remanence in a manner similar to the KTT experiments for thermal remanences using a technique known as ‘pseudo-Thellier’ normalization. ^{b0515}King *et al.* (1983) reminded us that anhysteretic remanence itself is a strong function of concentration with higher magnetite concentrations being less efficient at ARM acquisition than lower concentrations. As a result, zones with varying concentrations will be normalized differently (in effect, different α s in eqn [1] and violate the fundamental assumptions of the method. More recently, ^{b0095}Brachfeld and Banerjee (2000) proposed a secondary correction for normalized intensity that attempted to remove some of the nonlinear effects of the normalization process. ^{b1215}Tauxe and Wu (1990) argued that if the power spectrum of the normalizer was coherent with the normalized remanence, the normalization process was insufficient. ^{b0210}Constable *et al.* (1998) expanded on this idea, suggesting that the normalizer most coherent with the remanence should be used.

^{p0475} One of the important implications of the composite floc model of DRM of Tauxe *et al.* (2006) described in Section 5.13.4.1 is that current methods of normalizing sedimentary records for changes in magnetic grain size and concentration do not account for changes in floc size, hence will be only partially effective in isolating the geomagnetic contribution to changes in DRM. This has practical implications in the role of climate in influencing relative paleointensity records. For example, changes in the clay content could well lead to differences in flocculation, which in turn could influence paleointensity with no observable change in the magnetic mineralogy apart from a change in concentration. Other ‘stealth’ influences could be miniscule changes in salinity of lakes, which could result in profound changes in the paleointensity recorded, with no means of detecting it. However, in stable environments with only small changes in magnetic mineralogy and concentration, we can only hope that the normalization procedures chosen will give records that are reasonably linear with the applied field.

5.13.5 Remagnetization

s0110

Theoretical treatment of how rocks get magnetized ^{p0480} and how that magnetization might be used for paleointensity studies assume that the remanence was blocked either thermally (Section 5.13.3) or depositionally (Section 5.13.4). Yet almost no natural remanence remains completely unchanged for long. Thermodynamics teaches us that all substances out of equilibrium with their environments will approach equilibrium as the energy available permits. Magnetic particles out of equilibrium with the magnetic field in which they sit are subject to magnetic viscosity. If they are out of chemical equilibrium, they will alter chemically. The former results in the acquisition of a viscous remanence and the latter a chemical one. These are discussed in more detail in 00093. We will briefly describe their importance to paleointensity in the following.

5.13.5.1 Magnetic Viscosity

s0115

Returning to **Figure 2**, we see that magnetic ^{p0485} moments can respond to external fields even if the magnetic crystal itself is fixed on timescales determined by the magnetic relaxation time τ . When the relaxation time is short relative to the time span of observation, the magnetization is in equilibrium with the external field and the particles are called ‘superparamagnetic.’ This means that magnetic particles have sufficient thermal energy to overcome intervening energy barriers and flip their magnetic moments from one easy direction to another. The energy barrier is in part controlled by the external field, with a lower threshold into the direction of the applied field than out of it. Therefore magnetic moments will tend to ‘pool’ in the direction of the applied field.

The magnetization that is acquired in this isochemical, isothermal fashion is termed ‘viscous remanent magnetization’ or VRM. ^{p0490} With time, more and more grains will have sufficient thermal energy to overcome anisotropy energy barriers and flip their magnetizations to an angle more in alignment with the external field. The lower the value of τ , the quicker the approach to equilibrium.

According to eqn [2], relaxation time varies with ^{p0495} external factors such as temperature (as seen in **Figure 2**) and applied field B and with factors specific to the magnetic particle such as volume and its intrinsic resistance to changing external fields reflected in its anisotropy constant K . In any natural

substance, there will be a range of values for τ that could span from seconds (or less) to billions of years. It is interesting to note that a TRM is in effect the equilibrium magnetization (see, e.g., Yu and Tauxe, 2006) and TRMs will only be subject to magnetic viscosity if the field changes. DRMs, however, are typically one or two orders of magnitude less than the TRM that would be acquired in the same field, hence are almost never in equilibrium and therefore will nearly always be subject to viscous remagnetization, depending on the spectrum of τ values (see Kok and Tauxe, 1996a for discussion).

s0120 5.13.5.2 Chemical Alteration

p0500 Geological materials form in one environment (e.g., extruding red hot from the mouth of a volcano!) and wind up in quite different environments. Inevitably, they will break down as part of the rock cycle. Magnetic minerals are no exception and growth, alteration and dissolution of magnetic minerals change the original remanence. The magnetization that is fixed by growth or alteration of magnetic minerals is termed chemical remanent magnetization (CRM) and while this too is controlled in part by the external magnetic field, the theory of how to normalize CRM to retrieve the geomagnetic signal has never been properly developed. In general, paleointensity studies strive to recognize CRMs and exclude such remanences from interpretation.

s0125 5.13.6 Evaluating Paleointensity Data

s0130 5.13.6.1 Thermally blocked remanences

p0505 A well done paleointensity experiment allows us to test (1) whether the NRM was a single-component magnetization, (2) whether alteration occurred during laboratory reheating, and (3) whether blocking and unblocking were reciprocal, and (4) whether the TRM is a linear function of the applied field. Parameters can be calculated to provide measures of overall quality (scatter about the best-fit line, distribution of temperature steps, fraction of the NRM, etc.) of a given experiment. Some useful parameters are listed for convenience in **Table 1**.

s0135 5.13.6.2 Depositional Remanences

p0510 How can sedimentary relative paleointensity data be judged? Here are some thoughts:

1. The natural remanence must be carried by a detrital phase of high magnetic stability. Furthermore, the portion of the natural remanent vector used for paleointensity should be a single, well-defined component of magnetization. The nature of the NRM can be checked with progressive demagnetization using AF and thermal techniques. Supplementary information from hysteresis and rock-magnetic experiments can also be useful.
2. The detrital remanence must be an excellent recorder of the geomagnetic field, exhibit no inclination error, and if both polarities are present the two populations should be antipodal. The associated directional data should therefore be plotted on equal area projections (or at least histograms of inclination) whenever possible.
3. Large changes in concentration (more than about an order of magnitude) and changes in magnetic mineralogy or grain size should be minimized. These changes can be detected with the use of bi-plots of, for example, IRM versus χ . Such bi-plots should be linear, with low scatter.
4. The relative paleointensity estimates that are coherent with bulk rock-magnetic parameters should be treated with caution. Coherence can be assessed using standard spectral techniques.
5. Records from a given region should be coherent within the limits of a common timescale. Whenever possible duplicate records should be obtained and compared.
6. For a relative paleointensity record to have the maximum utility, it should have an independent timescale. Many deep-sea sediment records are calibrated using oxygen-isotopic curves or magnetostratigraphic age constraints (or both). Lake sediments are more difficult to date and rely for the most part on radiocarbon ages.

5.13.7 Current State of the Paleointensity Data

s0140

5.13.7.1 Paleomagnetic Databases

s0145

There has been an enormous effort in collecting and preserving paleomagnetic data since the early 1960s (e.g., Irving, 1964) but since the 1987 meeting of the IAGA in Vancouver the effort has been more concerted with seven IAGA-sponsored databases. Absolute paleointensities have been assembled in a series of compilations by Tanaka and Kono (1994), Perrin and Shcherbakov (1997), Perrin *et al.* (1998), and more recently Perrin and Schnepp (2004). This

p0515

t0005 **Table 1** Parameters

Parameter	Name	Definition/notes	Ref.
$ b $	Best-fit slope	Slope of pTRM acquired versus NRM remaining	1
B_{anc}	Ancient field estimate	$ b $ times the laboratory field	1
β	Scatter parameter	Standard error of the slope over $ b $	1
Q	Quality factor	Combines several parameters	1
VDS	Vector difference sum	Sum of vector differences of sequential demagnetization steps	3
F_{vds}	Fraction of the total NRM	Total NRM is VDS	2
δ_i	pTRM check	Difference between pTRM at pTRM check step at T_i	2
T_{max}	Maximum blocking temperature	Highest step in calculation of $ b $	2
DRATS	Difference RATio sum	$\sum \delta_i$ normalized by pTRM(T_{max})	2
N_{pTRM}	Number of pTRM checks	Below T_{max}	2
Δ_i	pTRM tail check	Difference between NRM remaining after first and second zero-field steps	2
MD%	Percent maximum difference	$100 \times$ maximum value of Δ_i/VDS	2
T	Orientation matrix	Matrix of sums of squares and products of demagnetization data	3
τ_i	Eigenvalues of T	$\tau_1 > \tau_2 > \tau_3$	3
V_i	Eigenvectors of T	Best-fit direction is V₁	3
MAD	Maximum angle of deviation	$\tan^{-1}(\sqrt{(\tau_2^2 + \tau_3^2)}/\tau_1)$	4
DANG	Deviation ANGLE	Angle between origin and V₁	2

1, Coe *et al.*, (1978); 2, Tauxe and Staudigel (2004); 3, Tauxe (1998); 4, Kirschvink (1980).
Table from Tauxe, 2006.

most recent version (here referred to as PINT03) contains data from 3128 cooling units from 215 references through 2003 and is available for downloading along with the other IAGA-sponsored databases at the National Geophysical Data Center (NGDC) website. There are also a number of paleointensity data (both relative and absolute) in the TRANS database also available at the NGDC website. This database contains data associated with polarity transitions.

p0520 In their assessment of the most recent release of the absolute paleointensity database, Perrin and Schnepp (2004) stated:

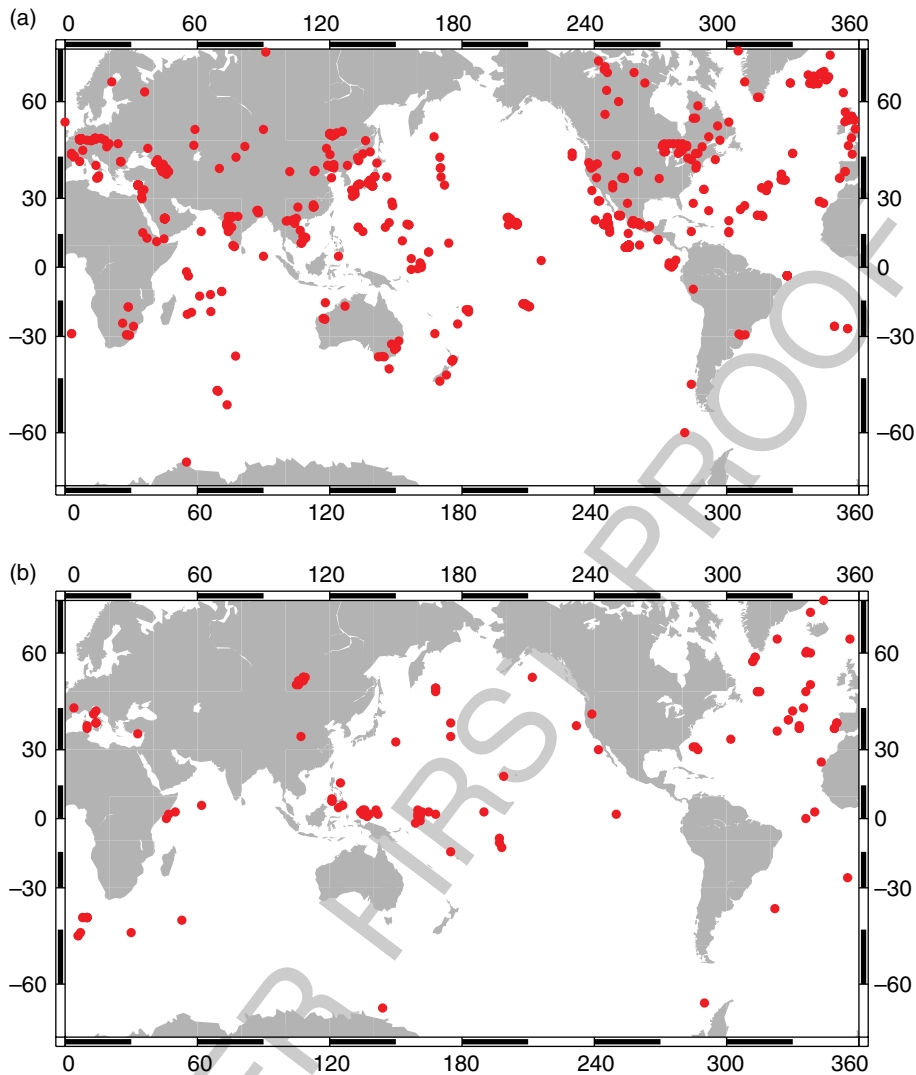
For the future, a harmonization or a combination of all IAGA databases would be desirable. Furthermore, the input of raw data at the specimen level would be useful in order to allow reinterpretation of data with more developed and sophisticated methods based on our increasing understanding of rock magnetism.

In order to address this widely felt sentiment, the MagIC database was created which can be accessed at its website. This database has merged several of the existing IAGA databases and allows for data ranging from original magnetometer output (including magnetometer, hysteresis, thermomagnetic, susceptibility, and other measurements) and their interpretations. Detailed descriptions of the data are possible by using 'method codes.'

The absolute paleointensity database of Perrin p0525 and Schnepp (2004) can now be accessed through the MagIC website by searching for that reference. We have updated it to include data published through late 2006 (Bowles *et al.* 2006; Carvallo *et al.*, 2004; Garcia *et al.*, 2006; Gee *et al.*, 2000; Halls *et al.* 2004; Herrero-Bervera and Valet, 2005; Leonhardt *et al.*, 2003; Macouin *et al.*, 2006; Riisager *et al.*, 2004; Smirnov and Tarduno, 2005; Tarduno and Cottrell, 2005; Tarduno *et al.*, 2002; Tauxe *et al.*, 2004a, 2004b; Tauxe and Staudigel, 2004; Tauxe, 2006; Yamamoto and Tsunakawa, 2005; Yoshihara and Hamano, 2004; Yoshihara *et al.*, 2003; Zhao *et al.*, 2004; Zhu *et al.*, 2004a, 2004b). Data can be retrieved through each individual reference, or by searching for this reference (Tauxe and Yamazaki, 2007) to retrieve the entire absolute paleointensity database. Data from the Tauxe references include everything down to the original measurement data as an example of the power of the MagIC database concept. We refer to our compilation of paleointensity data as PINT06 in the following.

The data in the PINT03 and PINT06 databases p0530 include information on geographic location (see map of data locations in **Figure 15(a)**), rock type and age of the sampling sites, type of paleointensity experiment, the remanence vector (including direction if available), and summary statistics such as the standard deviation of replicate specimens from a given

AU10



f0075 **Figure 15** Locations of all paleointensity data in the (a) absolute (PINT06) and (b) relative (SEDPI06) databases compiled for this paper.

cooling unit. If no measurement data are available, we may know that, for example, pTRM checks were performed (e.g. studies with pTRM listed under alteration check), but we do not know whether they ‘passed’ any particular criterion. The only reliability criteria included is the standard deviation of the replicate measurements from a given cooling unit. Because there are many useful reliability criteria for judging paleointensity data (see Section 5.13.6), efforts should be made to update the contributions in the MagIC database to include as many of these as are available.

p0535 Perrin and Schnepf (2004) ably summarized the characteristics of the PINT03 database and we will

not repeat their analysis here. Nonetheless, it is useful to reiterate that most of the data come from the last million years and are from the Northern Hemisphere. The temporal bias is particularly egregious when only the most ‘reliable’ data are used (i.e., that employed TRM normalization with pTRM checks.)

There was no IAGA database for relative paleointensity data (except those included in the TRANS database). As a step toward rectifying this problem, we summarize the published literature with relative paleointensity data in **Table 2**. Locations of records are shown in **Figure 15(b)**. We have obtained data from nearly 100 references and contributed them to

t0010 **Table 2** Summary of relative paleointensity records

AU11,12	Record	Latitude/Longitude	Age range	Dating method	Comp.	TS	Ref.
	10-pc03 ^a	-47/6	23-115 ka	RPI	69	44	69,7
	1010 ^a	30/-118	19-2036 ka	POL,MS	22	4,1	40,27
	1021 ^{a, b}	39/-128	13-1562 ka	POL	23	4,1	40,24
	1089 ^a	-41/10	20-578 ka	$\delta^{18}\text{O}$	69	44	70
	1092	-46/7	5.9-3.5 Ma	POL		4	18
	1101 ^{a, b}	-64/-70	706-1105 ka	POL,MS, $\delta^{18}\text{O}$	22	4,66	21
	21-pc02 ^a	-41/8	0-81 ka	$\delta^{18}\text{O}$	69	44	69,70,7
	305-a5 ^a	53/106	0-11 ka			44	54
	337-t2 ^a	53/106	13-84 ka	RPI		44	54
	4-pc03 ^a	-41/10	9-44 ka	RPI	69	44	69,7
	5-pc01 ^a	-41/10	8-64 ka	RPI	69	44	69,7
	522 ^a	-26/-5	22.8-34.7 Ma	POL		4	76
	606a ^a	37/323	773-792 ka	POL	26	4	13
	609b ^a	50/336	777-825 ka	POL	26	4	26
	664d ^a	0/336	670-807 ka	POL	26	4	81
	665a ^a	3/340	770-817 ka	POL	26	4	81
	767 ^{a, b}	5/124	601-1518 ka	POL	22	4	22,61
	767b ^a	5/124	759-829 ka	POL	22	4	22,61
	768a ^a	8/121	5-94 ka	$\delta^{18}\text{O}$, ^{14}C	23	41,79	63
	768b ^a	8/121	9-130 ka	$\delta^{18}\text{O}$, ^{14}C	23	41,79	63
	769 ^a	9/121	5-831 ka	$\delta^{18}\text{O}$, ^{14}C	23	41,79,66	62,63
	803a ^{a, b}	2/161	783-2178 ka	POL	22	4	33
	803b ^{a, b}	2/161	1487-2786 ka	POL	22	4	33
	804c ^a	1/161	1448-1470 ka	POL	26	4	26
	805b ^a	1/160	770-821 ka	POL	26	4	26
	848-851 ^a	2/-110	34-4035 ka	POL	23	4	82
	877 ^a	54/-148	9.4-11.3 Ma	POL		4	3
	882b	50/168	0-200 ka	~		66	52
	883	51/168	15-200 ka	$\delta^{18}\text{O}$		66	58
	884	51/168	15-200 ka	MS		66	58
	884 ^{a, b}	51/168	9.9-10.3 Ma	POL		4	56
	983 ^{a, b}	60/-24.1	0-1889 ka	POL, $\delta^{18}\text{O}$	22,34	4,66	10,11,12,6,8,9
	984 ^{a, b}	60.4/-23.6	0-2151 ka	POL, $\delta^{18}\text{O}$		4,66	11,8,9
	Chewaucan	43/-121	65-102 ka	^{14}C , ThL			57
	Sed-17aK ^a	25/-17	9-224 ka	$\delta^{18}\text{O}$		29	25
	ch88-10p ^a	30/-73	10-70 ka			44	64
	ch88-11p	31/-74	10-70 ka	~		44	64
	ch89-1p	31/-75	12-71 ka	~		44	65
	con-01-603-2	54/109	10-200 ka	POL, ^{14}C , ~			16
	con-01-604-2	52/106	0-60 ka	ARM			16
	con-01-605-3	52/105	0-40 ka	ARM			16
	ded8707 ^a	40/14	10-60 ka	Ash	23	29	80
	ded8708	40/14	40-80 ka	Ash		29	80
	e113p ^a	-2/159	4-380 ka	$\delta^{18}\text{O}$	22	1	74
	hu90-013-012	59/-47	10-110 ka	RPI, $\delta^{18}\text{O}$, ^{14}C			71
	hu90-013-013	58/-48	10-110 ka	RPI, ^{14}C			71
	hu91-045-094	50/-45	10-110 ka	RPI, $\delta^{18}\text{O}$, ^{14}C			71
	ket8251 ^a	40/14	8-95 ka	ash	23	29	80
	kh73-4-7	3/165	0-2000 ka	POL			59
	kh73-4-8	2/168	0-2000 ka	POL			59
	kh90-3-5	4/160	32-1159 ka	POL		4	60
	kk78-030 ^a	19/-161	601-1785 ka	POL	22	4	35
	kr9912-pc2 ^a	-11/-163	1003-3000 ka	POL, ARM		4,42	86
	kr9912-pc4 ^a	-13/-162	2002-2845 ka	POL		4,42	86
	kr9912-pc5 ^a	-9/-163	1295-2118 ka	POL		4,42	86
	ks87-752 ^{a, b}	-38/-38	311-1023 ka	POL, MS	23	4	83
	lc07 ^a	38/10	754-1033 ka	POL, ~	22	66	17
	ldb ^a	45/4	20-308 ka	MS, ^{14}C		15	85,78

(Continued)

28 Paleointensities

Table 2 (Continued)

Record	Latitude/Longitude	Age range	Dating method	Comp.	TS	Ref.
massicore	44/14	32–35 Ma	POL		4	37
md01-2440	38/–11	2–400 ka	RPI, MS		44	77
md01-2441	38/–11	30–54 ka	RPI, MS		44	77
md84-528	–42/53	15–80 ka	$\delta^{18}\text{O}$		29	80
md84-629	36/33	15–62 ka	$\delta^{18}\text{O}$		29	80
md85-668 ^a	0/46	21–187 ka	$\delta^{18}\text{O}$	23	44	45
md85-669 ^a	2/47	20–138 ka	RPI	23	44	45
md85-674 ^a	3/50	18–138 ka	RPI	23	44	45
md90-0940 ^a	6/62	108–1954 ka	POL, MS, fossils	23	4	46
md95-2009 ^a	63/–4	10–76 ka	ARM	34	20	32,34
md95-2024 ^a	50/–46	1–117 ka	MS, $\delta^{18}\text{O}$	68	2	68
md95-2034 ^a	34/–58	12–76 ka	ARM	34	20	32,34
md95-2039	40/–10	0–320 ka	$\delta^{18}\text{O}$, ^{14}C		44	77
md95-2042	40/–10	32–160 ka	$\delta^{18}\text{O}$, ^{14}C		44	77
md97-2140 ^{a, b}	2/142	568–1465 ka	POL		4	5
md97-2143 ^{a, b}	16/125	601–2226 ka	POL, $\delta^{18}\text{O}$	22	4,38	28
md98-2181 ^a	6/126	12–660 ka	$\delta^{18}\text{O}$, ^{14}C		67	73
md98-2183 ^{a, b}	2/135	20–1193 ka	POL, MS, ARM	86	4,42	86
md98-2185 ^{a, b}	3/134	9–2256 ka	POL, MS, ARM	22	4,42	86
md98-2187 ^{a, b}	4/135	51–3053 ka	POL, MS, ARM		4,42	86
md99-2334	38/–11	0–38 ka	RPI		44	77
ngc16 ^a	2/135	2–191 ka	MS	23	44	87
ngc26 ^a	3/135	1–120 ka	MS	23	44	87
ngc29 ^a	4/136	2–192 ka	MS	23	44	87
ngc36 ^a	–1/161	1–546 ka	$\delta^{18}\text{O}$	23	29,1	88
ngc38 ^a	–15/175	9–406 ka	$\delta^{18}\text{O}$	23	29,1	88
ngc65 ^a	35/175	6–635 ka	S		1	89
ngc69 ^{a, b}	40/175	7–881 ka	S		1	89
np35 ^a	4/141	127–798 ka	$\delta^{18}\text{O}$	23	29,1	88
np5 ^b	1/137	8–196 ka	$\delta^{18}\text{O}$	23	44	87
np7 ^a	2/138	6–199 ka	MS	23	44	87
p012 ^a	59/–47	14–177 ka	RPI	23	23	72
p013 ^a	58/–48	14–277 ka	RPI	23	23	72
p094 ^a	50/–46	2–111 ka	RPI	23	23	72
p226 ^a	3/–170	41–780 ka	POL	23	4	88
ps1535-10	79/2	0–100 ka	^{14}C			48
ps1535-6	79/2	0–100 ka	^{14}C			48
ps1535-8	79/2	0–100 ka	^{14}C			48
ps1707-2	73/–14	0–80 ka	MS		44	49
ps1852-2 ^a	70/–16	4–283 ka	MS		29,44	50
ps1878-3	73/–9	0–100 ka	^{14}C			48
ps1878-3	73/–10	0–45 ka	$\delta^{18}\text{O}$, ^{14}C		44	49
ps2138-1	82/31	10–75 ka	$\delta^{18}\text{O}$, ^{14}C			47
ps2644-5 ^a	68/–22	12–76 ka	ARM	34	20	32,34
rc10-167 ^a	33/150	11–781 ka	POL	26,23	4	30
rmdb75p ^a	2/160	124–668 ka	$\delta^{18}\text{O}$	23	29,66	75
su90-24 ^a	63/–37	11–76 ka	ARM	34	20	32,34
su90-33 ^a	60/–22	12–76 ka	ARM	34	20	32,34
su9003	41/–32	10–240 ka	Color		55	84
su9004	41/–32	0–240 ka	Color		55	84
su9008	44/–30	10–180 ka	$\delta^{18}\text{O}$		55	84
su9039	52/–22	0–240 ka	$\delta^{18}\text{O}$		55	84
su92-17 ^a	39/–27	4–280 ka	Color		44	39
su92-18 ^a	38/–27	4–280 ka	$\delta^{18}\text{O}$	23	44	39
su92-19 ^a	38/–27	4–279 ka	Color	23	44	39
v16-58 ^a	–46/30	767–770 ka	POL	26	4	31
ver98-1-1	53/108	20–60 ka	ARM			16
ver98-1-14	54/108	0–350 ka	ARM			16

(Continued)

Table 2 (Continued)

Record	Latitude/Longitude	Age range	Dating method	Comp.	TS	Ref.
ver98-1-3	54/108	50–250 ka	ARM			16
ver98-1-6 ^a	54/108	65–235 ka	Silica		44	51
Kotsiana	36/24	—				36
Lingtai ^a	35/107	10–73 ka	MS, ¹⁴ C, ThL			53
Potamida	36/24	—				36
Ir ^{a, b}	43/13	90–94.9 Ma	POL, fossils		19	14
WEGAstack	–65/144	0–800 ka	RPI, ¹⁴ C, fossils			43
MBstack ^a	3/162	32–1159 ka	POL	22	4	60
PMstack ^a	39/10	0–402 ka	RPI, $\delta^{18}\text{O}$, ¹⁴ C		44	77
NAstack ^a	45/–25	10–250 ka	$\delta^{18}\text{O}$		55	84

^aSubmitted to the MagIC database.

^bAges recalculated.

Dating methods: RPI, relative paleointensity; POL, polarity stratigraphy; MS, correlation of magnetic susceptibility; ARM, correlation of ARM; carb., correlation of calcium carbonate; ash, tephrostratigraphy; color, correlation of color; $\delta^{18}\text{O}$, oxygen isotopes; ¹⁴C, radiocarbon; ~, correlation of some unspecified wiggle; ThL, thermoluminescence; S, correlation of high to low coercivity IRM; silica, correlation of silica variations; fossil, correlation based on fossils.

References: 1, Bassinot *et al.*, 1994; 2, Bender *et al.*, 1994; 3, Bowles *et al.*, 2003; 4, Cande and Kent 1995; 5, Carcaillet *et al.*, 2003; 6, Channell *et al.*, 2000; 7, Channell and Kleiven, 2000; 8, Channell *et al.*, 2002; 9, Channell *et al.*, 2004; 10, Channell *et al.*, 1997; 11, Channell *et al.*, 1998; 12, Channell, 1999; 13, Clement and Kent, 1986; 14, Cronin *et al.*, 2001; 15, Dansgaard *et al.*, 1993; 16, Demory *et al.*, 2005; 17, Dinares-Turell *et al.*, 2002; 18, Evans and Channell, 2003; 19, Stratigraphy, 2004; 20, Grootes and Stuiver, 1997; 21, Guyodo *et al.*, 2001; 22, Guyodo and Valet, 2006; 23, Guyodo and Valet, 1999; 24, Guyodo *et al.*, 1999; 25, Haag, 2000; 26, Hartl and Tauxe, 1996; 27, Hayashida *et al.*, 1999; 28, Horg *et al.*, 2003; 29, 1984; 30, Kent and Opdyke, 1977; 31, Kent and Schneider, 1995; 32, Kissel *et al.*, 1999; 33, Kok and Tauxe, 1999; 34, Laj *et al.*, 2000; 35, Laj *et al.*, 1996; 36, Laj *et al.*, 1996b; 37, Lanci and Lowrie, 1997; 38, Laskar *et al.*, 1993; 39, Lehman *et al.*, 1996; 40, Leonhardt *et al.*, 1999; 41, Linsley and Thunnell, 1990; 42, Lisiecki and Raymo, 2005; 43, Macri *et al.*, 2005; 44, Martinson *et al.*, 1987; 45, Meynadier *et al.*, 1992; 46, Meynadier *et al.*, 1994; 47, Nowaczyk and Knies, 2000; 48, Nowaczyk *et al.*, 2003; 49, Nowaczyk and Antonow 1997; 50, Nowaczyk and Frederichs, 1999; 51, Oda *et al.*, 2002; 52, Okada, 1995; 53, Pan *et al.*, 2001; 54, Peck *et al.*, 1996; 55, Pisias *et al.*, 1984; 56, Roberts and Lewin-Harris, 2000; 57, Roberts *et al.*, 1994; 58, Roberts *et al.*, 1997; 59, Sato and Kobayashi, 1989; 60, Sato *et al.*, 1998; 61, Schneider *et al.*, 1992; 62, Schneider, 1993; 63, Schneider and Mello, 1996; 64, Schwartz *et al.*, 1996; 65, Schwartz *et al.*, 1998; 66, Shackleton *et al.*, 1990; 67, Sowers *et al.*, 1993; 68, Stoner *et al.*, 2000; 69, Stoner *et al.*, 2002; 70, Stoner *et al.*, 2003; 71, Stoner *et al.*, 1995; 72, Stoner *et al.*, 1998; 73, Stott *et al.*, 2002; 74, Tauxe and Wu, 1990; 75, Tauxe and Shackleton, 1994; 76, Tauxe and Hartl, 1997; 77, Thouveny *et al.*, 2004; 78, Thouveny *et al.*, 1994; 79, Tiedemann *et al.*, 1994; 80, Tric *et al.*, 1992; 81, Valet *et al.*, 1989; 82, Valet and Meynadier, 1993; 83, Valet *et al.*, 1994; 84, Weeks *et al.*, 1995; 85, Williams *et al.*, 1998; 86, Yamazaki and Oda, 2005; 87, Yamazaki and Ioka, 1994; 88, Yamazaki *et al.*, 1995; 89, Yamazaki, 1999.

AU13

the MagIC database (obtainable individually through the original reference or collectively through this reference). We refer to this compilation of relative paleointensity data as SEDPI06 in the following. Authors are encouraged to contribute or augment their own data in the database. In Section 5.13.8 we will discuss the highlights of the available paleointensity data from both the PINT06 (absolute) and SEDPI06 (relative) compilations. Before we discuss the global dataset, we will first describe methods of converting to virtual dipole moment.

converting intensities to ‘virtual dipole moments’ in both absolute and relative paleointensity data sets.

There are several ways to calculate equivalent ^{p0550} dipole moments for paleointensity data. Early studies tended to present a given intensity result as a ratio with some expected field. For example, Thellier and Thellier (1959) normalized intensity data to a reference inclination of 65°, using the paleomagnetically determined inclination and the relationship between inclination and field strength expected from a magnetic dipole. Most studies published over the last few decades however express paleointensity in terms of the equivalent geocentric dipole moment which would have produced the observed intensity at that (paleo) latitude. There are two ways in which this is done, the virtual dipole moment (VDM; **Figure 16(a)**) and the virtual axial dipole moment (VADM; **Figure 16(b)**). The VDM^(b1040) (Smith, 1967) is the moment of an geocentric dipole that would give rise to the observed magnetic field vector at location *P*. (The piercing point on the surface of the globe of this

s0150 5.13.7.2 Conversion to Virtual Dipole Moment

s0155 5.13.7.2.1 Absolute paleointensity data

p0545 The intensity of the magnetic field varies by a factor of two from equator to pole simply as a result of a dipole source, so data from different latitudes must be normalized to take this inherent dipole variation into account. In the following we discuss methods for

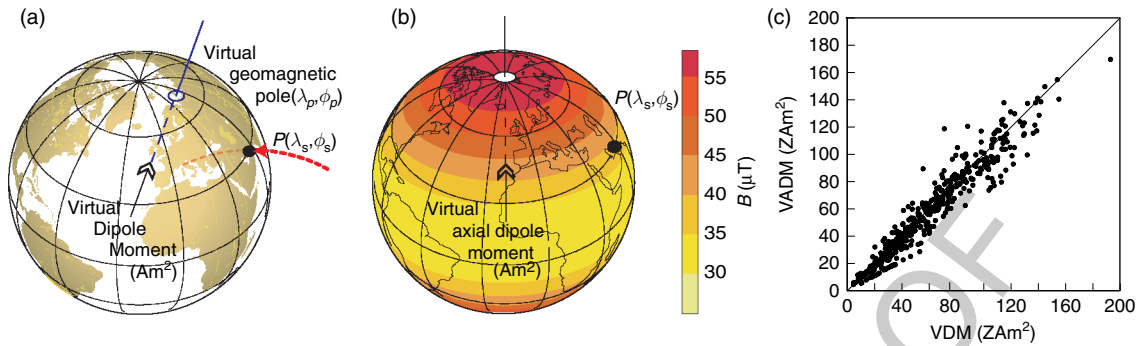


Figure 16 (a) The virtual dipole moment VDM is the geocentric dipole that would give rise to the observed geomagnetic field vector at the location P . λ_s , ϕ_s are the site latitude and longitude, respectively. (b) The virtual axial dipole moment is the geocentric axial dipole that would give rise to the observed intensity at P . (c) Comparison of VDM and VADM for paleointensity data (see text).

moment is the virtual geomagnetic pole or VGP.) To get the VDM, we first calculate the magnetic (paleo) colatitude θ_m from the observed inclination I and the so-called dipole formula ($\tan I = 2 \cot \theta_m$). Then, assuming a centered (but not axial) magnetic dipole with moment VDM we have

$$\text{VDM} = \frac{4\pi r^3}{\mu_0} B_{\text{anc}} (1 + 3 \cos^2 \theta_m)^{-1/2} \quad [11]$$

The VDM calculation requires a good estimate of the inclination, which is not always available, especially when unoriented specimens are used. In such cases, it may be possible to use either the site (co) latitude or a paleo (co) latitude estimated by a plate reconstruction in the place of magnetic colatitude in eqn [11]. This moment is known as the VADM (Barbetti *et al.*, 1977).

In order to compare the two forms of normalization, we selected data from the PINT06 database for the last 200 My that (1) were obtained with thermal normalization and used pTRM checks, (2) had multiple specimens that had standard deviations less than 15% of the mean or were less than 5 μT. We estimated paleolatitudes for the sampling sites using the global apparent polar wander paths of Besse and Courtillot (2002) and used these to calculate VADMs for many sites. We show the two estimates of dipole moment in **Figure 16(c)**; the two are essentially equivalent representations.

It is important to note here that neither VDMs nor VADMs actually represent the true dipole moment (see Korte and Constable, 2005). They do not take into account the rather substantial effect of the nondipole field contributions and in fact overestimate the true dipole moment based on an evaluation of data for the last 7000 years.

5.13.7.2.2 Relative paleointensity data s0160

Sedimentary paleointensity data are at best ‘relative’ paleointensity. Nonetheless several studies have attempted to calibrate relative paleointensity data into a quasi-absolute form and cast them as ‘VADMs’ in order to compare them with the igneous data sets. There are different strategies for accomplishing this conversion (see **Figure 17**): setting the ‘floor’ to some minimum value expected for the field (Constable and Tauxe, 1996), setting parts of the sedimentary record to be equal to coeval igneous records (e.g., Guyodo and Valet, 1999; Valet *et al.*, 2005) or setting the mean value to be some assumed value.

In the Constable and Tauxe (1996) method, the nonaxial dipole field is assumed to be on average 7.5 μT as it is for the present field. Reasoning that because the axial dipole must go through zero in a polarity transition, the average transitional field should be about 7.5 μT. **Figure 17(a)** illustrates an application of this method to calibrate the Oligocene relative paleointensity data from DSDP Site 522 of Tauxe and Hartl (1997; see **Table 2**) into VADM values. Setting the average value of the intensity in transitional records (red square in **Figure 17(a)**) to a value of 7.5 μT calibrates the entire record to B^* in μT. Assuming a paleolatitude of 32° S allows these B^* values to be converted to VADM values using eqn [11]. The problem with this method is that it is extremely sensitive to the choice of the nonaxial dipole field ‘floor’ value, which is not known for ancient times. Small changes in the choice of floor result in large changes for the calibrated record.

A different approach was taken by Guyodo and Valet (1999) who collected together many relative paleointensity records spanning the last 800 ky (see compilation reference #23 in **Table 2**). The ‘SINT-800’ stack

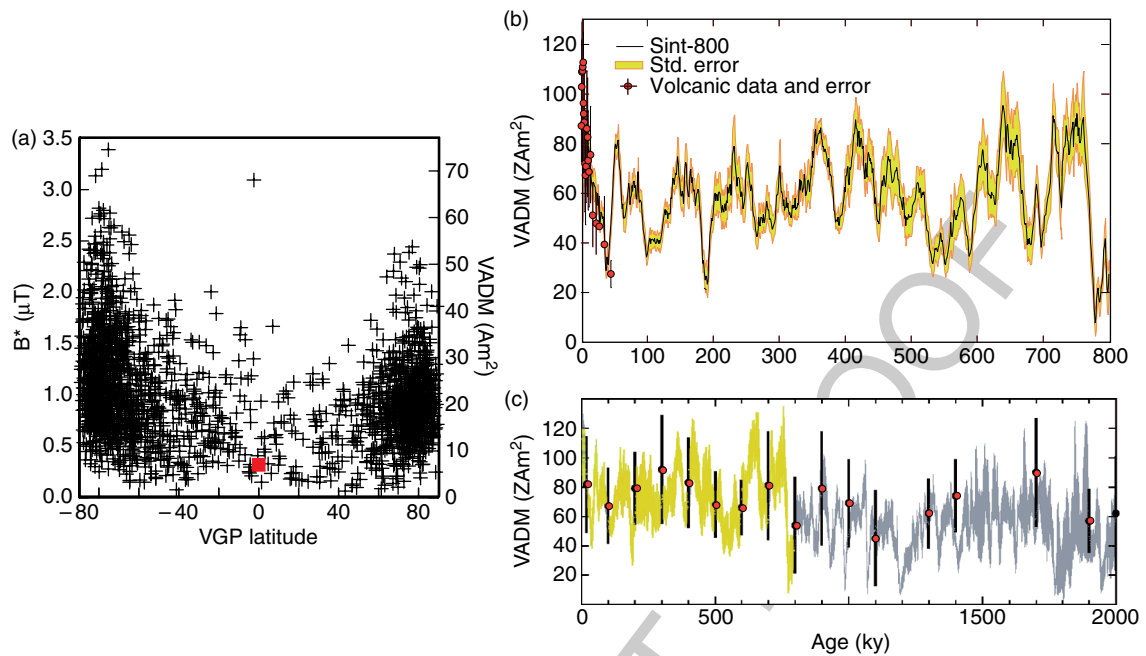


Figure 17 Calibration of sedimentary relative paleointensity data to quasi-absolute values. (a) Approach of Constable and Tauxe (1996) on relative paleointensity data from the Oligocene record at DSDP Site 522. Data associated with transitional fields (low VGP latitudes) are assumed to be on average $7.5 \mu\text{T}$, the value of the present average non-GAD field. This converts the relative intensity data to μT . Taking a paleolatitude of 32° , Tauxe and Staudigel (2004) converted these data to VADM using eqn [12]. (b) Stacked record of relative paleointensity data spanning the last 800 ky (SINT-800) of Guyodo and Valet (1999). They used the VADM data from contemporaneous lava flows to calibrate the record to VADM. (c) Similar to (b) but data span the last 2 My (SINT-2000) from Valet *et al.* (2005). They used averages of the PINT03 database (red dots) to calibrate the SINT record to VADM.

(see **Figure 17(b)**) overlapped a sequence of absolute paleointensity data whose ages were well known (red dots). These absolute data were used to calibrate the SINT-800 stack into VADM. Valet *et al.* (2005) extended the relative paleointensity stack to span the last 2 My (see **Figure 17(c)**). In this latest version, known as the SINT-2000 stack (a subset of the records compiled in reference #22), they took the global paleointensity data in the PINT03 database (with no selection criteria), and averaged them into 100 000 year bins (red dots). These were used to convert the SINT-2000 stack to VADM values. The two calibrations are somewhat different, with the latter version being higher on average.

Because amplitudes of relative paleointensity records must be related to latitude it is preferable to convert individual records to VADM prior to stacking, instead of stacking first and then converting to VADM. However, the ‘floor setting’ method of Constable and Tauxe (1996) required transitional data, which are not always available and has severe drawbacks of its own as mentioned before.

5.13.8 Discussion

s0165

In the following, we will discuss some of the ‘hot topics’ in paleointensity. The issues for many of these are still under debate and conclusions are still tentative. Nonetheless, the spirit of this volume is to present the ‘state of the field’ and we will endeavor to do so.

5.13.8.1 Selection Criteria from the PINT06 Database

s0170

For the purpose of this discussion, we selected data from the PINT06 database that had either standard deviations $\leq 5 \mu\text{T}$ or 15% or the mean. These were divided into those that used the so-called KTT experimental protocol with pTRM checks (here called ‘strict’) and those that did not (mostly KTT without pTRM checks and ‘Shaw’-type experiments; here called ‘loose’). Those that did not meet the consistency standard are labeled ‘rejected.’ As noted before, there is very little else to go on in the database as it currently stands. We plot these data versus age in **Figure 18**.

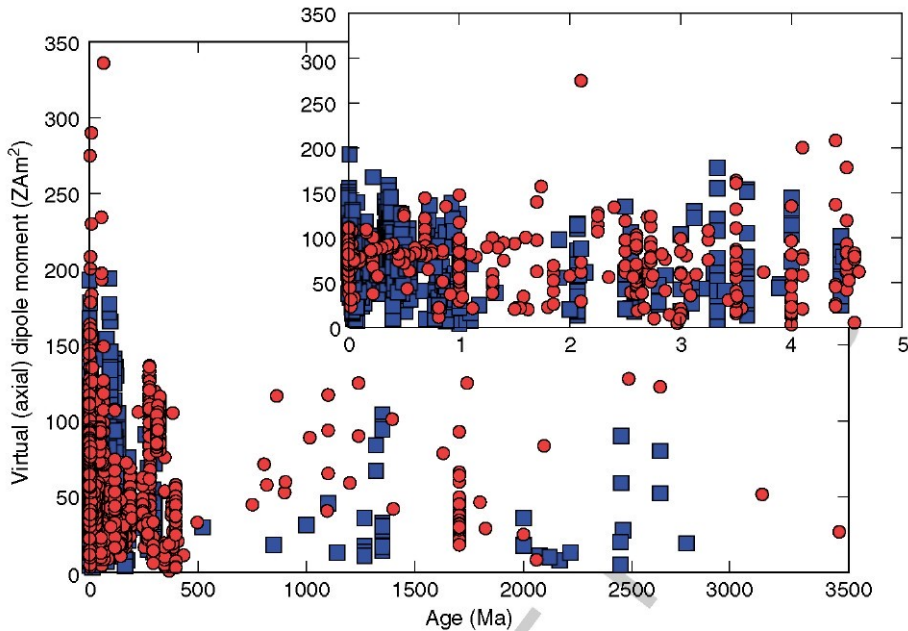


Figure 18 Summary of published data meeting the criteria of standard deviations of the mean being either less than 15% of the mean or less than 5 mT. Blue squares are the 'strict' data selection (KTT with pTRM checks) from the PINT06 database and the red dots are the 'loose' (mostly KTT without pTRM checks and 'Shaw'-type experiments); see text. The inset shows only data from the last 5 million years.

p0595 There are a total of 1504 cooling unit averages from the 'strict' group with a mean and standard deviation of $63.6 \pm 34 \text{ZAm}^2$ ('Z' stands for Zetta (10^{21})) and 1133 from the 'loose' experimental group with a mean of $62.8 \pm 37 \text{ZAm}^2$. A total of 1115 results were rejected on the grounds of poor within-cooling-unit reproducibility (or single-specimen results). These had a mean and standard deviation of $68.0 \pm 35.5 \text{ZAm}^2$. The standard errors of the means of these three data sets are: 0.9, 1.1, and 1.1, respectively, so while the 'strict' and 'loose' data sets have indistinguishable means, the rejected mean is significantly higher than the other two. The differences between the three data sets are illustrated using cumulative distributions in **Figure 19**. The strict and loose data sets have indistinguishable means, with the 'loose' data set having more scatter (more of both high and low values), while the mean of the 'rejected' group is significantly higher.

p0600 In this very large data set, there is no statistical difference between means of the 'strict' and 'loose' data sets (although the 'loose' data set has significantly more scatter) and the mean is significantly lower than the present field. While the highest values are in the 'loose' category, there are few of them and the means are indistinguishable. This does not mean that

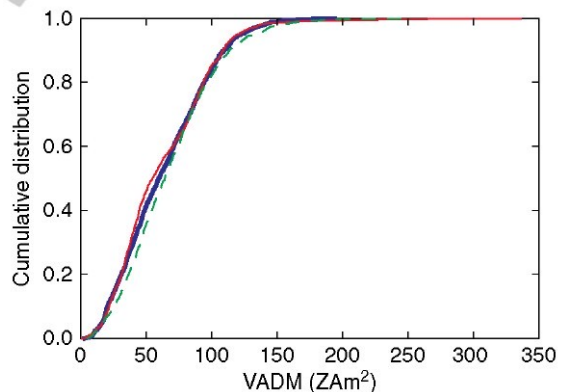


Figure 19 Cumulative distributions of 'strict' (heavy blue line; KTT-type experiment with pTRM checks), 'loose' (light red line; other experimental designs), and 'rejected' (dashed green line); all data points with standard deviations $>15\%$ of the mean and $>5 \text{mT}$. The strict and loose data sets are similar while the rejected data are significantly different with a higher mean.

experimental design makes no difference; the discussion of theory makes it quite clear that many things can give an erroneous result and these things should be tested for. The fact that there is higher scatter in the 'loose' criteria data set suggests that some of the scatter is not solely geomagnetic in origin. Furthermore,

using data with poor within-site consistency results in a significantly different and higher estimate for the mean value. We will not consider these ‘rejected’ data in the following discussion.

p0605 Although the data set is by now quite large, the age distribution of paleointensity data is still quite patchy with 39% of the data being younger than 1 Ma. By far the maximum data has come from the Northern Hemisphere (see **Figure 15(a)**). So one point of agreement among all papers on the subject and that is that more and better data would be helpful for defining the average paleofield intensity and its variation.

s0175 5.13.8.2 What is the Average Strength of the Geomagnetic Field?

p0610 The present Earth’s magnetic field is well approximated by a geocentric magnetic dipole with a moment of about 80 ZAm^2 . But what is the average value of the dipole moment? A great deal of effort has been put into assembling paleointensity databases over more than three decades, yet there remains little consensus on the answer to this most basic question.

p0615 Early studies suggested that the average field strength has either been quite a bit lower than the present (e.g., Smith (1967) and Coe (1967)) or approximately equivalent to today’s field (Kono, 1971; Bol’shakov and Solodnikov, 1980; and McFadden and McElhinny, 1982). Some studies found no trend with age in VDMs (e.g., Bol’shakov and Solodnikov, 1980) over the last few hundred million years, while others found a significant increase in dipole moment from the Mesozoic toward the present (e.g., Smith, 1967). Tanaka *et al.* (1995) estimated the average dipole moment for the last 20 My to be approximately 84 ZAm^2 with significantly lower values in the Mesozoic (the so-called ‘Mesozoic Dipole Low’ of Prévot *et al.*, 1990), a view also held by Perrin and Shcherbakov (1997) and recently reiterated by Biggin *et al.* (2003). But a series of recent papers have argued for a lower average (Juarez *et al.*, 1998; Juarez *et al.*, 2000; Selkin and Tauxe, 2000; Yamamoto and Tsunakawa, 2005; and Tauxe, 2006). In this view, the Mesozoic Dipole Low was not ‘low’ but was of average paleomagnetic intensity.

p0620 The lack of consensus stems in part from differing views on which data to include as well as the explosive growth of paleointensity data available (compare, e.g., Selkin and Tauxe, 2000; Heller *et al.*, 2002; Biggin *et al.*, 2003; and Goguitchaichvili *et al.*, 2004). While Biggin *et al.* (2003) argue that because such procedures, as the so-called ‘pTRM check’

designed to identify alteration during the paleointensity experiment, cannot guarantee the quality of a particular result, there is no need to reject data that do not have pTRM checks; others (e.g., Riisager and Riisager, (2001) and Tauxe and Staudigel (2004)) have tried to develop more rigorous experimental protocols to detect and reject ‘bad’ data. Here we take the broad view advocated by Biggin *et al.* (2003), relying strongly on strict consistency tests at the cooling unit level.

As a first look at what the average field might be, p0625 we consider the data from **Figure 18** (excluding the ‘rejected data’) that meet one of the following conditions: (1) they have ages less than 5 Ma and we can use the present latitude as the ‘paleolatitude’ (λ); (2) they have model latitudes based on plate reconstructions or derived from the apparent polar wander paths of Besse and Courtillot (2002); or (3) they have inclination (I) data associated with intensities whereby we can approximate paleolatitude using the dipole formula ($\tan(I) = 2 \tan \lambda$). We binned the data 10° latitudinal bins (see **Figure 20**). The error bars are the standard errors of the mean. Also shown is the intensity at each latitude expected from the average dipole moment of 63 ZAm^2 (the average estimated in the previous section for the whole data set).

Although there is some trend with latitude, the p0630 overall fit of the paleointensity data shown in **Figure 20** to a dipole field is poor. The equatorial results are ‘too high’ and mid-latitude results are ‘too low.’ Reasons for the failure of the dipole hypothesis in the PINT06 data compilation include: (1) the data may be ‘no good’; (2) there may be long-term

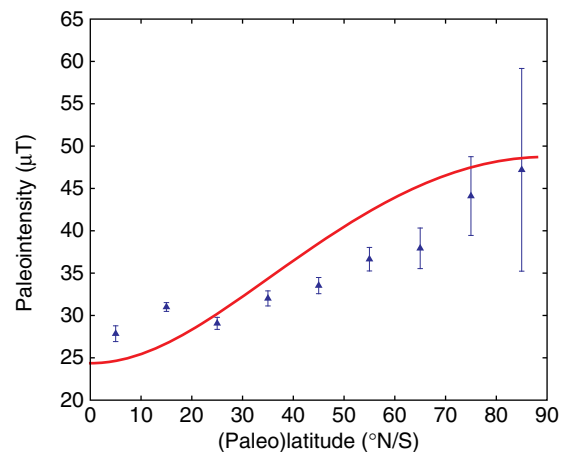


Figure 20 Paleointensity versus (paleo) latitude (see text). f0100 The error bars are the standard error of the mean for each paleolatitude bin.

nonaxial dipole field contributions to the geomagnetic field; (3) the average may be nonstationary and the data in different bins in **Figure 20** are from different ages and average fields. The first two hypotheses cannot be tested with the present data set, but the third can, to some extent by looking at the more recent past for which there are a lot of data.

p0635 In order to address the issue of the average field, we look at the data from the last 170 My meeting the consistency test described in the previous section in **Figure 18**. We have split these out into data from submarine basaltic glasses (SBG, blue dots), from single crystals (SX, red diamonds), and 'other' (mostly lava flows, triangles).

p0640 The present compilation is sufficient to clarify a few key misconceptions in the literature: (1) that SBG data are generally lower than other (mostly lava flow) data; (2) that single crystal results are 'high'; and (3) there is a stationary average field. The average of the 421 data points from SBG for the last 170 My is 66.9 ± 34 (standard error of the mean of 1.7) while that of all the other data is 62.6 ± 35.6 (standard error of the mean of 0.75); that is, the SBG data are in fact higher than the other data over this age interval. There are insufficient data in the database from single crystals, but it is clear from **Figure 21** that the single-crystal data are consistent with other data of similar age. Finally, the concept of a stationary average field is difficult to support with the data shown in **Figure 21**. It appears that there are periods of time (e.g., from about 20 Ma to about 55 Ma and older than about

125 Ma) during which the field was relatively low, with an average dipole moment of around 50 ZAm^2 . There are also periods of time during which the field is much higher (e.g., the last 20 My and the period from about 55 to 122 Ma).

Another clear result from the data in **Figure 18** is p0645 that the geomagnetic field is highly variable on both short and long timescales. Therefore it is likely that unless the same time period is considered in all latitudinal bins, in figures like **Figure 20** there will be scatter introduced from comparing times with different average field strength. Some effort should be put in obtaining data for certain time slices as a function of paleolatitude.

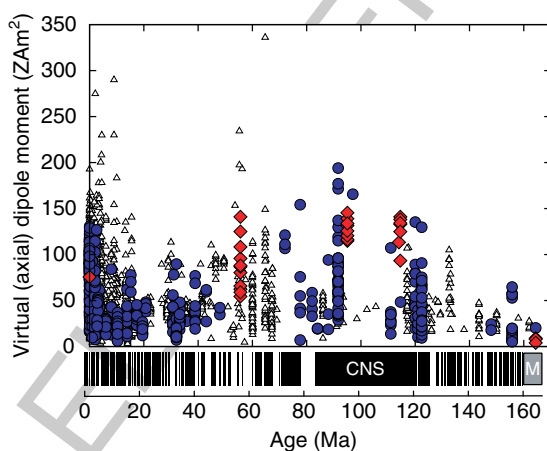
5.13.8.3 Are There Any Trends? s0180

5.13.8.3.1 Intensity versus polarity interval length s0185

Although there are no clear long-term trends in the paleointensity data shown in **Figures 18 and 21**, there are times when the field is stronger than others as noted previously. ^{b0230}Cox (1968) suggested that strong geomagnetic fields could inhibit reversals of the geomagnetic field and this makes sense with the observation that geomagnetic fields are low when the field is reversing.

^{b1180}Tauxe and Hartl (1997) and ^{b0210}Constable *et al.* (1998) p0655 demonstrated a weak correlation between the length of a given polarity interval and the average paleointensity in the relative paleointensity data from DSDP Site 522. So one of the primary motivations for initiating the study of the DSDP/ODP submarine basaltic glasses for paleointensity was to test the hypothesis that long intervals of stable polarity (like the Cretaceous Normal Superchron or CNS in **Figure 21**) were associated with unusually strong fields (see, e.g., ^{b0870}Pick and Tauxe, 1993). It was therefore puzzling and a bit disappointing when Selkin and Tauxe (2000) compared paleofield strength with reversal rate and found no clear relationship. There were just too few data from the CNS to make a definitive statement.

Now there are many more data from the last p0660 175 My with several data sets available from intervals whose polarity chron are known and the data can be associated with known polarity interval length. In **Figure 22** we also show the data from **Figure 21** associated with known polarity intervals. These data are from SBG obtained from holes drilled on clearly identifiable magnetic anomalies compiled by Tauxe (2006) and data from lava flows in



f0105 **Figure 21** Summary of published data meeting minimum criteria for last 200 My. Blue dots are submarine basaltic glass data. Red diamonds are single-crystal results. Triangles are all other data meeting the same consistency criteria ($\sigma < 5\%$ of mean or $< 5 \mu\text{T}$); VADMs calculated as in text.

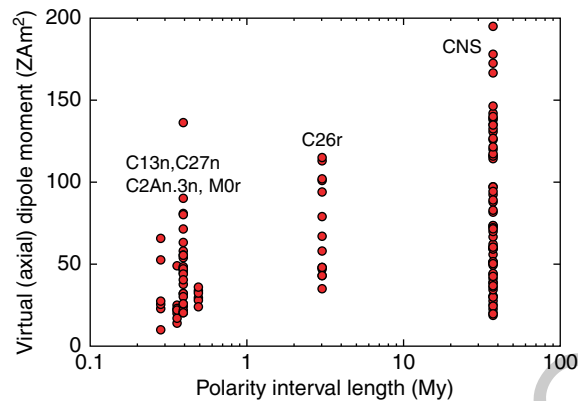


Figure 22 VADM data from the PINT06 database from polarity intervals of known duration. Data from the CNS are from Cottrell and Tarduno (2000); Riisager *et al.* (2003); Sherwood *et al.* (1993); Tarduno *et al.* (2001, 2002); Tauxe (2006); Tauxe and Staudigel (2004); Tanaka and Kono (2002); Zhao *et al.* (2004); Zhu *et al.* (2004b). C26r and C27n are from Riisager and Abrahmsen (2000); C12n, C13n, C32n are from Tauxe (2006); M0r are from Riisager *et al.* (2003), Tauxe (2006) and Zhu *et al.* (2001); and C2An.3n are from Herrero-Bervera and Valet (2005).

magnetostratigraphic sections correlated to the time-scale (Riisager *et al.*, 2003; Herrero-Bervera and Valet, 2005). It appears that the correlation suggested by Tauxe and Hartl (1997) and Constable *et al.* (1998) based on relative paleointensity in sediments is supported by the absolute paleointensity data set.

5.13.8.3.2 Source of scatter in the CNS

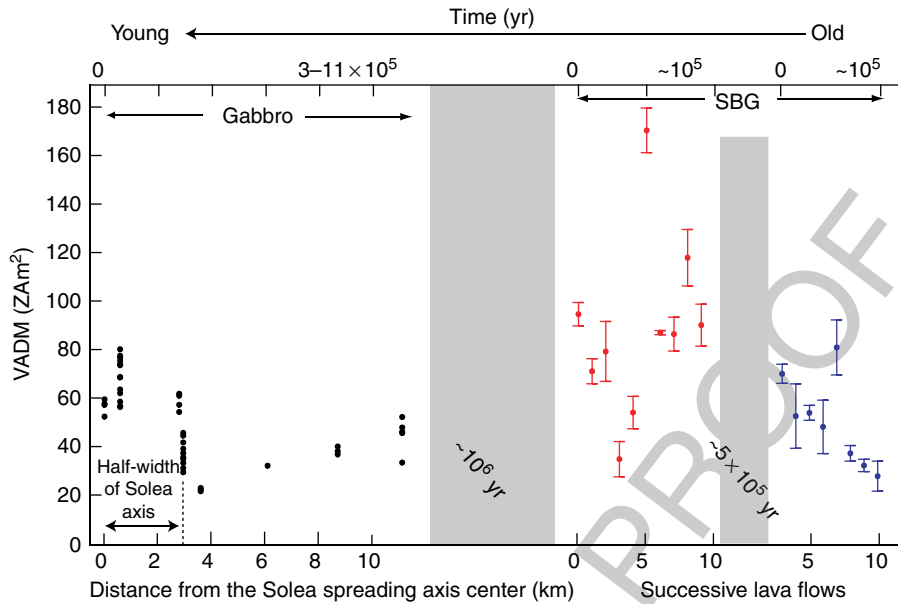
Another prediction made from the relative paleointensity data from Site 522 was that the scatter in the data is proportional to the average value and strongly linked to polarity interval length (Constable *et al.*, 1998). This observation also appears to be weakly supported by the absolute paleointensity data set. One question that springs to mind, however, is whether the scatter is geomagnetic in origin. To address this issue, Granot *et al.* (in press) assembled a data set from the Troodos ophiolite which formed during the CNS. Their data set includes new data from gabbros as well as the submarine basaltic glass data of Tauxe and Staudigel (2004). Many of the gabbro data came from a sequence of small plutons with a clear relationship to the ancient spreading axis and their relative age relationships were therefore known. Tauxe and Staudigel (2004) had sampled two transects through the entire oceanic extrusive layer, separated by some 10 km. Data from these two transects are in stratigraphic order, so their age relationships are also known. In **Figure 23** we show their plot of the three time sequences. The data exhibit remarkable serial correlation, which Granot *et al.* (in press) used to argue that the scatter in the CNS data is largely geomagnetic in origin.

5.13.8.3.3 The oldest paleointensity records

Under the topic of ‘trends in paleointensity,’ one of the most interesting questions concerns the earliest records of paleointensity. In **Figure 24** we show published results satisfying minimum consistency constraints obtained from Archean aged rocks. Until recently, there were very few studies that were based on experiments that used pTRM checks (triangles and diamonds in **Figure 24**). Recent data meet the highest experimental standards and show that the field had a large range in intensity, similar to more recent times, although the highest values come from experiments not done with pTRM checks (squares in **Figure 24**). The inescapable conclusion from these data is that the geomagnetic field was ‘alive and well’ by ~3 Ga.

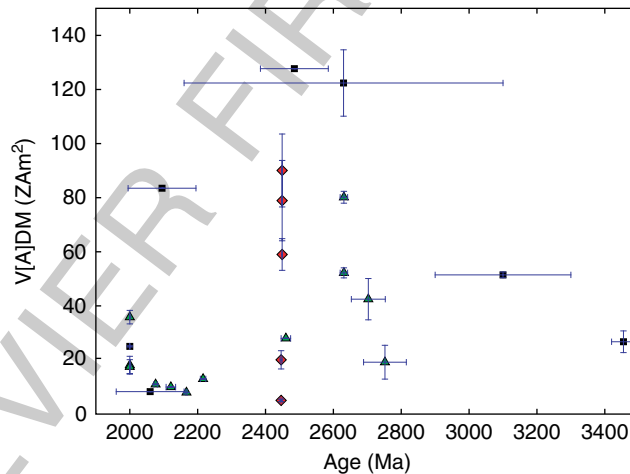
5.13.8.3.4 The paleointensity ‘saw-tooth’

Valet and Meynadier (1993) (detailed data set in Meynadier *et al.*, 1995) presented a relative paleointensity record for the last 4 My using sediment cores of ODP Leg 138 taken from the eastern equatorial Pacific (see **Figure 25**). They postulated an ‘asymmetric saw-tooth pattern’ of paleointensity variations, that is, a rapid intensity growth just after a polarity transition and a gradual decrease since then towards the next reversal (see **Figure 25**). They also suggested that the length of a polarity zone is proportional to the magnitude of the intensity jump. The latter observation is consistent with the data shown in **Figure 22** whereby long polarity intervals appear to have higher average fields. Nonetheless, the ‘saw-tooth’ idea became the subject of heated arguments.



f0115 **Figure 23** Three time-series of paleointensity data during the late CNS from the gabbros and glasses. Gray areas represent gaps in time estimated from moderate spreading rate (full spreading rate of $20\text{--}75\text{ mm yr}^{-1}$). Results for the gabbro specimens are shown as individual points and are corrected for cooling rate and anisotropy. Results for the SBG sites correspond to the average results from successive cooling units. Data are from Granot *et al.* (2006) and Tauxe and Staudigel (2004). Figure modified from Granot *et al.* (in press).

AU14

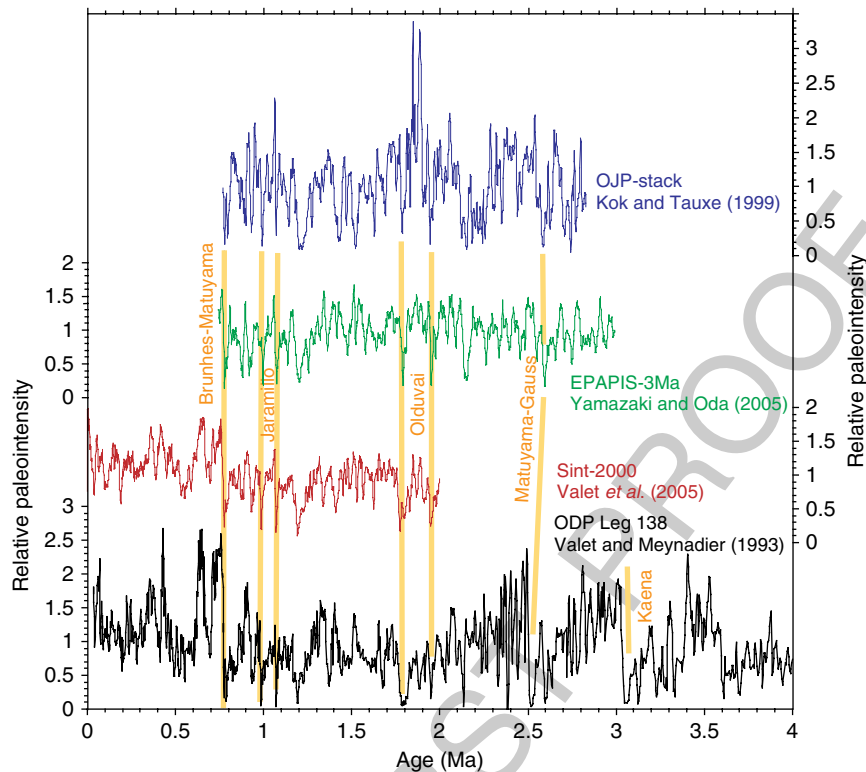


f0120 **Figure 24** Archean data from the database that have standard deviations of $<20\%$ of the mean or are $<5\text{ }\mu\text{T}$. Age uncertainties are indicated by the horizontal bars. Triangles are data from KTT-type experiments with pTRM checks and squares are from other types of experiments. The diamonds are from single-crystal experiments. Data are from Morimoto *et al.*, 1997; Yoshihara and Hamano, 2000; Sumita *et al.*, 2001; Macouin *et al.*, 2003; Bergh, 1970; Hale, 1987; McElhinny and Evans, 1968; Schwartz and Simons, 1969; Smirnov and Tarduno, 2003; Smirnov *et al.*, 2003, 2005; and Selkin *et al.*, 2000.

AU15

p0680 The saw-tooth was originally epitomized by the long-term decreasing trends observed in the Matuyama, one toward the Brunhes, one toward the Olduvai, and in the Gauss, one toward the Kaena, and one toward the Matuyama boundaries. The saw-tooth envisioned by Valet *et al.* (2005; see

SINT-2000 in **Figure 25**), however, is a shorter trend immediately preceding the reversal boundary. We will refer to this, more restricted view as the 'short saw-tooth' hypothesis in the following. First, we review the debate about the saw-tooth in the literature.



f0125 **Figure 25** The paleointensity record from ODP Leg 138 cores (Valet and Meynadier, 1993) showed the ‘asymmetric sawtooth pattern’, whereas other records which reached the Gauss–Matuyama boundary do not show such pattern: Ontong-Java Plateau stack of Kok and Tauxe (1999) and equatorial Pacific Paleointensity Stack of Yamazaki and Oda (2005).

p0685 While all transitional records with paleointensity data have low field intensities associated with transitional directions, not all records display a long-term decreasing trend toward a reversal. Arguments supporting the existence of the saw-tooth pattern were presented in rapid succession. Valet *et al.* (1994) examined paleointensity records near the Brunhes–Matuyama transition from the Atlantic, Indian, and Pacific Oceans, and found the rapid intensity growth after the transition. Meynadier *et al.* (1994) recognized the ‘saw-tooth pattern’ in a relative paleointensity record spanning the last 4 My obtained from a core in the Indian Ocean. Verosub *et al.* (1996) presented a record focused near the MBB and the Jaramillo Subchron of a sediment core from the central north Pacific which supported the ‘saw-tooth pattern.’

p0690 Counter arguments to the saw-tooth also began to appear. For example, Laj *et al.* (1996a, 1997 (for correction)) failed to see the ‘saw-tooth pattern’ utilizing the same core as that of Verosub *et al.* (1996) when examining a longer period of time up to the Olduvai Subchron. Laj *et al.* (1996b) reported that no rapid intensity increase after polarity transitions was observed in

relative paleointensity records from two Late Miocene sections in Crete (Kotsiana and Potamida in **Table 2**).

Arguments against the ‘saw-tooth pattern’ were **p0695** presented also from paleointensity estimations based on recording mechanisms different from sediments. Records of $^{10}\text{Be}/^9\text{Be}$ reflect geomagnetic paleointensity through a control on the production rate of the cosmogenic nuclide (^{10}Be). Raisbeck *et al.* (1994) argued that a $^{10}\text{Be}/^9\text{Be}$ record at Site 851 of ODP Leg 138, which is the same site as of Valet and Meynadier (1993), is inconsistent with the ‘saw-tooth pattern.’ Westphal and Munsch (1999) showed that the ‘saw-tooth pattern’ cannot explain the shape of stacked magnetic anomaly profiles over the East Indian Ridge, Juan de Fuca Ridge, and East Pacific Rise. McFadden and Merrill (1997) presented an analysis of the Cenozoic polarity reversal chronology that effective inhibition of a future reversal can only last for about 50 ky at most, which contradicts the ‘saw-tooth pattern’ requiring much longer inhibition.

The ‘saw-tooth pattern’ was also questioned from **p0700** remanent magnetization acquisition processes. Kok and Tauxe (1996a) proposed a cumulative viscous

remanence model for remanence acquisition of sediments that can yield intensity variations like the ‘saw-tooth’ pattern. Then, Kok and Tauxe (1996b) reproduced the ‘saw-tooth pattern’ of the ODP Leg 138 sediments by the cumulative viscous remanence model using the values of the equilibrium magnetization constrained by results of a Thellier-type paleointensity experiments applied to the ODP Leg 138 sediments. Furthermore, they resampled the Site 851 sediments near the Gauss–Gilbert boundary and showed that the ‘saw-tooth pattern’ disappeared by thermal demagnetization to 400° C.

p0705 Meynadier *et al.* (1998) made a counterargument to the cumulative viscous remanence model of Kok and Tauxe (1996a, 1996b). They suggested that to produce the saw-tooth pattern and to preserve the magnetostratigraphy with the cumulative viscous remanence model, a very narrow distribution of the relaxation times is required. They also showed that the saw-tooth pattern of the Site 851 sediments did not change by thermal demagnetization and AF demagnetization of stronger fields, which is inconsistent with the result of Kok and Tauxe (1996b) despite using the sediments from the same site. Kok and Tauxe (2000) on the comments to Meynadier *et al.* (1998) stressed the nonuniqueness of relaxation time distribution explaining the ‘saw-tooth pattern’, and pointed out that the τ distribution of Kok and Tauxe (1996b) is not all relaxation times present in the sediments, but merely a part of them that behave viscously. In the reply, Meynadier and Valet (2000) mentioned that the remanent magnetization with blocking temperatures between 150 and 300° C which may carry cumulative viscous remanence is only minor part of NRM of the sediments. The two groups also argued about the validity of thermal demagnetization on relative paleointensity estimation from sediments (Kok and Tauxe, 1999; Valet and Meynadier, 2001; Kok and Ynsen, 2002).

p0710 Mazaud (1996) proposed another model of magnetization acquisition which produces the ‘saw-tooth pattern’: a large fraction (say, two-thirds) of magnetic grains acquires NRM at deposition time while remaining grains reorientate or acquire magnetization after deposition. Although Meynadier and Valet (1996) considered this model unlikely from the knowledge of pDRM acquisition processes prevailing at that time, recent studies suggest that this model may have difficulties. As discussed in Section 5.13.4, the depth lag of pDRM acquisition is estimated to be very small (~2 cm) from the compilation of B/M boundary positions and the oxygen-isotope

chronology recorded in marine carbonate cores with various sedimentation rates (Tauxe *et al.*, 1996). An experiment of Katari *et al.* (2000) using natural undisturbed sediments suggests that pDRM (reorientation of magnetic particles) is a rare phenomenon, probably because of the effects of flocculation: magnetic minerals would be aggregated with clay.

In the 851 record of Valet and Meynadier (1993), p0715 the ‘saw-tooth pattern’ is most apparent in the early Matuyama Chron after the Gauss–Matuyama transition and during the Gauss Chron. The number of paleointensity records reported so far that reached the Gauss–Matuyama transition is still small. However, available records from different groups do not support the ‘saw-tooth pattern’: neither a stacked record since 2.8 Ma from the Ontong-Java Plateau (Kok and Tauxe, 1999; OJP-stack in Figure 25) nor a stacked record since 3.0 Ma from the equatorial Pacific (Yamazaki and Oda, 2005; EPAPIS stack in Figure 25) shows variations like the ‘saw-tooth pattern’ after the Gauss–Matuyama transition.

We do not yet understand well the rock-magnetic processes which produce the ‘saw-tooth pattern’ only for some sediments. If the DRM acquisition model of Mazaud (1996) works in general, all sedimentary paleointensity records should display ‘saw-tooth’-like changes. From the cumulative viscous remanence model of Kok and Tauxe (1996a), the sediments producing the ‘saw-tooth pattern’ are expected to have a particular magnetic grain-size distribution favorable for the long-term viscous remanence acquisition, but this has not yet been fully tested.

Recently, Valet *et al.* (2005) used 10 of the 15 records of relative paleointensity data compiled by Guyodo and Valet (2006) to create the so-called SINT-2000 stack (see Table 2 and Figure 25). Based on this subset of the data, Valet *et al.* (2000) argue for the ‘short saw-tooth’ pattern in the 80 ky interval immediately prior to the four reversals included in the stack. Of the four reversals in the SINT-2000 stack (figure 4 of Valet *et al.*, 2000), only the Upper Jaramillo and the lower Olduvai show convincing short saw-tooth patterns.

Relative paleointensity records spanning the last 2 My have steadily been produced (see, e.g., Table 2). Because the SINT-2000 is a stack which did not include many of the records in Table 2, we have plotted those records that span at least the period from 800 to 900 ky in Figure 26 for the interval including the Brunhes and Jaramillo. Considering all the records, it appears that even the short saw-tooth is only observed in a small subset of the records, although

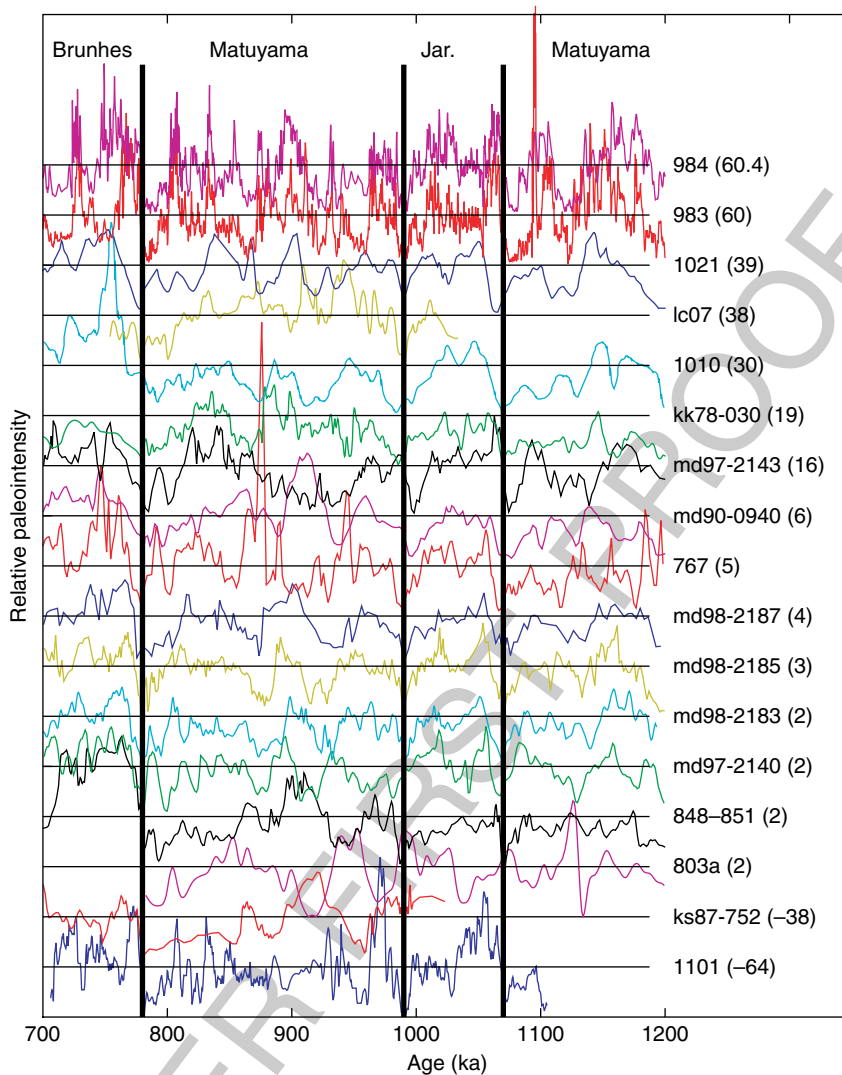


Figure 26 Plot of all records spanning at least the period from 800 to 900 ka in the MagIC database (see **Table 2**) for the range 700–1200 ka. Records are plotted in order of latitude (in parentheses to right of record name). The positions of the Matuyama/Brunhes, and the upper and lower Jaramillo transitions are indicated by heavy black lines.

an intensity peak just after the B/M boundary (Guyodo and Valet, 1999; Valet *et al.*, 2005) does appear in all records. In general, the long-term saw-tooth pattern originally observed by Valet and Meynadier (1993) has not been universally observed, as would be expected from the behavior of a dipole source.

(e.g., Hays *et al.*, 1976). Yet oxygen-isotope stratigraphy has its drawbacks. It cannot be applied in sediments deeper than the carbonate compensation depth or lakes. Oxygen-isotopic data are often difficult to interpret in marginal seas, where records may not reflect global ice-volume changes. Finally, temporal resolution better than 10^4 yr is critical for assessing the global nature of climatic events and their durations. The prospect of using relative paleointensity from sediments as a high-resolution correlation and dating tool has therefore been met with great enthusiasm (e.g., Stott *et al.*, 2002). Here we examine the prospects and problems with so-called ‘paleointensity-assisted chronology’ or PAC.

s0205 5.13.8.4 High-Resolution Temporal Correlation

s0210 5.13.8.4.1 Sediments

p0735 Oxygen-isotope stratigraphy revolutionized paleoceanography by providing a global signal with a resolution on the order of tens of thousands of years

p0740 The importance of PAC is not simply as a substitution for $\delta^{18}\text{O}$. It can also be used to examine consistency of other chronologies such as $\delta^{18}\text{O}$ and ^{14}C , because it is quasi-independent of them. Regional and global inter-core correlations tied by paleointensity variations revealed discrepancies of up to several thousand years between those based on ^{14}C and $\delta^{18}\text{O}$ (Stoner *et al.*, 1995), and between GISP2 and the $\delta^{18}\text{O}$ chronologies (Stoner *et al.*, 1995, 2000) during the last *c.* 100 ky. Moreover, paleointensity stratigraphy can have higher resolution than $\delta^{18}\text{O}$ stratigraphy because the variations contain shorter-wavelength components than those of $\delta^{18}\text{O}$. Truly dipolar features of geomagnetic field variations have a potential for providing a time reference for an inter-hemisphere paleoclimatic relationship with unprecedented resolution.

p0745 On a more limited scale, there is a possibility that inter-core correlation and age estimation can be performed using paleointensity by correlating patterns among cores with a standard curve such as SINT-800 (Guyodo *et al.*, 2001) and NAPIS-75 (Laj *et al.*, 2000), which is exemplified by Stoner *et al.* (1995; reference # 71 in Table 2) in the Labrador Sea, Demory *et al.* (2005; reference # 16 in Table 2) in the Lake Bikal, and Macri (2005; reference # 43 in Table 2) in the Wilkes Land Basin off Antarctica.

p0750 We feel that while regional correlations can be achieved, much is lost by using PAC as a primary dating tool. These records can no longer be used to constrain paleointensity models or global stacks, because the age information is not independent and features correlate by assumption. Such records have been clearly labeled in Table 2 (RPI) and in the MagIC database.

p0755 If we desire a global correlation tool, we require a dipolar signal. However, it is as yet unclear at which wavelength the dipole terms give way to nondipole terms. Korte and Constable (2005) caution us that variations in VADMs may not be global and their variations need not be synchronous because they can be strongly influenced by nondipole field effects. Moreover, the duration of a polarity reversal is known to be dependent on latitudes, ranging from about 2 ky near the equator to 10 ky at $\pm 60^\circ$ (Clement, 2004). Furthermore, the contribution of nondipole effects are probably higher when paleointensity is low, and both the duration and shape of a particular paleointensity low will be site dependent.

p0760 Doubts about the global nature of paleointensity features notwithstanding, global inter-core correlations on a millennial scale have been attempted.

A series of papers by Channell *et al.* (2000), Stoner *et al.* (2000), and Mazaud *et al.* (2002) correlated records between the high latitudes of the North Atlantic and the South Atlantic and Indian Ocean sectors. As an example of the method, we show the records of Stott *et al.* (2002), who tied cores together between the North Atlantic and the western equatorial Pacific (see Figure 27). The large-scale features (labeled H1–H10 and L1–L8 correlate reasonably well and are consistent with the oxygen-isotopic records from the two cores. These allow correlation with a resolution of 2–3 ky. The difficulty of identifying global features on a submillennial scale is made apparent by the rather unconvincing correlation of features marked by the stars. Although these features may well be synchronous, they do not resemble each other very much in the two hemispheres and without the excellent and very detailed chronological control of the independent oxygen-isotopic records, their identification would not have been possible. How much should these ‘millennial’ features look like each other and how synchronous they are expected to be requires much more detailed knowledge of the process of secular variation, a topic of active research (*see* 00092).

5.13.8.4.2 Ridge crest processes

The potential of paleointensity for high-resolution dating is not restricted to sediments. Thellier-type paleointensity data can be used to estimate ages of basalts near mid-ocean ridges, and it is expected that paleointensity will be useful for studying crustal accretion processes at ridges (Gee *et al.*, 2000; Ravilly *et al.*, 2001; Bowles *et al.*, 2006). This work is discussed in more detail by Gee and Kent (*see* 00097).

5.13.8.5 Atmospheric Interaction

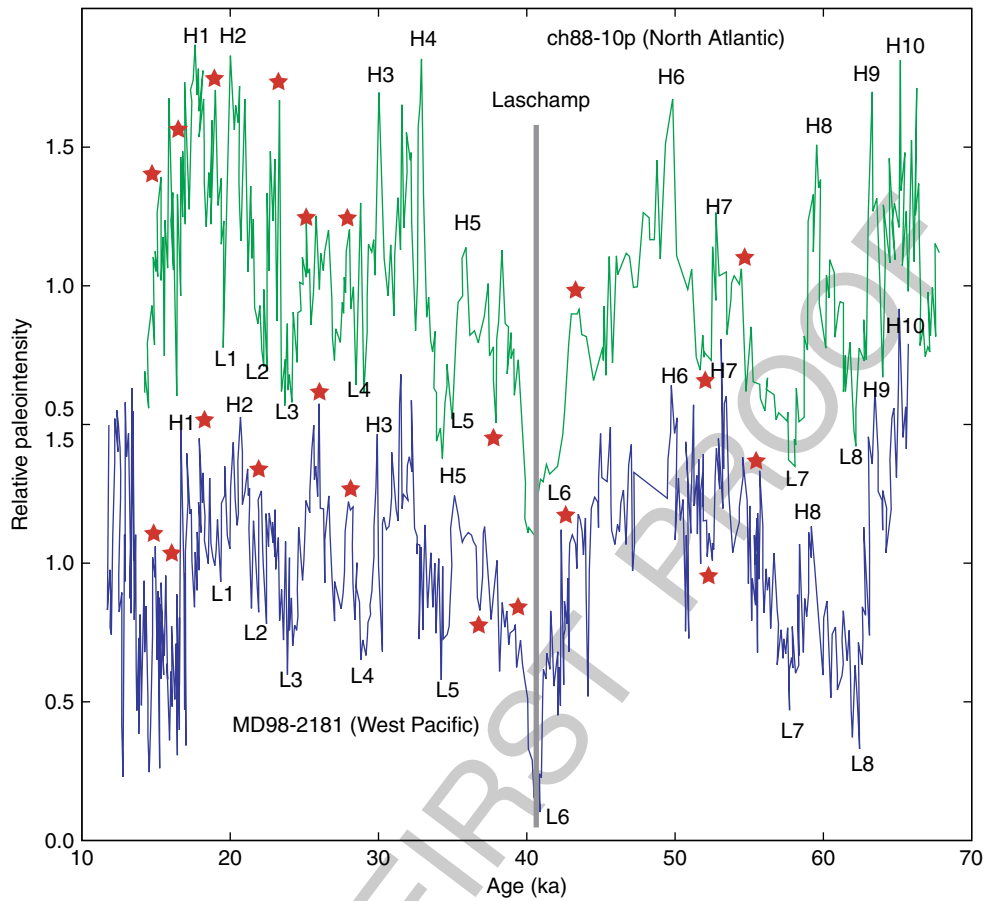
Radioactive forms of carbon, beryllium, and chlorine are produced in the atmosphere by cosmic ray bombardment. The decay of these isotopes is used for dating purposes in a wide variety of disciplines. There are large variations in ages predicted from tree ring, varve, ice layer counting or U/Th dating, and those estimated by radiocarbon dating. An example of such a comparison is shown in Figure 28(a) which shows the age based on ^{14}C dating from a core in the Cariaco Basin versus layer counting in the Greenland Ice Sheet Project 2 (GISP2) ice core from a core in the Cariaco Basin (Hughen *et al.*, 2004). The correlation of the marine sediment core

s0215

p0765

s0220

p0770



f0135 **Figure 27** Comparison of deep-sea sediment relative paleointensity records from md81-2181 and the North Atlantic Ocean site ch88-10p. The two records were dated by correlation of their individual oxygen-isotopic stratigraphies to the GISP2 record. Distinctive paleointensity highs (H1–10) and lows (L1–8) are identified in the two records. Less-convincing features (stars) are marked as well. The ages of the named features are synchronous to within an uncertainty of less than ± 500 years. The ‘Laschamp Excursion’ correlates with a distinctive ^{36}Cl excursion in the GISP2 record and provides an independent tie point to ice cores. Figure redrawn from supplement to Stott L, Poulsen C, Lund S, and Thunell R (2002) Super ENSO and global climate oscillations at millennial time scales. *Science* 297: 222–226.

to the ice core was based on tying dark sedimentary layers to interstadials in the GISP2 core.

p0775 The difference between radiocarbon and other age estimates in **Figure 28(a)** is used to calculate variations in initial radiocarbon in the atmosphere relative to the concentration in the modern atmosphere (see atmospheric $\Delta^{14}\text{C}$ plotted as dots in **Figure 28(b)**). An excess of radiocarbon (positive $\Delta^{14}\text{C}$) results in an underestimation of the age because there is ‘too much’ radiocarbon in the sample for its age. Changes in $\Delta^{14}\text{C}$ have been attributed to differences in the production of radiocarbon in the atmosphere by cosmic ray bombardment and changes in the carbon balance between the atmosphere and the deep ocean, which is a reservoir of old carbon (see, e.g., Bard *et al.*, 1990). If, for example, the transfer

of atmospheric carbon into the ocean was less efficient in the past or the release of old carbon from the deep ocean was less efficient (‘ventilation’ was slower), then there would be an excess of radiocarbon in the atmosphere relative to the modern atmosphere, resulting in ‘too young’ ^{14}C ages.

Radiocarbon production is thought to be strongly p0780 controlled by changes in magnetic field strength because the magnetic field shields the atmosphere from cosmic rays (see 00092). Changes in the intensity of the magnetic field should therefore result in changes in radiocarbon production (among other things); hence, the variation in intensity is a key parameter in deriving accurate age information. Hughen *et al.* (2004) used a paleointensity stack from the North Atlantic (the NAPIS stack of Laj

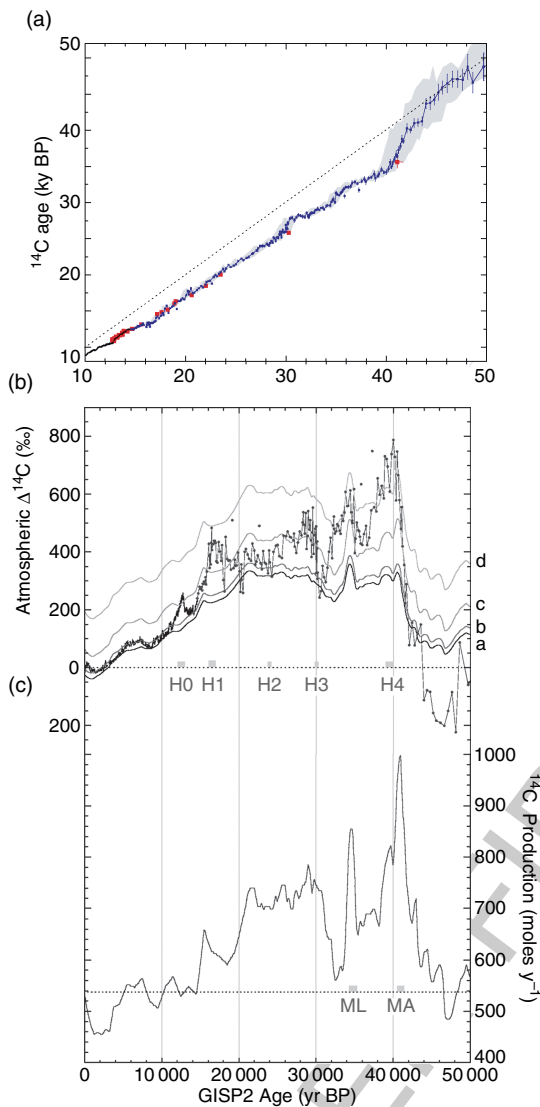


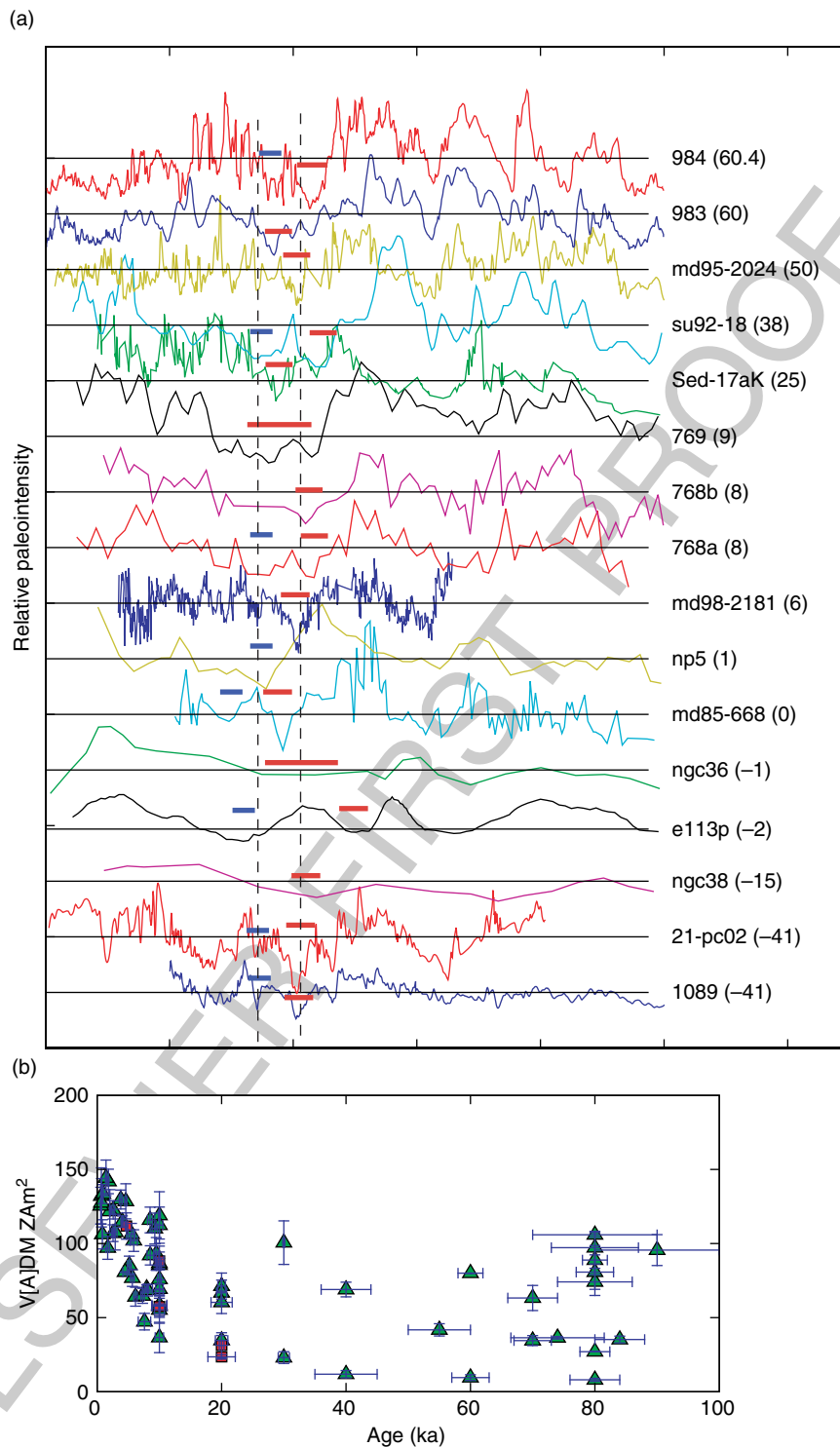
Figure 28 (a) Radiocarbon calibration data from Cariaco ODP Leg 165, Holes 1002D, and 1002E (blue circles), plotted versus calendar age assigned by correlation of detailed paleoclimate records to the Greenland Ice Core GISP2. The thin black line is high-resolution radiocarbon calibration data from tree rings joined at 12 cal. k BP to the varve counting chronology. Red squares are paired ^{14}C -U/Th dates from corals. Light gray shading represents the uncertainties in the Cariaco calibration. The radiocarbon dates are 'too young', falling well below the dashed line of 1:1 correlation. (b) Compilation of data interpreted as production rate changes in radiocarbon ($\Delta^{14}\text{C}$) versus calendar age (symbols same as in (a)). (c) Predicted variation of $\Delta^{14}\text{C}$ from the geomagnetic field intensity variations from sediments of the north Atlantic (Laj *et al.*, 2000) using the model of Masarik and Beer (1999). Figure modified from Hughen K, Lehman S, Southon J, *et al.*, (2004) C-14 activity and global carbon cycle changes over the past 50,000 years. *Science* 303(5655): 202–207.

et al., 2000) as a proxy for changes in the dipole moment of the Earth's magnetic field over the last 70 ky. By using the Monte Carlo simulations of the relationship between geomagnetic field strength and radiocarbon production of Masarik and Beer (1999), Hughen *et al.* (2004) predicted radiocarbon production for the past 50 ky (Figure 28(c)). The different curves in Figure 28(b) (a–d) use the predicted radiocarbon production values as input into box models using different ocean/atmosphere boundary conditions relating to different models of deep-sea ventilation, resulting in different estimates for atmospheric $\Delta^{14}\text{C}$.

None of the curves in Figure 28(b) based on the model predictions using the NAPIS stack provide a satisfactory fit to the observed variations. Hughen *et al.* (2002) suggested that either the model of Masarik and Beer (1999) for translating geomagnetic field intensity to radiocarbon production is incorrect at low field strengths or that our understanding of the global carbon cycle is insufficient. It is of course also possible that the NAPIS model of North Atlantic relative paleointensity is a poor proxy for the global paleomagnetic field intensity variations. We explore the latter in the following.

The NAPIS stack (compilation #34 in Table 2) based on a number of relative paleointensity records in the North Atlantic and as such it is a regional stack. Variations in cosmic ray bombardment are largely controlled by the strength of the dipole term, the estimation of which requires global coverage. In Figure 29 we plot all the records in the MagIC database that have independent age control based on oxygen isotopes. Hughen *et al.* (2004) labeled two peaks in predicted radiocarbon production 'LA' and 'ML' for the Laschamp and Mono Lake excursions (see Laj *et al.* (2000) for correlations) at 41 and 34 ka, respectively. Although excursions are defined on the basis of anomalous directions, they are thought to be related to low field strengths and decreases in paleointensity (DIPs) are frequently correlated to excursions (e.g., Guyodo and Valet, 1999).

The '41' and '34' ky ages are also marked in Figure 29(a) and the nearest DIPs are marked with red and blue bars for the so-called LA and ML features, respectively. Many records in the figure show only one DIP, or a broad low-paleointensity zone. The age agreement is rather poor. In particular, the two records from ODP Site 983 and 984 (see Table 2) were taken from very close to one another and have quite different character in the 41 ka DIP with 984 showing two distinct DIPs, but 983 only



f0145 **Figure 29** (a) Relative paleointensity records spanning the last 100 ky with independent age control based on $\delta^{18}\text{O}$. The solid red bars indicate intensity lows that are possibly related to the 'Laschamp Excursion' and the blue bars are a later paleointensity low, sometimes referred to as the 'Mono Lake Excursion.' (b) Absolute paleointensity data with age uncertainties of less than 20% meeting the 'strict' selection criteria (see text).

one. Moreover, Kent *et al.* (2002) argue that the Mono Lake is actually 38–41 ka and that it may well have the same feature as the Laschamp. Finally, as was discussed in Section 5.13.4, the response of sedimentary relative paleointensity may not be linear with the applied field and the amplitudes could be biased.

p0800 The absolute paleointensity data from the PINT06 database (with $\sigma_s < 15\%$ of the mean or $< 5 \mu\text{T}$) that had reasonable age uncertainties (better than 20%) are shown in **Figure 29(b)**. There is generally high scatter prior to about 15 ka, but after that there is a sharp upward trend toward the present.

p0805 While both the relative and absolute paleointensity data support a general period of low intensity spanning from perhaps 20 ka to as much as 50 ka, the details are at best unclear. There are not enough data to establish the existence of both the Mono Lake and the Laschamp as two separate globally observed excursions.

p0810 Rough agreement of paleointensity patterns between predictions based on cosmogenic radionuclide production rates and sedimentary relative paleointensity has been reported also for older ages: ^{36}Cl flux in GRIP Ice Core for the past 100 ky (Baumgartner *et al.*, 1998), a global ^{10}Be stack of the last 200 ky (Frank *et al.*, 1997), and $^{10}\text{Be}/^9\text{Be}$ -based paleointensity during the last 300 ky in the North Atlantic and from 500 to 1300 ka in the western equatorial Pacific (e.g., Carcaillet *et al.*, 2004). These results show the potential of ^{10}Be for providing independently geomagnetic field intensity information for the past several million years, although uncertainty originating from transportation and sedimentation processes of the radionuclide still remains (e.g., Christl *et al.*, 2003; McHargue and Donahue, 2005).

p0815 Overall, variations in dipole intensity are not as well constrained as we would like. As these variations are key to refining the radiocarbon calibration, more records with independent and accurate age constraints are needed.

s0225 5.13.8.6 Frequency of Intensity Fluctuations and the Climatic Connection

p0820 Arguments regarding the possible relationship between the intensity of the geomagnetic field and climate have a long history of more than 30 years (e.g., Wollin *et al.*, 1971). Discussions in the 1970s were based on the remanent intensity variations which were not corrected for differences in magnetizability of sediments. The relationship was convincingly rejected by Kent (1982), who showed that the remanent intensity variations of the relevant sediment cores were controlled by climatically

induced variations in carbonate contents. Kent and Opdyke (1977) were the first to suggest the presence of the obliquity frequency, ~ 43 ky in a normalized intensity record, but this idea was not seriously discussed at that time.

Rapid progress in relative paleointensity studies p0825 revived the orbital modulation issue in the late 1990s, and it has been heatedly argued since then. Tauxe and Shackleton (1997) found significant power in the power spectrum of a record from the Ontong-Java Plateau in the 30–50 ky band, but showed that the intensity fluctuations came in and out of phase of the associated oxygen-isotopic record, arguing against a strong relationship between climate and paleointensity. In contrast, Channell *et al.* (1998) and Channell (1999) proposed a ~ 40 ky obliquity frequency from a power spectrum analysis of their relative paleointensity records during the Brunhes Chron obtained from ODP Sites 983 and 984 in the North Atlantic. They interpreted it as geomagnetic field behavior from the observations that no power exists at ~ 40 ky in bulk magnetic properties and there is no coherence between the relative intensity and the normalizer (IRM), percent carbonate, and a magnetic grain-size proxy at ~ 40 ky. Their paleointensity records showed significant power also at the ~ 100 ky eccentricity frequency, but they rejected this because this frequency was observed also in bulk magnetic properties. Yamazaki (1999) instead proposed the possible presence of the ~ 100 ky frequency in his relative paleointensity records from the North Pacific based on the same logic as that of Channell *et al.* (1998): occurrence of ~ 100 ky power in relative paleointensity but not in the normalizer on the power spectra. Yokoyama and Yamazaki (2000) applied a wavelet analysis to five paleointensity records from the Pacific Ocean reported in Yamazaki *et al.* (1995) and Yamazaki (1999), and found a quasi-period of ~ 100 ky. They considered the ~ 100 ky period inherent to the geomagnetic field, because of the good coincidence of the relative intensity records in this scale despite significant phase differences in magnetic properties. Thouveny *et al.* (2004) reported a ~ 100 ky period in a paleointensity record during the last 400 ky from Portuguese Margin sediments, North Atlantic. Possible occurrence of 100 ky period in paleointensity would not be limited in the Brunhes Chron: Yamazaki and Oda (2005; see **Figure 30**) found significant power at ~ 100 ky period in paleointensity records from 0.8 to 3.0 Ma. Kok and Tauxe (1999) found point at ~ 150 ky in paleointensity

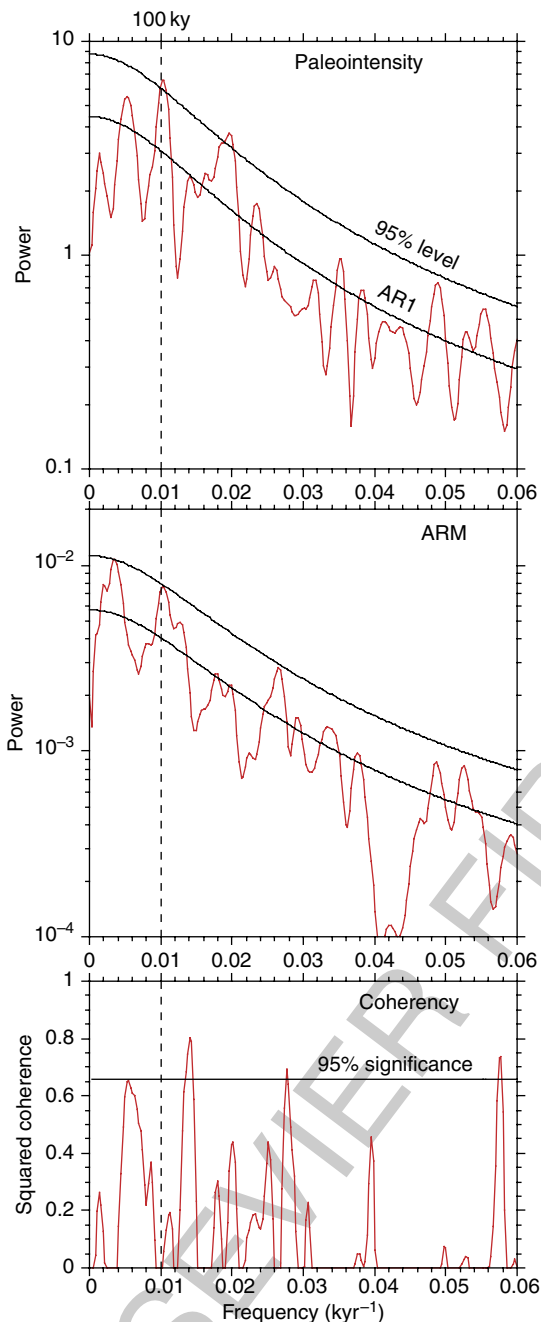


Figure 30 Power spectra of relative paleointensity and the normalizer (ARM), and cross-correlation between them of Core MD982187 in the western equatorial Pacific between 0.8 and 3.0 Ma (Yamazaki and Oda, 2005). This core is one of six cores which was used to construct the EPAPIS-3 Ma curve shown in **Figure 25** and covers the longest period of time among them. The relative paleointensity variations contain quasi-period of ~ 100 kyr, but no significant correlation between relative paleointensity and the normalizer. The statistical significance of the spectral peaks was tested against the red-noise background from a first-order autoregressive (AR1) process, and the 95% confidence level is indicated.

records during the Matuyama Chron from the Ontong-Java Plateau.

Whether the orbital frequencies found in sedimentary paleointensity records reflect geomagnetic field behavior or not has been discussed mainly on the following three points: significance and stability of the orbital periodicities, error in age control, and lithological contamination to paleointensity records. Guyodo and Valet (1999) argued that there is no stable periodicity during the Brunhes Chron by a spectrum analysis on the SINT-800 stack using sliding windows. However, the orbital modulation may be a nonstationary process. Sato *et al.* (1998) suggested that there is no constant period but continuous shifts between 50 and 140 ky based on a stacked paleointensity record from three cores in the western equatorial Pacific during the last 1.1 My. Horng *et al.* (2003) argued that the orbital frequencies in paleointensity variations are not statistically significant by applying a wavelet analysis on their relative paleointensity record during the last 2.14 My from the western Philippine Sea. On the other hand, Teanby and Gubbins (2000) proposed that the periodicities of several tens of thousand years observed from sedimentary paleointensity records could be due to aliasing, an artifact of coarse sampling, and simulated using archaeointensity data with a 2 ky period how false longer periods appear by aliasing. However, orbital periodicities have been reported even from sediment cores with significant variations in sedimentation rates, which is difficult to be explained by aliasing. Guyodo and Channell (2002) performed numerical simulation of paleointensity records with various sedimentation rates and variable quality of age control, and showed how spectral information is lost with decreasing sedimentation rates: the power spectra are reliable for periods as short as 4 ky in records with a sedimentation rate of 15 cm ky^{-1} with good age control, whereas periods of only $c. 50$ ky or longer are reliable in records with a sedimentation rate of 1 cm ky^{-1} . McMillan *et al.* (2002, 2004) evaluated effects of various sources of errors such as dating errors, misidentified tiepoints, changes in sedimentation rate, and the effect of non-dipole components. They simulated coherence of records among various sites, and evaluated the accuracy of a stacked record suggesting that dipole variations with periods of longer than 20 ky can be recovered (but shorter ones would be problematic).

Strong arguments against orbital modulation of the geomagnetic field come from possible lithological contamination to sedimentary paleointensity records.

Because paleointensity records during the last 200 ky look coherent with the oxygen-isotope curve, Kok (1999) suspected that sedimentary paleointensity records including those derived from ^{10}Be are controlled by paleoclimate due to inadequate normalization. Guyodo *et al.* (2000) performed a wavelet analysis on the records of paleointensity and magnetic properties from ODP Site 983, which was the same data set as those from which Channell *et al.* (1998), and Channell and Kleiven (2000) proposed the ~ 41 ky periodicity. They found that relative paleointensity has coherency with the normalizer and a magnetic grain-size proxy (ARM/k), and concluded that orbital frequencies in paleointensity records may be the expression of lithological variations.

p0840 At present, we cannot exclude a possibility that relative paleointensity estimation is significantly influenced by an unknown rock-magnetic mechanism which amplifies effects of minor variations in magnetic properties, because the mechanism of remanent-magnetization acquisition of sediments has not yet been fully understood, and no natural sediments are completely free from lithological variations induced by environmental changes. If variations of magnetic properties of sediments such as magnetic grain size and mineralogy contain the orbital periodicities and show coherence with paleointensity changes, this suggests the possible contamination of magnetic property changes to paleointensity records. However, this cannot exclude the possibility of orbital modulation of paleointensity, because the two can also have coherency if the orbital parameters affect both the geomagnetic field and depositional environment. To solve the problem, it is necessary to understand quantitative relation between the magnitude of magnetic property (e.g., magnetic grain size and mineralogy) changes and the magnitude of induced changes in normalized intensity. At present, we cannot even predict whether normalized intensity increases or decreases when magnetic grain size increases in a certain grain-size range. It is also important to examine phase relationships in coherency analyses. Patterns of lithological and magnetic property variations induced by paleoclimatic changes may vary place to place; for example, magnetic grain size would increase in a certain period of time in some areas, but in other areas it would decrease in the same period of time. Paleointensity, on the other hand, should be globally synchronous. Thus, even when paleointensity and magnetic property variations have coherency, lithological contamination is suggested to be minor if the

phase angles between the two from various places differ significantly.

On the possibility of orbital modulation of the p0845 geomagnetic field, a relationship of excursions and reversals with paleoclimate has also been discussed since 1970s. Rampino (1979, 1981) suggested that excursions may have occurred at about 100 ky intervals, and the ages of the excursions seem to coincide with times of peak eccentricity of the Earth's orbit (but see Rampino and Kent, 1983). Worm (1997) revisited the problem, and suggested that excursions and reversals tend to have occurred during periods of global cooling or during cold stages. He also gave an explanation to the intriguing observation that Arctic sediments seem to have recorded apparently longer duration of excursions (e.g., Nowaczyk *et al.*, 2001): larger sedimentation rates during glacials would cause a higher chance to record excursions if probability of excursions is higher during glacials. On the contrary, Kent and Carlut (2001) rejected the relationship. They concluded that six excursions in the Brunhes Chron and 21 reversals since 5.3 Ma have no tendency to occur at a consistent amplitude or phase of obliquity and eccentricity. Recently, the number of possible excursions during the Brunhes Chron have increased significantly (up to *c.* 20) (Lund *et al.*, 2001). Hence the problem of the possible connection between excursions and paleoclimate is not independent to the arguments on the orbital frequencies in relative paleointensity. Besides paleointensity and excursions, a discussion of orbital frequencies in paleomagnetic directions has been revitalized. Yamazaki and Oda (2002) reported a ~ 100 ky periodicity in an inclination record during the last 2.2 My from the western equatorial Pacific, whereas Roberts *et al.* (2003) concluded that it is not statistically significant.

As noted in Section 5.13.4, there can be a 'stealth' p0850 link between lithological factors, like clay content, which are controlled by climate and the relative paleointensity records which would be difficult to detect using the standard methods of normalization. To date, the significance and implications of possible climatic controls on paleointensity have not yet been adequately addressed.

5.13.9 Conclusions

s0230

Scientists have dreamed of analyzing the ancient p0855 magnetic field intensity for over four centuries. Since the first serious attempts to acquire paleointensity data in the 1930s, experimental design has

improved dramatically. The theoretical foundations for interpreting paleointensity data from both thermal and depositional remanences are steadily improving and there has been explosive growth in publications with paleointensity data. The data are slowly being contributed to the communal database whose scope has increased dramatically recently.

p0860 We have highlighted some of the major topics involving paleointensity data in this treatise. While these topics are still fresh and arguments abound, we can make the following statements regarding paleointensity:

1. Everyone agrees that more and better data could resolve many of the current debates. Experiments with built-in assessments of the fundamental assumptions of the method and the ability to estimate reliability indices are essential. Data sets are being contributed to the MagIC database, including measurements and full documentation of methods and data processing. This new generation of a database has the potential to go a long way toward settling some of the major issues discussed in this chapter.
2. In general, the ancient magnetic field has been highly variable on both short and long timescales. There have been extended periods of time with intensities lower than the present field but there have also been intervals with field strengths greater than the present field in the past. These periods of increased field strength may be related to the length of the polarity interval in which they are found.
3. The geomagnetic field in the Archean appears to have been 'alive and well.'
4. Arguments against the 'asymmetric saw-tooth' in paleointensity data associated with polarity reversals appear to be winning while arguments about the coherence of paleointensity with orbital frequencies and the ability to correlate globally paleointensity features on a millennial scale remain unresolved.

Acknowledgments

We thank the individuals who supplied data for the MagIC database compilation: J.E.T. Channell, C. Laj, Y. Guyodo, M. Perrin, L. Schnepf, J. Stoner, N. Thouveny, and J.-P. Valet. This work was in part supported by NSF Grant EAR 033-7399 and the Grant-in-Aid for Scientific Research

((A)(2) No. 16204034) of the Japan Society for the Promotion of Science to TY. Acknowledgment is also made to the donors of the American Chemical Society Petroleum Research Fund for partial support of this research.

References

- AU16
- Aitken MJ, Allsop AL, Bussell GD, and Winter MB (1988) Determination of the intensity of the Earth's magnetic field during archeological times: Reliability of the Thellier technique. *Reviews of Geophysics* 26: 3–12. b0005
- Anson GL and Kodama KP (1987) Compaction-induced inclination shallowing of the post-depositional remanent magnetization in a synthetic sediment. *Geophysical Journal of the Royal Astronomical Society* 88: 673–692. b0010
- Barbetti M (1977) Measurements of recent geomagnetic secular variation in southeastern Australia and the question of dipole wobble. *Earth and Planetary Science Letters* 36: 207–218. b0015
- Bard E, Hamelin B, Fairbanks RG, and Zindler A (1990) Calibration of the 14C timescale over the past 30,000 years using mass spectrometric U–Th ages from Barbados corals. *Nature* 345: 405–410. b0020
- Bassinot FC, Labeyrie LD, Vincent E, Quidelleur X, Shackleton NJ, and Lancelot Y (1994) The astronomical theory of climate and the age of the Brunhes–Matuyama magnetic reversal. *Earth and Planetary Science Letters* 126: 91–108. b0025
- Baumgartner S, Beer J, Masarik J, Wagner G, Meynadier L, and Synal H-A (1998) Geomagnetic modulation of the ³⁶Cl flux in the GRIP Ice Core, Greenland. *Science* 279: 1330–1331. b0030
- Ben Yosef E, Tauxe L, Ron H, et al. (2005) The intensity of the geomagnetic field during the last 6 millennia as recorded by slag deposits from archaeological sites in the Southern Levant. *EOS Transactions of the American Geophysical Union, Fall Meeting Supplement* 86(62): GP21A-0007. b0035
- Bender M, Sowers T, Dickson ML, et al. (1994) Climate correlations between Greenland and Antarctica during the past 100,000 years. *Nature* 372(6507): 663–666. b0040
- Besse J and Courtillot V (2002) Apparent and true polar wander and the geometry of the geomagnetic field over the last 200 Myr. *Journal of Geophysical Research* 107: 2300 (doi:10.1029/2000JB000050). b0045
- Biggin AJ, Böhnel HN, and Zuniga FR (2003) How many paleointensity determinations are required from a single lava flow to constitute a reliable average? *Geophysical Research Letters* 30(11): 1575. b0050
- Bleil U and von Dobeneck T (1999) Geomagnetic events and relative paleointensity records: Clues to high-resolution paleomagnetic chronostratigraphies of Late Quaternary marine sediments. In: Fischer G and Wefer G (eds.) *Use of Proxies in Paleoceanography: Examples from the South Atlantic*, pp. 635–654. Hiedelberg, Germany: Springer-Verlag. b0055
- Böhnel H, Biggin AJ, Walton D, Shaw J, and Share JA (2003) Microwave palaeointensities from a recent Mexican lava flow, baked sediments and reheated pottery. *Earth and Planetary Science Letters* 214(1–2): 221–236. b0060
- Bol'shakov A and Shcherbakova V (1979) A thermomagnetic criterion for determining the domain structure of ferrimagnetics. *Izvestiya, Physics of the Solid Earth* 15: 111–117. b0065
- Bol'shakov A and Solodnikov GM (1980) Paleomagnetic data on the intensity of the magnetic field of the Earth. *Izvestiya Earth Physics* 16: 602–614. b0070

- b0075** Bowles J, Gee J, Kent D, Bergmanis E, and Sinton J (2005) Cooling rate effects on paleointensity estimates in submarine basaltic glass and implications for dating young flows. *Geochemistry, Geophysics, Geosystems* 6: Q07002 (doi:10.1029/2004GC000900).
- b0080** Bowles J, Gee J, Kent DV, Perfit M, Soule A, and Fornari D (2006) Paleointensity applications to timing and extent of eruptive activity, 9°–10°N East Pacific rise. *Geochemistry, Geophysics, Geosystems* 7: Q06006 (doi:10.1029/2005GC001141).
- b0085** Bowles J, Tauxe L, Gee J, McMillan D, and Cande SC (2003) Source of tiny wiggles in Chron C5: A comparison of sedimentary relative intensity and marine magnetic anomalies. *Geochemistry, Geophysics, Geosystems* 4(6): 1049 (doi:10.1029/2002GC000489).
- b0090** Boyd M (1986) A new method for measuring paleomagnetic intensities. *Nature* 3196: 208–209.
- b0095** Brachfeld SA and Banerjee SK (2000) A new high-resolution geomagnetic relative paleointensity record for the North American Holocene: A comparison of sedimentary and absolute intensity data. *Journal of Geophysical Research* 105(B1): 821–834.
- b0100** Cande SC and Kent DV (1995) Revised calibration of the geomagnetic polarity timescale for the late Cretaceous and Cenozoic. *Journal of Geophysical Research* 100: 6093–6095.
- b0105** Carcaillet J, Bourles DL, Thouveny N, and Arnold M (2004) A high resolution authigenic ¹⁰Be/⁹Be record of geomagnetic moment variations over the last 300 ka from sedimentary cores of the Portuguese margin. *Earth and Planetary Science Letters* 219(3–4): 397–412.
- b0110** Carcaillet JT, Thouveny N, and Bourles DL (2003) Geomagnetic moment instability between 0.6 and 1.3 Ma from cosmnuclide evidence. *Geophysical Research Letters* 30(15): 1792.
- b0115** Carter-Stiglitz B, Jackson M, and Moskowitz B (2002) Low-temperature remanence in stable single domain magnetite. *Geophysical Research Letters* 29: 1129 (doi:10.1029/2001GL014197).
- b0120** Carter-Stiglitz B, Moskowitz B, and Jackson M (2003) Low-temperature remanence in stable single domain magnetite. *Geophysical Research Letters* 30(21): 2113.
- b0125** Carvallo C, Ozdemir O, and Dunlop DJ (2004) Palaeointensity determinations, palaeodirections and magnetic properties of basalts from the Emperor seamounts. *Geophysical Journal International* 156(1): 29–38.
- b0130** Channell JET (1999) Geomagnetic paleointensity and directional secular variation at Ocean Drilling Program (ODP) Site 984 (Bjorn Drift) since 500 ka: Comparisons with ODP Site 983 (Gardar Drift). *Journal of Geophysical Research* 104(B10): 22937–22951.
- b0135** Channell JET, Curtis JH, and Flower BP (2004) The Matuyama-Brunhes boundary interval (500–900 ka) in North Atlantic drift sediments. *Geophysical Journal International* 158(2): 489–505.
- b0140** Channell JET, Hodell DA, and Lehman B (1997) Relative geomagnetic paleointensity and ¹⁸O at ODP Site 983 (Gardar Drift, North Atlantic) since 350 ka. *Earth and Planetary Science Letters* 153: 103–118.
- b0145** Channell JET, Hodell DA, McManus J, and Lehman B (1998) Orbital modulation of the Earth's magnetic field intensity. *Nature* 394(6692): 464–468.
- b0150** Channell JET and Kleiven HF (2000) Geomagnetic palaeointensities and astrochronological ages for the Matuyama-Brunhes boundary and the boundaries of the Jaramillo Subchron: Palaeomagnetic and oxygen isotope records from ODP Site 983. *Philosophical Transactions of the Royal Society of London, Series A* 358(1768): 1027–1047.
- b0155** Channell JET, Mazaud A, Sullivan P, Turner S, and Raymo ME (2002) Geomagnetic excursions and paleointensities in the Matuyama Chron at Ocean Drilling Program Sites 983 and 984 (Iceland Basin). *Journal of Geophysical Research* 107(B6): 2114.
- Channell J, Stoner J, Hodell D, and Charles C (2000) Geomagnetic paleointensity for the last 100 kyr from the subantarctic South Atlantic: A tool for inter-hemispheric correlation. *Earth and Planetary Science Letters* 175: 145–160. **b0160**
- Chauvin A, Roperch P, and Levi S (2005) Reliability of geomagnetic paleointensity data: The effects of the NRM fraction and concave-up behavior on paleointensity determinations by the Thellier method. *Physics of the Earth and Planetary Interiors* 150(4): 265–286. **b0165**
- Christl M, Strobl C, and Mangini A (2003) Beryllium-10 in deep-sea sediments: A tracer for the Earth's magnetic field intensity during the last 200,000 years. *Quaternary Science Reviews* 22: 725–739. **b0170**
- Cisowski S and Fuller M (1986) Lunar paleointensities via the IRM(s) normalization method and the early magnetic history of the moon. In: Hartmann W, Phillips R, and Taylor G (eds.) *The Origin of the Moon*, pp. 411–421. Houston, TX: Lunar and Planetary Science Institute. **b0175**
- Clement BM (2004) Dependence of the duration of geomagnetic polarity reversals on site latitude. *Nature* 428(6983): 637–640. **b0180**
- Clement BM and Kent DV (1986) Short polarity intervals within the Matuyama: Transitional field records from hydraulic piston cored sediments from the North Atlantic. *Earth and Planetary Science Letters* 81: 253–264. **b0185**
- Coe RS (1967) The determination of paleo-intensities of the Earth's magnetic field with emphasis on mechanisms which could cause non-ideal behavior in Thellier's method. *Journal of Geomagnetism and Geoelectricity* 19: 157–178. **b0190**
- Coe RS, Grommé S, and Mankinen EA (1978) Geomagnetic paleointensities from radiocarbonated lava flows on Hawaii and the question of the Pacific nondipole low. *Journal of Geophysical Research* 83: 1740–1756. **b0195**
- Coffey W, Kalmykov Y, and Waldron J (1996) *World Scientific Series in Contemporary Chemical Physics, Vol. 11: The Langevin Equation with Applications in Physics, Chemistry and Electrical Engineering*. Singapore: World Scientific. **b0200**
- Collinson DW (1965) DRM in sediments. *Journal of Geophysical Research* 70: 4663–4668. **b0205**
- Constable CG, Tauxe L, and Parker RL (1998) Analysis of 11 Myr of geomagnetic intensity variation. *Journal of Geophysical Research* 103(B8): 17735–17748. **b0210**
- Constable C and Tauxe L (1996) Towards absolute calibration of sedimentary paleointensity records. *Earth and Planetary Science Letters* 143: 269–274. **b0215**
- Cottrell R and Tarduno J (1999) Geomagnetic paleointensity derived from single plagioclase crystals. *Earth and Planetary Science Letters* 169: 1–5. **b0220**
- Cottrell R and Tarduno J (2000) Late Cretaceous true polar wander: Not so fast. *Science* 288: 2283a. **b0225**
- Cox AV (1968) Lengths of geomagnetic polarity intervals. *Journal of Geophysical Research* 73: 3247–3260. **b0230**
- Cronin M, Tauxe L, Constable C, Selkin P, and Pick T (2001) Noise in the quiet zone. *Earth and Planetary Science Letters* 190: 13–30. **b0235**
- Dansgaard W, Johnsen S, Clausen H, et al. (1993) Evidence for general instability of past climate from a 250-kyr ice core record. *Nature* 364: 218–220. **b0240**
- Deamer GA and Kodama KP (1990) Compaction-induced inclination shallowing in synthetic and natural clay-rich sediments. *Journal of Geophysical Research* 95: 4511–4529. **b0245**
- Dekkers M and Bönhel H (2006) Reliable absolute paleointensities independent of magnetic domain state. *Earth and Planetary Science Letters* 248: 508–517. **b0250**

- [b0255](#) deMenocal PB, Ruddiman WF, and Kent DV (1990) Depth of p-DRM acquisition in deep-sea sediments – A case study of the B/M reversal and oxygen isotopic stage 19.1. *Earth and Planetary Science Letters* 99: 1–13.
- [b0260](#) Demory F, Nowaczyk NR, Witt A, and Oberhansli H (2005) High-resolution magnetostratigraphy of late Quaternary sediments from Lake Baikal, Siberia: Timing of intracontinental paleoclimatic responses. *Global and Planetary Change* 46(1–4): 167–186.
- [b0265](#) Denham CR and Chave AD (1982) Detrital remanent magnetization: Viscosity theory of the lock-in zone. *Journal of Geophysical Research* 87: 7126–7130.
- [b0270](#) Dinares-Turell J, Sagnotti L, and Roberts AP (2002) Relative geomagnetic paleointensity from the Jaramillo Subchron to the Matuyama/Brunhes boundary as recorded in a Mediterranean piston core. *Earth and Planetary Science Letters* 194(3–4): 327–341.
- [b0275](#) Dunlop D and Argyle K (1997) Thermoremanence, anhysteretic remanence and susceptibility of submicron magnetites: Nonlinear field dependence and variation with grain size. *Journal of Geophysical Research* 102: 20199–20210.
- [b0280](#) Dunlop DJ and Xu S (1994) Theory of partial thermoremanent magnetization in multidomain grains, 1 repeated identical barriers to wall motion (single microcoercivity). *Journal of Geophysical Research* 99: 9005–9023.
- [b0285](#) Dunlop D and Ozdemir O (1997) *Cambridge Studies in Magnetism: Rock Magnetism: Fundamentals and Frontiers*. Cambridge, UK: Cambridge University Press.
- [b0290](#) Evans HF and Channell JET (2003) Upper Miocene magnetic stratigraphy at ODP site 1092 (sub-Antarctic South Atlantic): Recognition of ‘cryptochrons’ in C5n.2n. *Geophysical Journal International* 153(2): 483–496.
- [b0295](#) Fabian K (2003) Some additional parameters to estimate domain state from isothermal magnetization measurements. *Earth and Planetary Science Letters* 213(3–4): 337–345.
- [b0300](#) Folgheraiter M (1899) Sur les variations séculaires de l’inclinaison magnétique dans l’antiquité. *Journal de Physique* 5: 660–667.
- [b0305](#) Fox JMW and Aitken MJ (1980) Cooling-rate dependence of thermoremanent magnetization. *Nature* 283: 462–463.
- [b0310](#) Frank M, Schwarz B, Baumann S, Kubik P, Suter M, and Mangini A (1997) A 200 kyr record of cosmogenic radionuclide production rate and geomagnetic field intensity from ¹⁰Be in globally stacked deep-sea sediments. *Earth and Planetary Science Letters* 149: 121–129.
- [b0315](#) Garcia AS, Thomas DN, Liss D, and Shaw J (2006) Low geomagnetic field intensity during the Kiaman superchron: Thellier and microwave results from the Great Whin Sill intrusive complex, northern United Kingdom. *Geophysical Research Letters* 33(16): L11701.
- [b0320](#) Gee J, Cande S, Hildebrand J, Donnelly K, and Parker R (2000) Geomagnetic intensity variations over the past 780 kyr obtained from near-seafloor magnetic anomalies. *Nature* 408: 827–832.
- [b0325](#) Genevey A and Gallet Y (2003) Eight thousand years of geomagnetic field intensity variations in the eastern Mediterranean. *Journal of Geophysical Research* 108: 2228 (doi:10.1029/2001JB001612).
- [b0330](#) Gibbs R (1985) Estuarine flocs: Their size, settling velocity and density. *Journal of Geophysical Research* 90: 3249–3251.
- [b0335](#) Goguitchaichvili A, Alva-Valdivia LM, Luis M, Rosas-Elguera J, Urrutia-Fucugauchi J, and Sole J (2004) Absolute geomagnetic paleointensity after the Cretaceous Normal Superchron and just prior to the Cretaceous–Tertiary transition. *Journal of Geophysical Research* 109: B01105 (doi:10.1029/2003JB002477).
- [b0340](#) Granot R, Tauxe L, Gee JS, and Ron H (in press) A view into the Cretaceous geomagnetic field from analysis of gabbros and submarine glasses. *Earth and Planetary Science Letters*.
- Grootes P and Stuiver M (1997) Oxygen 18/16 variability in Greenland snow and ice with 10⁻³ to 10⁵ year time resolution. *Journal of Geophysical Research* 102: 26455–26470.
- [b0345](#) Guyodo Y, Acton GD, Brachfeld S, and Channell JET (2001) A sedimentary paleomagnetic record of the Matuyama chron from the Western Antarctic margin (ODP Site 1101). *Earth and Planetary Science Letters* 191(1–2): 61–74.
- [b0355](#) Guyodo Y and Channell JET (2002) Effects of variable sedimentation rates and age errors on the resolution of sedimentary paleointensity records. *Geochemistry, Geophysics, Geosystems* 3: 1048.
- [b0360](#) Guyodo Y, Gaillot P, and Channell JET (2000) Wavelet analysis of relative geomagnetic paleointensity at ODP Site 983. *Earth and Planetary Science Letters* 184(1): 109–123.
- [b0365](#) Guyodo Y, Richter C, and Valet JP (1999) Paleointensity record from Pleistocene sediments off the California Margin. *Journal of Geophysics* 104: 22953–22965.
- [b0370](#) Guyodo Y and Valet JP (1999) Global changes in intensity of the Earth’s magnetic field during the past 800 kyr. *Nature* 399(6733): 249–252.
- [b0375](#) Guyodo Y and Valet JP (2006) A comparison of relative paleointensity records of the Matuyama Chron for the period 0.75–1.25 Ma. *Physics of the Earth and Planetary Interiors* 156: 205–212.
- [b0380](#) Haag M (2000) Reliability of relative palaeointensities of a sediment core with climatically-triggered strong magnetisation changes. *Earth and Planetary Science Letters* 180(1–2): 49–59.
- [b0385](#) Halgedahl S, Day R, and Fuller M (1980) The effect of cooling rate on the intensity of weak-field TRM in single-domain magnetite. *Journal of Geophysical Research* 85: 3690–3698.
- [b0390](#) Halls H and Davis D (2004) Paleomagnetism and UPb geochronology of the 2.17 Ga Biscotasing dyke swarm, Ontario, Canada: Evidence for vertical-axis crustal rotation across the Kapuskasing Zone. *Canadian Journal of Earth Sciences* 41: 255–269.
- [b0395](#) Harrison CGA (1966) The paleomagnetism of deep sea sediments. *Journal of Geophysical Research* 71: 3033–3043.
- [b0400](#) Hartl P and Tauxe L (1996) A precursor to the Matuyama/Brunhes transition- field instability as recorded in pelagic sediments. *Earth and Planetary Science Letters* 138: 121–135.
- [b0405](#) Hayashida A, Verosub KL, Heider F, and Leonhardt R (1999) Magnetostratigraphy and relative palaeointensity of late Neogene sediments at ODP Leg 167 Site 1010 off Baja California. *Geophysical Journal International* 139(3): 829–840.
- [b0410](#) Hays JD, Imbrie J, and Shackleton NJ (1976) Variations in the Earth’s orbit: Pacemaker of the ice ages. *Science* 194: 1121–1132.
- [b0415](#) Heller F and Liu T (1982a) Magnetostratigraphical dating of loess deposits in China. *Nature* 300: 431–433.
- [b0420](#) Herrero-Bervera E and Valet JP (2005) Absolute paleointensity and reversal records from the Waianae sequence (Oahu, Hawaii, USA). *Earth and Planetary Science Letters* 234(1–2): 279–296.
- [b0425](#) Hoffman KA and Biggin AJ (2005) A rapid multi-sample approach to the determination of absolute paleointensity. *Journal of Geophysical Research* 110: B12108 (doi:10.1029/2005JB003646).
- [b0430](#) Hoffman KA, Constantine VL, and Morse DL (1989) Determination of absolute palaeointensity using a multi-specimen procedure. *Nature* 339: 295–297.
- [b0435](#) Horng CS, Roberts AP, and Liang WT (2003) A 2.14-Myr astronomically tuned record of relative geomagnetic paleointensity from the western Philippine Sea. *Journal of Geophysical Research* 108(B1): 2059.

- b0440** Hughen K, Lehman S, Southon J, *et al.* (2004) C-14 activity and global carbon cycle changes over the past 50,000 years. *Science* 303(5655): 202–207.
- b0445** Imbrie J, Hays JD, Martinson DG, *et al.* (eds.) (1984) *Milankovitch and Climate, Part 1: The Orbital Theory of Pleistocene Climate: Support from a Revised Chronology of the Marine $\delta^{18}\text{O}$ Record*, Hingham, MA Reidel.
- b0450** Irving E (1964) *Paleomagnetism and Its Application to Geological and Geophysical Problems*. New York: John Wiley.
- b0455** Johnson EA, Murphy T, and Torreson OW (1948) Pre-history of the Earth's magnetic field. *Terrestrial Magnetism and Atmospheric Electricity* 53: 349–372.
- b0460** Johnson HP, Lowrie W, and Kent DV (1975) Stability of anhysteretic remanent magnetization in fine and coarse magnetite and maghemite particles. *Geophysical Journal of the Royal Astronomical Society* 41: 1–10.
- b0465** Juarez M and Tauxe L (2000) The intensity of the time averaged geomagnetic field: The last 5 m.y. *Earth and Planetary Science Letters* 175: 169–180.
- b0470** Juarez T, Tauxe L, Gee JS, and Pick T (1998) The intensity of the Earth's magnetic field over the past 160 million years. *Nature* 394: 878–881.
- b0475** Katari K and Bloxham J (2001) Effects of sediment aggregate size on DRM intensity: A new theory. *Earth and Planetary Science Letters* 186(1): 113–122.
- b0480** Katari K, Tauxe L, and King J (2000) A reassessment of post depositional remanent magnetism: Preliminary experiments with natural sediments. *Earth and Planetary Science Letters* 183: 147–160.
- b0485** Kent D, Hemming S, and Turrin B (2002) Laschamp excursion at Mono Lake? *Earth and Planetary Science Letters* 197: 151–164.
- b0490** Kent DV (1973) Post-depositional remanent magnetization in deep-sea sediment. *Nature* 246: 32–34.
- b0495** Kent DV (1982) Apparent correlation of paleomagnetic intensity and climatic records in deep-sea sediments. *Nature* 299: 538–539.
- b0500** Kent DV and Carlucci J (2001) A negative test of orbital control of geomagnetic reversals and excursions. *Geophysical Research Letters* 28(18): 3561–3564.
- b0505** Kent DV and Opdyke ND (1977) Paleomagnetic field intensity variation recorded in a Brunhes epoch deep-sea sediment core. *Nature* 266: 156–159.
- b0510** Kent DV and Schneider DA (1995) Correlation of paleointensity variation records in the Brunhes/Matuyama polarity transition interval. *Earth and Planetary Science Letters* 129: 135–144.
- b0515** King JW, Banerjee SK, and Marvin J (1983) A new rock magnetic approach to selecting sediments for geomagnetic paleointensity studies: Application to paleointensity for the last 4000 years. *Journal of Geophysical Research* 88: 5911–5921.
- b0520** King RF and Rees AI (1966) Detrital magnetism in sediments: An examination of some theoretical models. *Journal of Geophysical Research* 71: 561–571.
- b0525** Kirschvink JL (1980) The least-squares line and plane and the analysis of paleomagnetic data. *Geophysical Journal of the Royal Astronomical Society* 62: 699–718.
- b0530** Kissel C, Laj C, Labeyrie L, Dokken T, Voelker A, and Blamart D (1999) Rapid climatic variations during marine isotopic stage 3: Magnetic analysis of sediments from Nordic Seas and North Atlantic. *Earth and Planetary Science Letters* 171(3): 489–502.
- b0535** Kletetschka G, Acuna MH, Kohout T, Wasilewski PJ, and Connerney JEP (2004) An empirical scaling law for acquisition of thermoremanent magnetization. *Earth and Planetary Science Letters* 226(3–4): 521–528.
- b0540** Kletetschka G, Fuller M, Kohout T, *et al.* (2006) TRM in low magnetic fields: A minimum field that can be recorded by large multidomain grains. *Physics of the Earth and Planetary Interiors* 154: 290–298.
- Koenigsberger J (1936) Die abhaengigkeit der natuerlichen remanenten magnetisierung bei eruptivgesteinen von deren alter und zusammensetzung. *Beitriige zur Angewandte Geophysik* 5: 193–246. **b0545**
- Koenigsberger J (1938a) Natural residual magnetism of eruptive rocks, Pt I. *Terrestrial Magnetism and Atmospheric Electricity* 43: 119–127. **b0550**
- Koenigsberger J (1938b) Natural residual magnetism of eruptive rocks, Pt II. *Terrestrial Magnetism and Atmospheric Electricity* 43: 299–320. **b0555**
- Kok YS and Tauxe L (1996a) Saw-toothed pattern of relative paleointensity records and cumulative viscous remanence. *Earth and Planetary Science Letters* 137: 101–108. **b0560**
- Kok YS and Tauxe L (1996b) Saw-toothed pattern of sedimentary paleointensity records explained by cumulative viscous remanence. *Earth and Planetary Science Letters* 144: E9–E14. **b0565**
- Kok YS and Tauxe L (1999) A relative geomagnetic paleointensity stack from Ontong-Java Plateau sediments for the Matuyama. *Journal of Geophysical Research, Solid Earth* 104(B11): 25401–25413. **b0570**
- Kok YS and Yensen I (2002) Reply to comment by J.-P. Valet and L. Meynadier on 'A relative geomagnetic paleointensity stack from Ontong-Java Plateau sediments for the Matuyama'. *Journal of Geophysical Research* 107(B3): 2051. **b0575**
- Kok Y and Tauxe L (2000) Comment on 'Saw-toothed variations of relative paleointensity and cumulative viscous remanence: Testing the records and the model', by L. Meynadier, J.-P. Valet, Y. Guyodo, and C. Richter. *Journal of Geophysical Research* 105: 16609–16612. **b0580**
- Kono M (1971) Intensity of the Earth's magnetic field during the Pliocene and Pleistocene in relation to the amplitude of mid-ocean ridge magnetic anomalies. *Earth and Planetary Science Letters* 11: 10–17. **b0585**
- Kono M (1974) Intensities of the Earth's magnetic field about 60 m.y. ago determined from the Deccan Trap basalts, India. *Journal of Geophysical Research* 79: 1135–1141. **b0590**
- Kono M and Ueno N (1977) Paleointensity determination by a modified Thellier method. *Physics of the Earth and Planetary Interiors* 13: 305–314. **b0595**
- Korte M and Constable C (2005) The geomagnetic dipole moment over the last 7000 years – New results from a global model. *Earth and Planetary Science Letters* 236: 348–358. **b0600**
- Laj C, Kissel C, and Garnier F (1996a) Relative geomagnetic field intensity and reversals for the last 1.8 My from a central equatorial Pacific core. *Geophysical Research Letters* 23: 3393–3396. **b0605**
- Laj C, Kissel C, and Lefevre I (1996b) Relative geomagnetic field intensity and reversals from Upper Miocene sections in Crete. *Earth and Planetary Science Letters* 141(1–4): 67–78. **b0610**
- Laj C, Kissel C, Mazaud A, Channell JET, and Beer J (2000) North Atlantic palaeointensity stack since 75 ka (NAPIS-75) and the duration of the Laschamp event. *Philosophical Transactions of the Royal Society of London* 358(1768): 1009–1025. **b0615**
- Laj C, Rais A, Surmont J, *et al.* (1997) Changes of the geomagnetic field vector obtained from lava sequences on the island of Vulcano (Aeolian Islands, Sicily). *Physics of the Earth and Planetary Interiors* 99: 161–177. **b0620**
- Lanci L and Lowrie W (1997) Magnetostratigraphic evidence that 'tiny wiggles' in the oceanic magnetic anomaly record represent geomagnetic paleointensity variations. *Earth and Planetary Science Letters* 148(3–4): 581–592. **b0625**
- Laskar J, Joutel F, and Boudin F (1993) Orbital, precessional, and insolation quantities for the Earth from –20 Myr to +10 Myr. *Astronomy and Astrophysics* 270(1–2): 522–533. **b0630**

- [b0635](#) Le Goff M and Gallet Y (2004) A new three-axis vibrating sample magnetometer for continuous high-temperature magnetization measurements: Applications to paleo- and archeo-intensity determinations. *Earth and Planetary Science Letters* 229(1–2): 31–43.
- [b0640](#) Lehman B, Laj C, Kissel C, Mazaud A, Paterne M, and Labeyrie L (1996) Relative changes of the geomagnetic field intensity during the last 280 kyr from piston cores in the Acores area. *Physics of the Earth and Planetary Interiors* 93: 269–284.
- [b0645](#) Leonhardt R, Heider F, and Hayashida A (1999) Relative geomagnetic field intensity across the Jaramillo subchron in sediments from the California margin: ODP Leg 167. *Journal of Geophysical Research* 104: 29133–29146.
- [b0650](#) Leonhardt R, Matzka J, and Menor EA (2003) Absolute paleointensities and paleodirections of miocene and Pliocene lavas from Fernando de Noronha, Brazil. *Physics of the Earth and Planetary Interiors* 139(3–4): 285–303.
- [b0655](#) Levi S and Banerjee SK (1976) On the possibility of obtaining relative paleointensities from lake sediments. *Earth and Planetary Science Letters* 29: 219–226.
- [b0660](#) Linsley B and Thunnell R (1990) The record of deglaciation in the Sulu Sea: Evidence for the Younger Dryas event in the western tropical Pacific. *Paleoceanography* 5: 1025–1039.
- [b0665](#) Lisiecki L and Raymo ME (2005) A Pliocene–Pleistocene stack of 57 globally distributed benthic $\delta^{18}\text{O}$ records. *Paleoceanography* 20: PA1003 (doi:10.1029/2004PA001071).
- [b0670](#) Liu Q, Banerjee SK, Jackson MJ, Deng C, Pan Y, and Zhu R (2005) Inter-profile correlation of the Chinese loess/paleosol sequences during Marine Oxygen Isotope Stage 5 and indications of pedogenesis. *Quaternary Science Reviews* 24(1–2): 195–210.
- [b0675](#) Lovlie R (1974) Post-depositional remanent magnetization in a re-deposited deep-sea sediment. *Earth and Planetary Science Letters* 21: 315–320.
- [b0680](#) Lu R, Banerjee SK, and Marvin J (1990) Effects of clay mineralogy and the electrical conductivity of water on the acquisition of depositional remanent magnetization in sediments. *Journal of Geophysical Research* 95: 4531–4538.
- [b0685](#) Lund SP and Keigwin L (1994) Measurement of the degree of smoothing in sediment paleomagnetic secular variation records: An example from late Quaternary deep-sea sediments of the Bermuda Rise, western North Atlantic Ocean. *Earth and Planetary Science Letters* 122: 317–330.
- [b0690](#) Lund S, Williams T, Acton GD, Clement BM and Okada M (2001) Proceedings of the ocean Drilling Program, Scientific Results 17, Vol. 172: *Brunhes Chron magnetic field excursions recovered from Leg 172 sediments*. Ocean Drilling Program.
- [b0695](#) Macouin M, Valet J, Besse J, and Ernst R (2006) Absolute paleointensity at 1.27 Ga from the Mackenzie dyke swarm (Canada). *Geochemistry, Geophysics, Geosystems* 7: Q06H21 (doi:10.1029/2005GC000960).
- [b0700](#) Macri P, Sagnotti L, Dinares-Turell J, and Caburlotto A (2005) A composite record of Late Pleistocene relative geomagnetic paleointensity from the Wilkes Land Basin (Antarctica). *Physics of the Earth and Planetary Interiors* 151(3–4): 223–242.
- [b0705](#) Martinson DG, Pisias NG, Hays JD, Imbrie J, Moore TC, Jr., and Shackleton NJ (1987) Age dating and the orbital theory of the Ice ages: Development of a high-resolution 0–300,000 year chronostratigraphy. *Quaternary Research* 27: 1–29.
- [b0710](#) Masarik J and Beer J (1999) Simulation of particle fluxes and cosmogenic nuclide production in the Earth's atmosphere. *Journal of Geophysical Research* 104(D10): 12099–12111.
- [b0715](#) Mazaud A (1996) 'Sawtooth' variation in magnetic intensity profiles and delayed acquisition of magnetization in deep sea cores. *Earth and Planetary Science Letters* 139: 379–386.
- Mazaud A, Sicre MA, Ezat U, *et al.* (2002) Geomagnetic-assisted stratigraphy and sea surface temperature changes in core MD94-103 (Southern Indian Ocean): Possible implications for North-South climatic relationships around H4. *Earth and Planetary Science Letters* 201(1): 159–170.
- McClelland E and Briden J (1996) An improved methodology for Thellier-type paleointensity determination in igneous rocks and its usefulness for verifying primary thermoremanence. *Journal of Geophysical Research* 101: 21995–22013.
- McElhinny MW (1973) Paleomagnetism and Plate Tectonics. [b0730](#) [AU18](#)
- McFadden PL and McElhinny MW (1982) Variations in the geomagnetic dipole 2: Statistical analysis of VDM's for the past 5 million years. *Journal of Geomagnetism and Geoelectricity* 34: 163. [b0735](#)
- McFadden P and Merrill R (1997) Sawtooth paleointensity and reversals of the geomagnetic field. *Physics of the Earth and Planetary Interiors* 103: 247–252. [b0740](#)
- McHargue L and Donahue D (2005) Effects of climate and the cosmic-ray flux on the ^{10}Be content of marine sediments. *Earth and Planetary Science Letters* 232: 193–207. [b0745](#)
- McMillan DG, Constable CG, and Parker RL (2002) Limitations on stratigraphic analyses due to incomplete age control and their relevance to sedimentary paleomagnetism. *Earth and Planetary Science Letters* 201(3–4): 509–523. [b0750](#)
- McMillan DG, Constable C, and Parker RL (2004) Assessing the dipolar signal in stacked paleointensity records using a statistical error model and geodynamo simulations. *Physics of the Earth and Planetary Interiors* 145: 37–54. [b0755](#)
- Meynadier L and Valet JP (1995) Relative geomagnetic intensity during the last 4 m.y. from the equatorial Pacific. *Proceedings of the Ocean Drilling Program, Scientific Results* 138: 779–795. [b0760](#)
- Meynadier L and Valet JP (1996) Post-depositional realignment of magnetic grains and asymmetrical saw-tooth patterns of magnetization intensity. *Earth and Planetary Science Letters* 126: 109–127. [b0765](#)
- Meynadier L, Valet JP, Bassinot F, Shackleton NJ, and Guyodo Y (1994) Asymmetrical saw-tooth pattern of the geomagnetic field intensity from equatorial sediments in the Pacific and Indian Oceans. *Earth and Planetary Science Letters* 126: 109–127. [b0770](#)
- Meynadier L, Valet JP, Guyodo Y, and Richter C (1998) Saw-toothed variations of relative paleointensity and cumulative viscous remanence: Testing the records and the model. *Journal of Geophysical Research* 103: 7095–7105. [b0775](#)
- Meynadier L, Valet JP, Weeks R, Shackleton NJ, and Hagee VL (1992) Relative geomagnetic intensity of the field during the last 140 ka. *Earth and Planetary Science Letters* 114: 39–57. [b0780](#)
- Nagata T (1961) Rock Magnetism. [b0785](#) [AU19](#)
- Nagata T, Arai Y, and Momose K (1963) Secular variation of the geomagnetic total force during the last 5000 years. *Journal of Geophysical Research* 68: 5277–5282. [b0790](#)
- Néel L (1949) Théorie du trainage magnétique des ferromagnétiques en grains fines avec applications aux terres cuites. *Annales de Géophysique* 5: 99–136. [b0795](#)
- Néel L (1955) Some theoretical aspects of rock-magnetism. *Advances in Physics* 4: 191–243. [b0800](#)
- Nowaczyk NR and Antonow M (1997) High-resolution magnetostratigraphy of four sediment cores from the Greenland Sea. 1. Identification of the Mono Lake excursion, Laschamp and Biwa I Jamaica geomagnetic polarity events. *Geophysical Journal International* 131(2): 310–324. [b0805](#)
- Nowaczyk NR, Antonow M, Knies J, and Spielhagen RF (2003) Further rock magnetic and chronostratigraphic results on reversal excursions during the last 50 ka as derived from northern high latitudes and discrepancies in precise AMS C-14 dating. *Geophysical Journal International* 155(3): 1065–1080. [b0810](#)

- [b0815](#) Nowaczyk NR and Frederichs TW (1999) Geomagnetic events and relative palaeointensity variations during the past 300 ka as recorded in Kolbeinsey Ridge sediments, Iceland Sea: Indication for a strongly variable geomagnetic field. *International Journal of Earth Sciences* 88(1): 116–131.
- [b0820](#) Nowaczyk NR, Harwat S, and Melles M (2001) Impact of early diagenesis and bulk particle grain size distribution on estimates of relative geomagnetic palaeointensity variations in sediments from Lama Lake, northern Central Siberia. *Geophysical Journal International* 145(1): 300–306.
- [b0825](#) Nowaczyk NR and Knies J (2000) Magnetostratigraphic results from the eastern Arctic Ocean: AMS ¹⁴C ages and relative palaeointensity data of the Mono Lake and Laschamp geomagnetic reversal excursions. *Geophysical Journal International* 140(1): 185–197.
- [b0830](#) Oda H, Nakamura K, Ikehara K, Nakano T, Nishimura M, and Khlystov O (2002) Paleomagnetic record from Academician Ridge, Lake Baikal: A reversal excursion at the base of marine oxygen isotope stage 6. *Earth and Planetary Science Letters* 202(1): 117–132.
- [b0835](#) Okada M (1995) Detailed variation of geomagnetic field intensity during the late Pleistocene at Site 882. *Proceedings of the Ocean Drilling Program, Scientific Results* 145: 469–474.
- [b0840](#) Ozima M, Ozima M, and Akimoto S (1964) Low temperature characteristics of remanent magnetization of magnetite. *Journal of Geomagnetism and Geoelectricity* 16: 165–177.
- [b0845](#) Pan Y, Zhu R, Shaw J, Liu Q, and Guo B (2001) Can relative paleointensities be determined from the normalized magnetization of the wind-blown loess of China? *Journal of Geophysical Research* 106: 19221–19232.
- [b0850](#) Peck J, King J, Colman S, and Kravchinsky V (1996) An 84-kyr paleomagnetic record from the sediments of Lake Baikal, Siberia. *Journal of Geophysical Research* 101: 1365–1385.
- [b0855](#) Perrin M and Schnepf E (2004) IAGA paleointensity database: Distribution and quality of the data set. *Physics of the Earth and Planetary Interiors* 147(2–3): 255–267.
- [b0860](#) Perrin M, Schnepf E, and Shcherbakov V (1998) Paleointensity database updated. *EOS Transactions of the American Geophysical Union* 79: 198.
- [b0865](#) Perrin M and Shcherbakov V (1997) Paleointensity of the Earth's magnetic field for the past 400 Ma: Evidence for a dipole structure during the Mesozoic low. *Journal of Geomagnetism and Geoelectricity* 49: 601–614.
- [b0870](#) Pick T and Tauxe L (1993) Geomagnetic paleointensities during the Cretaceous normal superchron measured using submarine basaltic glass. *Nature* 366: 238–242.
- [b0875](#) Pisis NG, Martinson DG, Moore TC, et al. (1984) High-resolution stratigraphic correlation of benthic oxygen isotopic records spanning the last 300,000 years. *Marine Geology* 56(1–4): 119–136.
- [b0880](#) Prévot M, Derder MEM, McWilliams M, and Thompson J (1990) Intensity of the Earth's magnetic field: Evidence for a Mesozoic dipole low. *Earth and Planetary Science Letters* 97: 129–139.
- [b0885](#) Raisbeck G, Yiou F, and Zhou S (1994) Paleointensity puzzle. *Nature* 371: 207–208.
- [b0890](#) Rampino M (1979) Possible relations between changes in global ice volume, geomagnetic excursions, and the eccentricity of the Earth's orbit. *Geology* 7: 584–587.
- [b0895](#) Rampino MR (1981) Revised age estimates of Brunhis paleomagnetic events: Support for a link between geomagnetism and eccentricity. *Earth and Planetary Science Letters* 8: 1047–1050.
- [b0900](#) Rampino MR and Kent DV (1983) Geomagnetic excursions and climate change. *Nature* 302: 455.
- [b0905](#) Ravilly M, Horen H, Perrin M, Dymant J, Gente P, and Guillou H (2001) NRM intensity of altered oceanic basalts across the MAR (21 degrees N, 0–1.5 Ma): A record of geomagnetic palaeointensity variations? *Geophysical Journal International* 145(2): 401–422.
- [b0910](#) Riisager J, Riisager P, and Pedersen A (2003) The C27n–C26r geomagnetic polarity reversal recorded in the west Greenland flood basalt province: How complex is the transitional field? *Journal of Geophysical Research* 108: 2155 (doi:10.1029/2002JB002124).
- [b0915](#) Riisager J, Riisager P, Zhao XX, Coe RS, and Pedersen AK (2004) Paleointensity during a chron C26r excursion recorded in west Greenland lava flows. *Journal of Geophysical Research, Solid Earth* 109(B4): B04107.
- [b0920](#) Riisager P and Abrahamsen N (2000) Palaeointensity of West Greenland Palaeocene basalts: Asymmetric intensity around the C27n–C26r transition. *Physics of the Earth and Planetary Interiors* 118(1–2): 53–64.
- [b0925](#) Riisager P and Riisager J (2001) Detecting multidomain magnetic grains in Thellier palaeointensity experiments. *Physics of the Earth and Planetary Interiors* 125(1–4): 111–117.
- [b0930](#) Roberts A, Lehman B, Weeks R, Verosub K, and Laj C (1997) Relative paleointensity of the geomagnetic field over the last 200,000 years from ODP Sites 883 and 884, North Pacific Ocean. *Earth and Planetary Science Letters* 152: 11–23.
- [b0935](#) Roberts AP (1995) Magnetic properties of sedimentary greigite (Fe₃S₄). *Earth and Planetary Science Letters* 134: 227–236.
- [b0940](#) Roberts AP and Lewin-Harris JC (2000) Marine magnetic anomalies: Evidence that 'tiny wiggles' represent short-period geomagnetic polarity intervals. *Earth and Planetary Science Letters* 183(3–4): 375–388.
- [b0945](#) Roberts AP, Verosub KL, and Negrini RM (1994) Middle Late Pleistocene relative paleointensity of the geomagnetic-field from lacustrine sediments, Lake Chewaucan, Western United States. *Geophysical Journal International* 118(1): 101–110.
- [b0950](#) Roberts AP, Winklhofer M, Liang WT, and Horng CS (2003) Testing the hypothesis of orbital (eccentricity) influence on Earth's magnetic field. *Earth and Planetary Science Letters* 216(1–2): 187–192.
- [b0955](#) Rolph TC and Shaw J (1985) A new method of palaeofield magnitude correction for thermally altered samples and its application to Lower Carboniferous lavas. *Geophysical Journal of the Royal Astronomical Society* 80: 773–781.
- [b0960](#) Sato T, Kikuchi H, Nakashizuka M, and Okada M (1998) Quaternary geomagnetic field intensity: Constant periodicity or variable period? *Geophysical Research Letters* 25: 2221–2224.
- [b0965](#) Sato T and Kobayashi K (1989) Long-period secular variations of the Earth's magnetic field revealed by Pacific deep-sea sediment cores. *Journal of Geomagnetism and Geoelectricity* 41: 147–159.
- [b0970](#) Schneider DA (1993) An estimate of Late Pleistocene geomagnetic intensity variation from Sulu Sea sediments. *Earth and Planetary Science Letters* 120(3–4): 301–310.
- [b0975](#) Schneider DA, Kent DV, and Mello GA (1992) A detailed chronology of the Australasian impact event, the Brunhes–Matuyama geomagnetic polarity reversal and global climate change. *Earth and Planetary Science Letters* 111: 395–405.
- [b0980](#) Schneider D and Mello G (1996) A high-resolution marine sedimentary record of geomagnetic intensity during the Brunhes chron. *Earth and Planetary Science Letters* 144: 297–314.
- [b0985](#) Schwartz M, Lund SP, and Johnson TC (1996) Environmental factors as complicating influences in the recovery of quantitative geomagnetic-field paleointensity estimates from sediments. *Geophysical Research Letters* 23: 2693–2696.
- [b0990](#) Schwartz M, Lund SP, and Johnson TC (1998) Geomagnetic field intensity from 71 to 12 ka as recorded in deep-sea sediments of the Blake Outer Ridge, North Atlantic Ocean. *Journal of Geophysical Research, Solid Earth* 103(B12): 30407–30416.
- [b0995](#) Selkin P, Gee JS, and Tauxe L (in press) Nonlinear thermoremanence acquisition and implications for paleointensity data. *Earth and Planetary Science Letters*. AU20

- b1000** Selkin P, Gee J, Tauxe L, Meurer W, and Newell A (2000a) The effect of remanence anisotropy on paleointensity estimates: A case study from the Archaean Stillwater complex. *Earth and Planetary Science Letters* 182: 403–416.
- b1005** Selkin P and Tauxe L (2000b) Long-term variations in paleointensity. *Philosophical Transactions of the Royal Society of London* 358: 1065–1088.
- b1010** Shackleton NJ, Berger A, and Peltier WR (1990) An alternative astronomical calibration of the lower Pleistocene timescale based on ODP Site 677. *Transactions of the Royal Society of Edinburgh, Earth Sciences* 81: 251–261.
- b1015** Shaw J (1974) A new method of determining the magnitude of the paleomagnetic field application to 5 historic lavas and five archeological samples. *Geophysical Journal of the Royal Astronomical Society* 39: 133–141.
- b1020** Shcherbakov V and Shcherbakova V (1983) On the theory of depositional remanent magnetization in sedimentary rocks. *Geophysical Surveys* 5: 369–380.
- b1025** Shcherbakova V, Shcherbakov V, and Heider F (2000) Properties of partial thermoremanent magnetization in PSD and MD magnetite grains. *Journal of Geophysical Research* 105: 767–782.
- b1030** Sherwood G, Shaw J, Baer G, and Mallik S (1993) The strength of the geomagnetic field during the Cretaceous Quiet Zone: Paleointensity results from Israeli and Indian Lavas. *Journal of Geomagnetism and Geoelectricity* 45: 339–360.
- b1035** Smirnov AV and Tarduno JA (2005) Thermochemical remanent magnetization in precambrian rocks: Are we sure the geomagnetic field was weak? *Journal of Geophysical Research* 110: B06103 (doi:10.1029/2004JB003445).
- b1040** Smith PJ (1967) The intensity of the ancient geomagnetic field: A review and analysis. *Geophysical Journal of the Royal Astronomical Society* 12: 321–362.
- b1045** Sowers T, Bender M, Labeyrie L, et al. (1993) A 135,000 year Vostok–Specmap common temporal framework. *Paleoceanography* 8: 737–766.
- b1050** Spassov S, Heller F, Evans ME, Yue LP, and Dobeneck Tv (2003) A lock-in model for the complex Matuyama–Brunhes boundary record of the loess/palaeosol sequence at Lingtai (Central Chinese Loess Plateau). *Geophysical Journal International* 155(2): 350–366.
- b1055** Stacey FD (1972) On the role of Brownian motion in the control of detrital remanent magnetization of sediments. *Pure and Applied Geophysics* 98: 139–145.
- b1060** Stern DP (2003) A millennium of geomagnetism. *Reviews of Geophysics* 41(2): 1007.
- b1065** Stoner J, Channell J, Hillaire-Marcel C, and Kissel C (2000) Geomagnetic paleointensity and environmental record from Labrador Sea core MD95-2024: Global marine sediment and ice core chronostratigraphy for the last 110 kyr. *Earth and Planetary Science Letters* 5626: 1–17.
- b1070** Stoner JS, Channell JET, and Hillaire-Marcel C (1995) Late Pleistocene relative geomagnetic paleointensity from the deep Labrador Sea: Regional and global correlations. *Earth and Planetary Science Letters* 134: 237–252.
- b1075** Stoner JS, Channell JET, and Hillaire-Marcel C (1998) A 200 ka geomagnetic chronostratigraphy for the Labrador Sea: Indirect correlation of the sediment record to SPECMAP. *Earth and Planetary Science Letters* 159(3–4): 165–181.
- b1080** Stoner JS, Channell JET, Hodell DA, and Charles CD (2003) A ~580 kyr paleomagnetic record from the sub-Antarctic South Atlantic (Ocean Drilling Program Site 1089). *Journal of Geophysical Research* 108(B5): 2244.
- b1085** Stoner JS, Laj C, Channell JET, and Kissel C (2002) South Atlantic and North Atlantic geomagnetic paleointensity stacks (0–80 ka): Implications for inter-hemispheric correlation. *Quaternary Science Reviews* 21(10): 1141–1151.
- Stott L, Poulsen C, Lund S, and Thunell R (2002) Super ENSO and global climate oscillations at millennial time scales. *Science* 297: 222–226.
- Stratigraphy ICo (2004) *Geologic Time Scale 2004*. Cambridge, UK: Cambridge University Press.
- Sugiura N, Strangway D, Pearce G, Wu Y, and Taylor L (1979) A new magnetic paleointensity value for a ‘young lunar glass’. *Proceedings of the Lunar and Planetary Science Conference X*: 2189–2197.
- Tanaka H and Kono M (1991) Preliminary results and reliability of palaeointensity studies on historical and C14 dated Hawaiian lavas. *Journal of Geomagnetism and Geoelectricity* 43: 375–388.
- Tanaka H and Kono M (2002) Paleointensities from a Cretaceous basalt platform in inner Mongolia, Northeastern China. *Physics of the Earth and Planetary Interiors* 133(1–4): 147–157.
- Tanaka H, Kono M, and Uchimura H (1995) Some global features of paleointensity in geological time. *Geophysical Journal International* 120: 97–102.
- Tanaka H, Otsuka A, Tachibana T, and Kono M (1994) Paleointensities for 10–22 ka from volcanic rocks in Japan and New Zealand. *Earth and Planetary Science Letters* 122: 29–42.
- Tarduno JA and Cottrell RD (2005) Dipole strength and variation of the time-averaged reversing and nonreversing geodynamo based on Thellier analyses of single plagioclase crystals. *Journal of Geophysical Research* 110: B11101 (doi:10.1029JB003970).
- Tarduno JA, Cottrell RD, and Smirnov AV (2001) High geomagnetic intensity during the mid-Cretaceous from Thellier analyses of single plagioclase crystals. *Science* 291(5509): 1779–1783.
- Tarduno JA, Cottrell RD, and Smirnov AV (2002) The Cretaceous superchron geodynamo: Observations near the tangent cylinder. *Proceedings of the National Academy of Sciences of the United States of America* 99(22): 14020–14025.
- Tarduno J, Cottrell R, and Smirnov A (2006) The paleomagnetism of single silicate crystals: Recording geomagnetic field strength during mixed polarity intervals, superchrons, and inner core growth. *Reviews of Geophysics* 44: RG1002 (doi:10.1029/2005RG000189).
- Tauxe L (1993) Sedimentary records of relative paleointensity of the geomagnetic field: Theory and practice. *Reviews of Geophysics* 31: 319–354.
- Tauxe L (1998) *Paleomagnetic Principles and Practice*. Dordrecht, The Netherlands: Kluwer.
- Tauxe L (2005) *Lectures in Paleomagnetism*, earthref.org/Magic/Books/Tauxe/2005, San Diego.
- Tauxe L (2006a) Depositional remanent magnetization: Toward an improved theoretical and experimental foundation. *Earth and Planetary Science Letters* 244: 515–529.
- Tauxe L (2006b) Long term trends in paleointensity: The contribution of DSDP/ODP submarine basaltic glass collections. *Physics of the Earth and Planetary Interiors* 244: 515–529.
- Tauxe L, Bertram H, and Seberino C (2002) Physical interpretation of hysteresis loops: Micromagnetic modelling of fine particle magnetite. *Geochemistry, Geophysics, Geosystems* 3, (doi:10.1029/2001GC000280).
- Tauxe L, Gans PB, and Mankinen E (2004a) Paleomagnetic and ⁴⁰Ar/³⁹Ar ages from Matuyama/Brunhes aged volcanics near McMurdo Sound, Antarctica. *Geochemistry, Geophysics, Geosystems* 5: Q06H12 (doi:10.1029/2003GC000656).
- Tauxe L and Hartl P (1997) 11 million years of Oligocene geomagnetic field behaviour. *Geophysical Journal International* 128: 217–229.
- Tauxe L, Herbert T, Shackleton NJ, and Kok YS (1996) Astronomical calibration of the Matuyama–Brunhes

AU21

b1175

b1180

b1185

- Boundary: Consequences for magnetic remanence acquisition in marine carbonates and the Asian loess sequences. *Earth and Planetary Science Letters* 140: 133–146.
- b1190** Tauxe L and Love J (2003) Paleointensity in Hawaiian Scientific Drilling project Hole (HSDP2): Results from submarine basaltic glass. *Geochemistry, Geophysics, Geosystems* 4: 8702 (doi:10.1029/2001GC000276).
- b1195** Tauxe L, Lusk J, Selkin P, Gans PB, and Calvert A (2004b) Paleomagnetic results from the Snake River Plain: Contribution to the global time averaged field database. *Geochemistry, Geophysics, Geosystems* 5: Q08H13 (doi:10.1029/2003GC000661).
- b1200** Tauxe L, Pick T, and Kok YS (1995) Relative paleointensity in sediments; a pseudo-Thellier approach. *Geophysical Research Letters* 22: 2885–2888.
- b1205** Tauxe L and Shackleton NJ (1994) Relative paleointensity records from the Ontong-Java Plateau. *Geophysical Journal International* 117: 769–782.
- b1210** Tauxe L and Staudigel H (2004) Strength of the geomagnetic field in the Cretaceous Normal Superchron: New data from submarine basaltic glass of the Troodos Ophiolite. *Geochemistry, Geophysics, Geosystems* 5(2): Q02H06 (doi:10.1029/2003GC000635).
- b1215** Tauxe L and Wu G (1990) Normalized remanence in sediments of the Western Equatorial Pacific: Relative paleointensity of the geomagnetic field? *Journal of Geophysical Research* 95(B8): 12337–12350.
- b1220** Taylor L (1979) An effective sample preparation technique for paleointensity determinations at elevated temperatures. *Proceedings of the Lunar and Planetary Science Conference X*: 1209–1211.
- b1225** Teanby N and Gubbins D (2000) The effects of aliasing and lock-in processes on palaeosecular variation records from sediments. *Geophysical Journal International* 142(2): 563–570.
- b1230** Thellier E (1938) Sur l'aimantation des terres cuites et ses applications géophysiques. *Annales de l'Institut de Physique du Globe Université, Paris* 16: 157–302.
- b1235** Thellier E and Thellier O (1959) Sur l'intensité du champ magnétique terrestre dans le passé historique et géologique. *Annales de Géophysique* 15: 285–378.
- b1240** Thouveny N, Carcaillet J, Moreno E, Leduc G, and Nerini D (2004) Geomagnetic moment variation and paleomagnetic excursions since 400 kyr BP: A stacked record from sedimentary sequences of the Portuguese margin, Pt 1. *Earth and Planetary Science Letters* 219(3–4): 377–396.
- b1245** Thouveny N, Debeaulieu JL, Bonifay E, et al. (1994) Climate variations in Europe over the past 140-Kyr deduced from rock magnetism. *Nature* 371(6497): 503–506.
- b1250** Tiedemann R, Sarnthein M, and Shackleton NJ (1994) Astronomical timescale for the Pliocene Atlantic delta ¹⁸O and dust flux record of Ocean Drilling Program Site 659. *Paleoceanography* 9: 619–638.
- b1255** Tric E, Valet JP, Turcholka P, et al. (1992) Paleointensity of the geomagnetic field during the last 80,000 years. *Journal of Geophysical Research* 97: 9337–9351.
- b1260** Tsunakawa H and Shaw J (1994) The Shaw method of paleointensity determinations and its application to recent volcanic rocks. *Geophysical Journal International* 118: 781–787.
- b1265** Valet J-P (2003) Time variations in geomagnetic intensity. *Reviews of Geophysics* 41: 1004 (doi:10.1029/2001RG000104).
- b1270** Valet JP, Brassart J, Lemeur I, et al. (1996) Absolute paleointensity and magnetomineralogical changes. *Journal of Geophysical Research* 101(B11): 25029–25044.
- b1275** Valet J-P and Herrero-Bervera E (2000) Paleointensity experiments using alternating field demagnetization. *Earth and Planetary Science Letters* 177: 43–58.
- Valet JP and Meynadier L (1993) Geomagnetic field intensity and reversals during the past four million years. *Nature* 366: 234–238.
- b1285** Valet JP and Meynadier L (2001) Comment on 'A relative geomagnetic paleointensity stack from Ontong-Java plateau sediments for the Matuyama' by Yvo S. Kok and Lisa Tauxe. *Journal of Geophysical Research* 106: 11013–11015.
- b1290** Valet JP, Meynadier L, Bassinot FC, and Garnier F (1994) Relative paleointensity across the last geomagnetic reversal form sediments of the Atlantic, Indian and Pacific Oceans. *Geophysical Research Letters* 21: 485–488.
- b1295** Valet JP, Meynadier L, and Guyodo Y (2005) Geomagnetic dipole strength and reversal rate over the past two million years. *Nature* 435: 802–805.
- b1300** Valet JP, Tauxe L, and Clement BM (1989) Equatorial and mid-latitude records of the last geomagnetic reversal from the Atlantic Ocean. *Earth and Planetary Science Letters* 94: 371–384.
- b1305** Valet JP, Tric E, Herrero-Bervera E, Meynadier L, and Lockwood JP (1998) Absolute paleointensity from Hawaiian lavas younger than 35 ka. *Earth and Planetary Science Letters* 161: 19–32.
- b1310** van Vreumingen M (1993a) The magnetization intensity of some artificial suspensions while flocculating in a magnetic field. *Geophysical Journal International* 114: 601–606.
- b1315** van Vreumingen M (1993b) The influence of salinity and flocculation upon the acquisition of remanent magnetization in some artificial sediments. *Geophysical Journal International* 114: 607–614.
- b1320** van Zijl JSU, Graham KWT, and Hales AL (1962a) The paleomagnetism of the Stormberg Lavas 1. *Geophysical Journal of the Royal Astronomical Society* 7: 23–39.
- b1325** van Zijl JSU, Graham KWT, and Hales AL (1962b) The paleomagnetism of the Stormberg Lavas, 2. The behavior of the Earth's magnetic field during a reversal. *Geophysical Journal of the Royal Astronomical Society* 7: 169–182.
- b1330** Verosub KL (1977) Depositional and postdepositional processes in the magnetization of sediments. *Reviews in Geophysics and Space Physics* 15: 129–143.
- b1335** Verosub KL, Herrero-Bervera E, and Roberts AP (1996) Relative geomagnetic paleointensity across the Jaramillo Subchron and the Matuyama/Brunhes boundary. *Geophysical Research Letters* 23(5): 467–470.
- b1340** Walton D (2004) Avoiding mineral alteration during microwave magnetization. *Geophysical Research Letters* 31: L03606 (doi:10.1029/2003GL019011).
- b1345** Walton D (2005) Isolating viscous overprints with microwaves. *EOS Transactions of the American Geophysical Union, Fall Meeting Supplement* 86: GP12A-05.
- b1350** Walton D, Share J, Rolph TC, and Shaw J (1993) Microwave magnetisation. *Geophysical Research Letters* 20: 109–111.
- b1355** Weeks RJ, Laj C, Endignoux L, et al. (1995) Normalised natural remanent magnetisation intensity during the last 240000 years in piston cores from the central North Atlantic Ocean: Geomagnetic field intensity or environmental signal? *Physics of the Earth and Planetary Interiors* 87: 213–229.
- b1360** Westphal M and Munschy M (1994) Saw-tooth pattern of the Earth's magnetic field tested by magnetic anomalies over oceanic spreading ridges. *Comptes Rendus de l'Académie des Sciences Series IIA Earth and Planetary Science* 329: 565–571.
- b1365** Williams T, Thouveny N, and Creer KM (1998) A normalised intensity record from Lac du Bouchet: Geomagnetic palaeointensity for the last 300 kyr? *Earth and Planetary Science Letters* 156(1–2): 33–46.
- b1370** Winterwerp J and van Kesteren W (2004) *Developments in Sedimentology, Vol. 56: Introduction to the Physics of Cohesive Sediment in the Marine Environment*. Amsterdam, The Netherlands: Elsevier.

- b1375** Wollin G, Ericson D, and Ryan WBF (1971) Variations in magnetic intensity and climatic changes. *Nature* 232: 549–550.
- b1380** Worm H (1997) A link between geomagnetic reversals and events and glaciations. *Earth and Planetary Science Letters* 147: 55–67.
- b1385** Xu S and Dunlop DJ (1994) Theory of partial thermoremanent magnetization in multidomain grains 2 Effect of microcoercivity distribution and comparison with experiment. *Journal of Geophysical Research* 99: 9025–9033.
- b1390** Yamamoto Y and Tsunakawa H (2005) Geomagnetic field intensity during the last 5 Myr: LTD-DHT Shaw palaeointensities from volcanic rocks of the Society Islands, French Polynesia. *Geophysical Journal International* 162(1): 79–114.
- b1395** Yamamoto Y, Tsunakawa H, and Shibuya H (2003) Palaeointensity study of the Hawaiian 1960 lava: Implications for possible causes of erroneously high intensities. *Geophysical Journal International* 153(1): 263–276.
- b1400** Yamazaki T (1999) Relative paleointensity of the geomagnetic field during Brunhes Chron recorded in North Pacific deep-sea sediment cores: Orbital influence? *Earth and Planetary Science Letters* 169(1–2): 23–35.
- b1405** Yamazaki T and Ioka N (1994) Long-term secular variation of the geomagnetic field during the last 200 kyr recorded in sediment cores from the western equatorial Pacific. *Earth and Planetary Science Letters* 128: 527–544.
- b1410** Yamazaki T, Ioka N, and Eguchi N (1995) Relative paleointensity of the geomagnetic field during the Brunhes Chron. *Earth and Planetary Science Letters* 136: 525–540.
- b1415** Yamazaki T and Oda H (2002) Orbital influence on Earth's magnetic field: 100,000-year periodicity in inclination. *Science* 295(5664): 2435–2438.
- b1420** Yamazaki T and Oda H (2005) A geomagnetic paleointensity stack between 0.8 and 3.0 Ma from equatorial Pacific sediment cores. *Geochemistry, Geophysics, Geosystems* 6: Q11H20 (doi:10.203/2005GC001001).
- b1425** Yokoyama Y and Yamazaki T (2000) Geomagnetic paleointensity variation with a 100 kyr quasiperiod. *Earth and Planetary Science Letters* 181(1–2): 7–14.
- b1430** Yoshida S and Katsura I (1985) Characterization of fine magnetic grains in sediments by the suspension method. *Geophysical Journal of the Royal Astronomical Society* 82: 301–317.
- b1435** Yoshihara A and Hamano Y (2004) Paleomagnetic constraints on the Archean geomagnetic field intensity obtained from komatiites of the Barberton and Belingwe greenstone belts, South Africa and Zimbabwe. *Precambrian Research* 131(1–2): 111–142.
- Yoshihara A, Kondo A, Ohno M, and Hamano Y (2003) Secular variation of the geomagnetic field intensity during the past 2000 years in Japan. *Earth and Planetary Science Letters* 210(1–2): 219–231.
- b1445** Yu Y and Tauxe L (2004) On the use of magnetic transient hysteresis in paleomagnetism for granulometry. *Geochemistry, Geophysics, Geosystems* 6: Q01H14 (doi: 10.1029/2004GC000839).
- b1450** Yu Y and Tauxe L (2006) Acquisition of viscous remanent magnetization. *Physics of the Earth and Planetary Interiors* 159: 32–42.
- b1455** Zhao X, Riisager P, Riisager J, Draeger U, Coe R, and Zheng Z (2004) New paleointensity results from Cretaceous basalt of Inner Mongolia, China. *Physics of the Earth and Planetary Interiors* 141: 131–140.
- b1460** Zhu R, Laj C, and Mazaud A (1994) The Matuyama–Brunhes and upper Jaramillo transitions recorded in a loess section at Weinan, north-central China. *Earth and Planetary Science Letters* 125: 143–158.
- b1465** Zhu RX, Lo CH, Shi RP, Pan YX, Shi GH, and Shao J (2004a) Is there a precursor to the Cretaceous normal superchron? New paleointensity and age determination from Liaoning province, northeastern China. *Physics of the Earth and Planetary Interiors* 147(2–3): 117–126.
- b1470** Zhu RX, Lo CH, Shi RP, Shi GH, Pan YX, and Shao J (2004b) Palaeointensities determined from the middle Cretaceous basalt in Liaoning Province, northeastern China. *Physics of the Earth and Planetary Interiors* 142(1–2): 49–59.
- b1475** Zhu RX, Pan YX, Shaw J, Li DM, and Li Q (2001) Geomagnetic palaeointensity just prior to the Cretaceous normal superchron. *Physics of the Earth and Planetary Interiors* 128(1–4): 207–222.

Relevant Websites

- <http://earthref.org/MAGIC/> – Magnetics Information Consortium (MAGIC).
- <http://www.ngdc.noaa.gov/seg> – National Geophysical Data Center (NGDC).

Author's Contact Information**[AU1] L. Tauxe**

Scripps Institution of Oceanography
University of California, San Diego
Mail Code 0208
La Jolla
CA 92093-0220
USA

T. Yamazaki

Geological Survey of Japan
AIST Tsukuba Central 7
1-1-3 Higashi
Tsukuba
Ibaraki 305-8567
Japan

Keywords: DRM; Geomagnetic field behavior; Paleointensity; TRM

Abstract

G. Folgheraiter suggested over a century ago that baked materials could in principle be used to study variations of the Earth's magnetic field intensity in the past although he foresaw great difficulties. Over the last century, enormous progress has been made in laying the theoretical foundations for using archeological and geological materials to study variations in the strength of the magnetic field. Along with better theoretical foundations have come improvements in experimental design. Over the last decade, there has been an explosion of papers presenting data concerning variations in paleointensity through time, using both igneous and sedimentary records. In this chapter we will explore the theoretical basis for paleointensity experiments in igneous and sedimentary environments, review the existing data, and highlight current topics of interest.